ELECTRONICALLY TUNABLE MICROWAVE BANDSTOP FILTER DESIGN AND IMPLEMENTATION

A THESIS SUBMITTED TO
THE GRADUATE SCHOOL OF NATURAL AND APPLIED SCIENCES
OF
MIDDLE EAST TECHNICAL UNIVERSITY

BY

SACİD ORUÇ

IN PARTIAL FULFILLMENT OF THE REQUIREMENTS
FOR
THE DEGREE OF MASTER OF SCIENCE
IN
ELECTRICAL AND ELECTRONICS ENGINEERING

SEPTEMBER 2010

Approval of the thesis:

ELECTRONICALLY TUNABLE MICROWAVE BANDSTOP FILTER DESIGN AND IMPLEMENTATION

submitted by **SACİD ORUÇ** in partial fulfillment of the requirements for the degree of **Master of Science in Electrical and Electronics Engineering Department, Middle East Technical University** by,

Prof. Dr. Canan Özgen _____
Dean, Graduate School of **Natural and Applied Sciences**

Prof. Dr. İsmet Erkmen _____
Head of Department, **Electrical and Electronics Engineering**

Prof. Dr. Nevzat Yıldırım _____
Supervisor, **Electrical and Electronics Engineering Dept., METU**

Examining Committee Members:

Prof. Dr. Canan Toker _____
Electrical and Electronics Engineering Dept., METU

Prof. Dr. Nevzat Yıldırım _____
Electrical and Electronics Engineering Dept., METU

Assoc. Prof. Dr. Sencer Koç _____
Electrical and Electronics Engineering Dept., METU

Assoc. Prof. Dr. Şimşek Demir _____
Electrical and Electronics Engineering Dept., METU

Dr. Mustafa Akkul _____
Manager, ASELSAN Inc.

Date: 17.09.2010

I hereby declare that all information in this document has been obtained and presented in accordance with academic rules and ethical conduct. I also declare that, as required by these rules and conduct, I have fully cited and referenced all material and results that are not original to this work.

Name, Last name : Sacid ORUÇ
Signature :

ABSTRACT

ELECTRONICALLY TUNABLE MICROWAVE BANDSTOP FILTER DESIGN AND IMPLEMENTATION

Oruç, Sacid
M.Sc., Department of Electrical and Electronics Engineering
Supervisor: Prof. Dr. Nevzat Yıldırım

September 2010, 173 pages

In modern broadband microwave applications, receivers are very sensitive to interference signals which can come from the system itself or from hostile emitters. Electronically tunable bandstop filters can be used to eliminate these interference signals with adaptation to changing frequency conditions. In this thesis, electronically tunable bandstop filter design techniques are investigated for microwave frequencies. The aim is to find filter topologies which allow narrowband bandstop or 'notch' filter designs with low-Q resonators and with tuning capability. Tunability will be provided by the use of electronically tunable capacitors, specifically varactor diodes. For this purpose, firstly direct bandstop filter techniques are investigated and their performances are analyzed. Then phase cancellation approach, which enables high quality bandstop filter design with lossy circuit elements, is introduced and analyzed. Lastly, a novel notch filter design technique called as all-pass filter approach is introduced. This approach allows a systematic design method and enables to design very good tunable notch filter characteristics with low-Q resonators. Three filter topologies using this approach are given and their

performances are analyzed. Also prototype tunable notch filters operating in X-Band are designed and implemented by using these three topologies.

Keywords: Bandstop Filter, Notch Filter, Tunable, Varactor Diode, All-Pass Filter, X-Band

ÖZ

ELEKTRİKSEL OLARAK AYARLANABİLİR MİKRODALGA BANT DURDURAN SÜZGEÇ TASARIM VE ÜRETİMİ

Oruç, Sacid
Yüksek Lisans, Elektrik ve Elektronik Mühendisliği Bölümü
Tez Yöneticisi: Prof. Dr. Nevzat Yıldırım

Eylül 2010, 173 sayfa

Günümüz geniş bantlı mikrodalga uygulamalarında almaçlar, sistemin kendisinden veya düşman vericilerinden kaynaklanan parazit sinyallere karşı oldukça duyarlıdır. Elektriksel olarak ayarlanabilir bant durduran süzgeçler kullanılarak bu parazit sinyaller değişen frekans koşullarına uyum sağlayacak şekilde engellenebilmektedir. Bu tezde, mikrodalga frekanslarında çalışan elektriksel olarak ayarlanabilen süzgeç tasarım teknikleri araştırılmaktadır. Burada amaç düşük Q faktörlü rezonatörler ile ayarlanabilme yeteneği olan dar bantlı bant durduran (ya da çentik) süzgeç tasarımına izin veren topolojileri bulmaktır. Ayarlanabilme özelliği elektriksel olarak ayarlanabilir kapasiteler, özellikle varaktör diyotlar, kullanarak sağlanacaktır. Bu amaçla, ilk olarak doğrudan bant durduran süzgeç teknikleri araştırılmış ve performansları incelenmiştir. Daha sonra kayıplı devre elemanları ile yüksek kalitede bant durduran süzgeç tasarımına imkan veren faz iptalleşmesi yaklaşımı tanıtılmış ve incelenmiştir. Son olarak ise tüm-geçiren süzgeç yaklaşımı denilen yeni bir çentik süzgeç tasarım tekniği tanıtılmıştır. Bu yaklaşım sistematik bir tasarım yöntemi kullanılmasını sağlamaktadır ve düşük Q faktörlü rezonatörler ile oldukça iyi ayarlanabilir çentik süzgeçlerin tasarlanabilmesini sağlamaktadır. Bu yaklaşımını

kullanan üç süzgeç topolojisi verilmiştir ve performansları incelenmiştir. Ayrıca bu üç topoloji kullanılarak X-Bantta çalışan ilk örnek ayarlanabilir çentik süzgeçler tasarlanmış ve üretilmiştir.

Anahtar Kelimeler: Bant Durduran Süzgeç, Çentik Süzgeç, Ayarlanabilir, Varaktör Diyot, Tüm-Geçiren Süzgeç, X-Bant

To my beloved family

ACKNOWLEDGEMENTS

I would like to express my sincere gratitude to my supervisor Prof. Dr. Nevzat Yıldırım for his supervision, invaluable guidance and support during the development of this thesis.

I would like to thank Dr. Mustafa Akkul, Zeynep Eymür, Bülent Alıcıoğlu, Galip Keçelioğlu and Gökhan Boyacıoğlu for their precious suggestions, support and technical help during this thesis study. I also wish to express my sincere appreciation to Tülay Can and Turan Yıldırım for their great help in assembling and measurement processes.

I would like to thank ASELSAN Inc. for allowing me to use their facilities for fabrication and measurement processes.

I would also like to thank TÜBİTAK for their financial support during my graduate study.

Finally, I feel grateful to my dear family for their absolute support, patience and encouragement.

TABLE OF CONTENTS

LIST OF FIGURES

FIGURES

LIST OF ABBREVIATIONS

ADS	: Advanced Design System
CAD	: Computer-Aided Design
CST	: Computer Simulation Technology
BLC	: Branch Line Coupler
BW	: Bandwidth
BPF	: Bandpass Filter
BSF	: Bandstop Filter
EM	: Electromagnetic
GAAS	: Gallium Arsenide
LNA	: Low Noise Amplifier
OC	: Open Circuit
PCB	: Printed Circuit Board
PCL	: Parallel Coupled Line
Q	: Quality Factor
RF	: Radio Frequency
RX	: Receiver
SC	: Short Circuit
SSS	: Suspended Stripline Substrate
TL	: Transmission Line
TZ	: Transmission Zero

CHAPTER 1

INTRODUCTION

1.1 Overview

Tunable narrowband bandstop or 'notch' filters have wide applications in both communication and electronic warfare systems. In modern broadband system applications, receivers are very sensitive to interference signals. So incident unwanted signals that can degrade receiver dynamic range and desensitize the receiver should be prevented. These unwanted signals can be fixed frequency interferences or changing frequency interferences which can result from collocated transmitters and hostile emitters. In order to suppress the effects of interfering signals, a highly selective tunable notch filter is required in receivers' front-end. These notch filters are placed in front of receivers' low noise amplifier as shown in Figure 1.1 to eliminate potential interferers with frequency tunability included for adaptation to changing unwanted signal conditions.

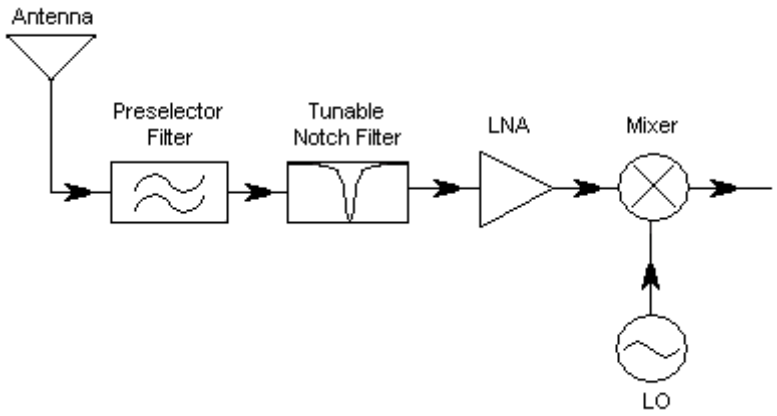

Figure 1.1 Tunable Notch Filter Position in Receiver Front-End.

Since typical position of these filters is before LNA of receivers, it is important that losses and nonlinearities at passband of the circuit should be very small for minimal additional noise, signal distortion and degradation in receiver sensitivity. Also suppression or 'notch depth' at tuned frequency should be high to eliminate strong interferences and suppressed frequency band should not be too wide in order to avoid decreasing the operational bandwidth of the receiver which is defined by the preselector filter. These expected properties for a proper tunable notch filter can only be satisfied by using high-Q resonators. High-Q resonators enable low passband loss, high selectivity or 'notch depth' and narrow stopband bandwidth. However the required Q values of resonators for a high performance tunable notch filter are considerably high. So cavity filters and YIG tuned filters are used for high frequency microwave applications instead of planar transmission mediums which are generally lossy. Cavity filters and YIG filters can have very high Q resonators and center frequency of the notch filter can be tuned by mechanically adjusting the cavity dimensions of cavity resonators and by magnetically changing the resonance frequencies of a ferromagnetic YIG element. However these type of filters have bulky and expensive physical structure and have slow tuning speed due to mechanical and magnetical tuning. Also they are not suitable for large production volumes since they need to be custom machined, carefully assembled, tuned and calibrated. In today's commercial and military high frequency systems, filters must not only provide good frequency selectivity, but also offer small size, fast tuning speed, affordable cost and high production volumes.

When compactness, low cost and ease of production are considered, planar structures come forward. Tunable notch filters can also be formed by using planar transmission mediums. However planar structures have significant circuit losses which limit to obtain high Q resonators. Tunability of resonators is achieved by variable capacitors. There are a few tunable capacitor types that can be used in planar structures like solid state varactor diodes, RF MEMS digital capacitors and ferroelectric capacitors. Due to their ease of production, assembly, low cost and speed, solid state varactor diodes or just 'varactors' are widely used for planar tunable circuits. In this thesis, main goal is to design varactor tunable notch filters.

Although varactors enable compact, fast tunable and easily constructed filters, varactor tuned notch filters traditionally suffer from high insertion loss in passband, insufficient rejection at notch frequency and inadequate selectivity due to inherent dissipation losses in varactors and circuit losses of planar transmission media. Notch depth of these low-Q notch filters can be improved by increasing notch bandwidth or by increasing order of the filter. However, these approaches have negative impact on selectivity and passband insertion loss. In order to be able to design high performance tunable notch filters by using varactors and by using planar structures, filter topologies which take effects of circuit losses into account are necessary.

Historically, narrowband bandstop filter topologies are used in the first varactor tunable notch filters [1]. In these approaches, first a notch filter is synthesized by using available narrowband bandstop filter topologies and then tuning capacitors are added to the resonators of the filter. This classical approach suffers greatly from low Q resonators. Notch depth and selectivity becomes insufficient when low order bandstop filters are used. Also notch depth varies significantly during tuning of notch frequency. There are a few ways to improve notch filter characteristics of these low-Q notch filters. First of all, loss of resonators can be eliminated using negative resistance approach by addition of transistors to the resonators [2]. So very high-Q resonators can be achieved by this way and these high-Q values can be preserved during tuning of resonators. However due to addition of transistors, complexity of the filter increases. Secondly, notch depth can be increased by introduction of a cross-coupling bridge line which creates a transmission zero (TZ) at notch frequency [3]. This enables to obtain high notch depths by addition of only a simple transmission line (TL). So notch depth can be increased by this way without increasing circuit complexity. However, this high notch depth can be tuned within a very limited frequency range. There are also approaches using cross coupling bridge lines and amplifiers to obtain high performance tunable notch filter characteristics [4]-[5] at the expense of increasing circuit element number and complexity.

There are also various works which enable high notch depth, wide tuning range and low tuning notch depth variations from low-Q resonators. For example, all-pass filter networks formed by 3-dB hybrids whose direct and couple ports are loaded by

identical resonators and the isolated port of the coupler are treated as the output port can be used for this purpose [6]-[7]. If the resonances of two resonators are detuned then a notch appears at the output port through phase cancellation. The notch frequency can be shifted by tuning the resonance frequencies. A number of papers exist on the design of such notch filters based on this approach [6]-[10].

1.2 Description of the Thesis

The aim of this thesis work is to design electronically tunable microwave notch filters. These designs will be suitable for planar transmission mediums like microstrip, coplanar, suspended stripline substrate (SSS) etc. and varactor diodes will be used as tuning elements.

Throughout the thesis, many notch filter topologies are introduced. Some of them are direct narrowband bandstop topologies and others are bridged structures. The bridge structures are composed of either a BLC with two resonators or a bandpass / bandstop main filter with a delay line cross-coupling input & output of the main filter. All these topologies are analyzed by linear simulation with only tuning capacitors as lossy elements. Their convenience for tunable notch filter designing is investigated.

A novel, systematic design method called as all-pass filter approach is introduced. This approach enables high performance tunable notch filters with low-Q varactors. Various filter topologies using this approach are given and analyzed. 3 prototype notch filters using this approach are designed by using linear & EM simulations and implemented in SSS medium. Measurement results of these implemented designs are presented.

1.3 Outline of the Thesis

In Chapter 2, after a brief introduction of bandstop filters, direct narrowband bandstop filter topologies are introduced. Design steps of different filter topologies

are presented. Then responses of these topologies with lossy tuning capacitors are investigated and evaluated for their convenience as tunable notch filter designing.

In Chapter 3, amplitude balanced phase cancellation approach, which improves performances of direct notch filter topologies in Chapter 2, is introduced. This method also enables bandpass filters and BLC containing topologies to design tunable notch filters. Details of various topologies are presented and their performances with lossy tuning capacitors are investigated.

In Chapter 4, the all-pass filter approach, which enables much better tunable notch filter characteristics with low-Q resonators compared to the topologies given in Chapter 2 and 3, is introduced. A systematic design approach is given and various filter topologies that can be used with this approach are presented and investigated.

In Chapter 5, design stages of 3 prototype filters using all-pass filter approach are presented. Linear and EM simulation results are given and the results of the implemented circuits are shown. Finally the thesis work is summarized with conclusion in Chapter 6.

CHAPTER 2

DIRECT BANDSTOP FILTER DESIGN

2.1 Bandstop / Notch Filter Basics

Bandstop filters or band-reject filters, reject signals within a frequency band bounded by a lower and an upper limit and allow transmission at frequencies out of this band. The ideal bandstop filter amplitude response in frequency domain is given in Figure 2.1.

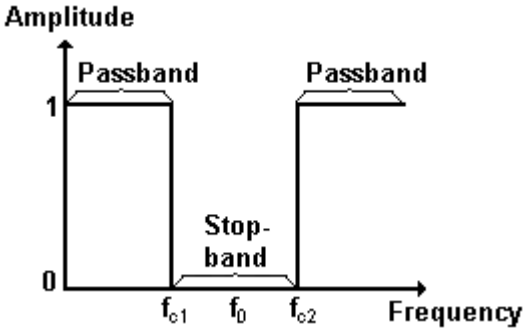

Figure 2.1 Ideal (Brick Wall) Bandstop Filter.

In Figure 2.1, f_{c1} & f_{c2} are the lower and upper corner frequencies and f_0 is the center frequency of the ideal bandstop filter. In ideal bandstop filter, attenuation in passband is zero, attenuation in stopband is infinite, and transition from passband to stopband is infinitely sharp. Such an ideal filter (brick wall filter) characteristics is not possible to obtain in practice. Practical filter responses have smoother passband to stopband transitions. Passband insertion losses are desired to be as small as possible and stopband attenuations are desired to be as high as possible. Ideal characteristics can be approximated using approximating functions like Butterworth,

Chebyshev, Elliptic etc. within an acceptable tolerance. Typical approximate bandstop amplitude responses using these functions are given in Figure 2.2.

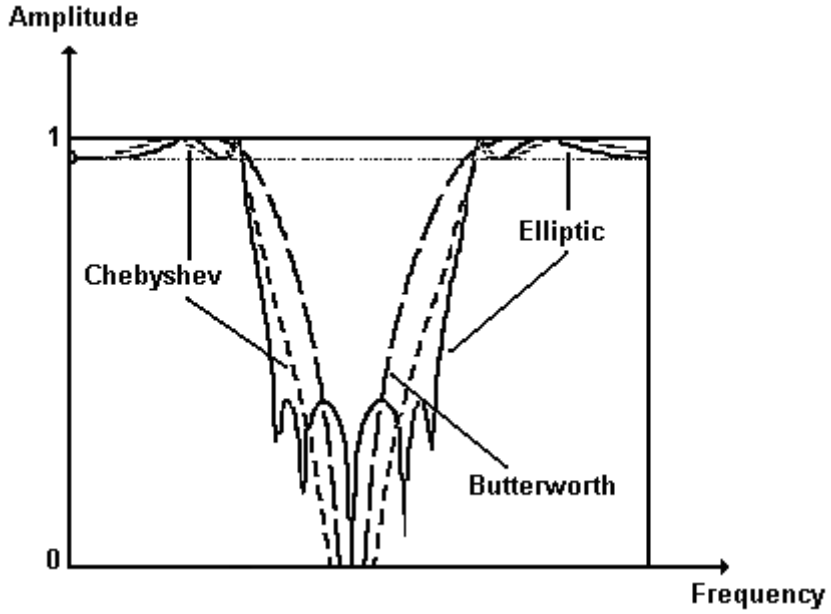

Figure 2.2 Approximations for Ideal Bandstop Filter.

A bandstop filter (BSF) with a narrow stopband is called a notch filter. Notch filters basically reject or 'notch' out a specific frequency. So ideally they are like allpass filters except an abrupt attenuation at a specific frequency. Typical response of a notch filter and its important characteristics are shown in Figure 2.3.

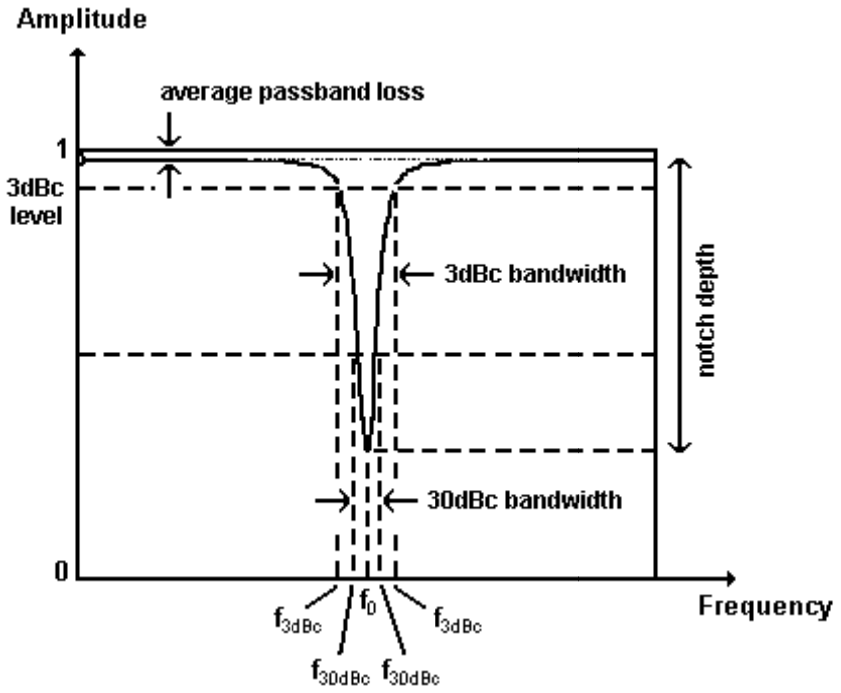

Figure 2.3 A Typical Notch Filter and its Characteristics.

The performance of a notch filter is mainly evaluated by four parameters:

- stopband attenuation level (or notch depth) at center frequency
- stopband frequency bandwidth for a given attenuation level (for example 30dBc frequency bandwidth)
- frequency bandwidth for a given attenuation level at which passband to stopband transition starts (for example 3dBc frequency bandwidth)
- average insertion loss at passband

Designing notch filters seems at first nothing different from designing bandstop filters with a narrow bandwidth. However using direct bandstop filter topologies for notch filter designs most probably gives poor results. This is because of two main reasons. Firstly, as stopband bandwidth decreases for a bandstop filter, circuit elements get unrealizable values. Secondly, circuit losses, especially finite Q of resonators, severely degrade the stopband attenuation level. In this chapter of this thesis, direct bandstop filter topologies are introduced and their notch performances are investigated.

The main goal of this thesis is to design electronically tunable notch filters. So besides investigating appropriate notch filter topologies, tunability of center frequency is also a primary concern. Theoretically it is possible to convert fixed frequency bandstop/notch filters into mechanically or electronically tunable bandstop filters by varying the capacitance or inductance of the resonators. Resonators are the main circuit elements which determine the center frequency of a bandstop filter. So in order to be able to change the center frequency, they are the primary actor. However in order not to distort the proper frequency response, all the circuit parameters should be tuned. This cannot be implemented for a practical circuit. In most filter circuits, only resonators are suitable for tuning. Hence the distortion of frequency responses of notches when only resonators are tuned is an important parameter to be investigated for notch filter topologies. The additional performance parameters of a tunable notch filter besides the previous given four performance parameters are as follows:

- notch depth variations during tuning
- notch bandwidth variations during tuning (3dBc, 30dBc, etc.)
- frequency tuning range

Typical variations in amplitude response characteristics of a notch filter when center frequency is changed are shown in Figure 2.4.

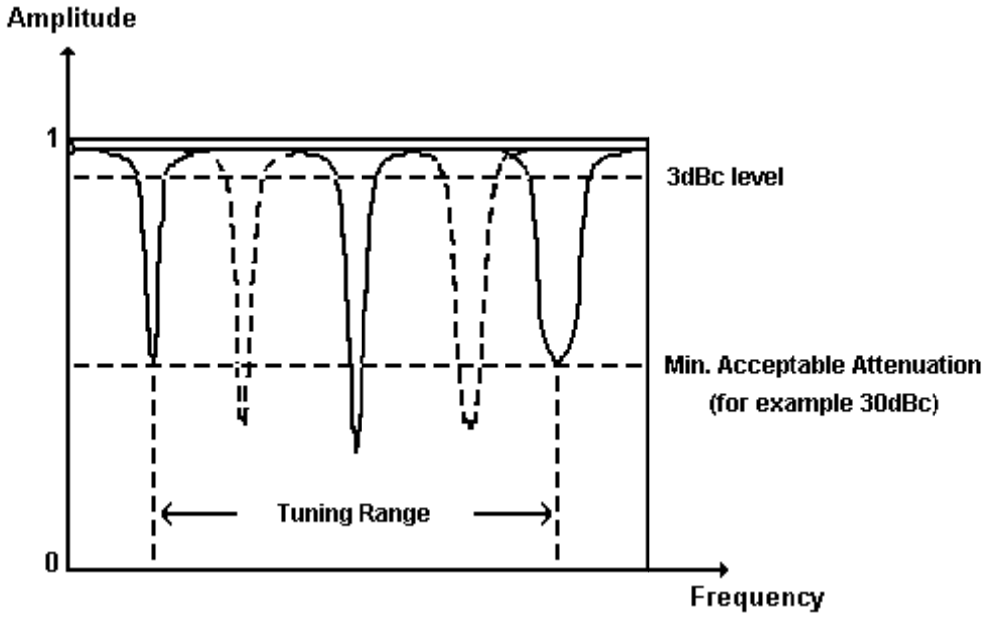

Figure 2.4 Typical Changes During Tuning of Notch Center Frequency.

In this chapter and the following two chapters many filter topologies are introduced and their convenience to be used as a high quality notch filter are investigated according to the previously given performance parameters. More details and examples for filter topologies that will be given throughout this thesis can be found in [11]. For a high quality tunable notch filter, the following properties are generally expected:

- notch depth is very high
- notch bandwidth is narrow
- passband to stopband transition is very sharp
- average insertion loss is very low
- deep notch depth is conserved during tuning
- notch bandwidth does not change significantly during tuning
- deep notch can be tuned over a broad frequency range
- passband return loss is high

2.2 Direct Bandstop Filter Design Methods

Simply, a notch filter can easily be synthesized from bandstop filter by using modern filter design method, namely insertion loss method. Starting with lowpass filter prototypes that are based on approximation functions such as Butterworth, Chebyshev, Elliptic, etc. and are normalized in terms of impedance and frequency, various transformations are applied to convert the prototype designs to the desired frequency range and impedance level. The insertion and return losses in the passband and attenuation in the stopband can be defined and controlled based on ripple level and degree of filter. The details of this classic method can be found in various books [12]-[13].

The standard insertion loss method gives filter circuits consisting of only lumped inductance and capacitances. At frequencies up to a few hundred MHz, commercial lumped elements (capacitor, inductor, and resistor) are available. But above these frequencies, performances of commercially available lumped element performances are not as desired because of element dimensions and parasitic effects. So, at microwave frequencies, lumped filter circuits obtained from standard insertion loss method are not realizable. To overcome this problem, the elements obtained from standard insertion loss method are converted to distributed elements using the Richard's Transformation and Kuroda Identities. Using this distributed approach, both waveguide and printed circuits can be implemented. For printed circuit implementations, the resultant circuit can be composed of transmission lines, OC and SC stubs, stepped impedances and coupled lines. Due to periodic nature of transmission lines in frequency, the responses in distributed filters are repetitive and spurious passbands are unavoidable.

In the scope of this thesis, frequency of interest will be X-Band (8-12GHz). So at this frequency band, distributed filters are a must. But for the sake of completeness and generality, both lumped and distributed designs are to be introduced.

2.3 Standart Lumped Element Designs

The modern procedure used to design filters is called the insertion loss method. This method uses network synthesis techniques to design filters with a completely specified frequency response. The design is simplified by beginning with lowpass prototypes that are normalized in terms of impedance and frequency. Transformations are then applied to convert the prototype designs to the desired frequency range and impedance level. This method gives lumped element circuits.

Well known design formulations of this method can be found in many books. Also there are sophisticated computer-aided design (CAD) packages available to design filter circuits based on this method. In this thesis, all linear filter designs are synthesized by FILPRO.

There are 4 standard circuit topology derived from insertion loss method. The first two are the basic designs (dual of each other) consisting of series and parallel LC resonators and the other two are modified versions of the first two designs by using impedance inverters so that only one type (series or parallel) resonators are used.

These standard designs are not useful for designing narrowband bandstop filters or in other words notch filters. As stopband bandwidth decreases, element values become unrealizable. This is shown in the following designs in Figure 2.5. For a notch filter at center frequency of 10GHz, two designs are done using FILPRO tools By Built-in LC Prototypes and By Prototype with Inverters, which applies standard lowpass prototype method.

Built-in LC Prototypes	Lumped, BSF, Cheby
Ripple (dB)	0.01
Passband Corners (MHz)	9800-10200
Proto. Degree	3

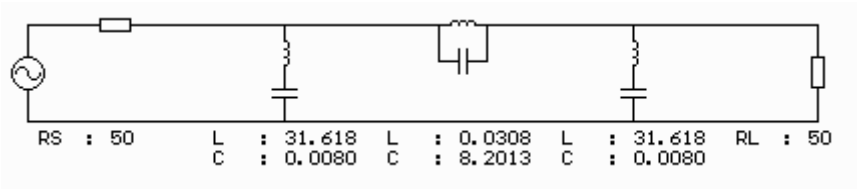

(a)

By Prototype with Inverters	Lumped, BSF, Cheby, Shunt Caps+ Inverters
Ripple (dB)	0.01
Passband Corners (MHz)	9800-10200
Proto. Degree	3

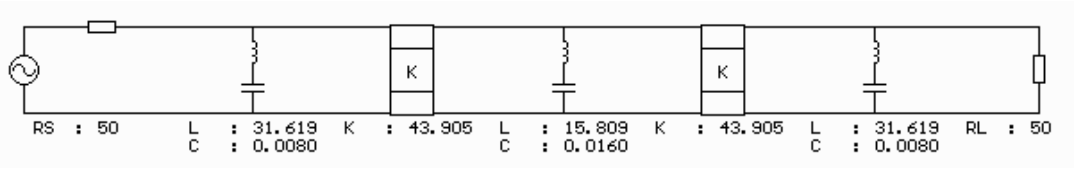

(b)

Figure 2.5 FILPRO Standard Lumped Designs. (a) By Built-in LC Prototypes. (b) By Prototype with Inverters.

In Figure 2.5, it is seen that inductor values are very high for microwave frequencies and capacitor values are too low to be realized in any frequency. As stated before, in high frequencies, especially above 2 GHz, distributed elements should be used instead of lumped elements.

2.4 Distributed Element Designs

Distributed element filter design method is more general form of standard insertion loss method. In this case, using Richard's transformation, lumped elements are replaced by distributed elements. Resistors stay the same but capacitors are replaced by OC stubs and inductors are replaced by SC stubs. In addition to these elements, transmission lines (namely unit element), stepped impedances and coupled lines are

also present as elements in distributed circuits which do not have any equivalents in lumped elements. Distributed circuit theory establishes a simple relationship between lumped and distributed circuits by mapping frequency plane to Ω- plane, which repeats with a period of $wl/v_p=2\pi$. This transformation converts lumped elements to transmission line (TL) sections. Also Kuroda's identities can be used to separate filter elements by using TL sections. These additional TL sections do not affect the filter response so this type of design is called redundant filter synthesis. It is possible to design microwave filters that take advantage of these sections to improve filter response; such nonredundant synthesis does not have a lumped element counterpart [14].

Due to this periodic mapping, responses of distributed filters are repetitive. This is generally considered to be a negative aspect for distributed filters. But this enables distributed lowpass filters (LPF) to be used also as bandstop filters. Distributed lowpass filters whose corner frequency is close to the periodicity frequency (or quarter wavelength frequency) have a response of bandstop/notch filter around the quarter wavelength frequency. Hence in distributed element approach, both bandstop filter designs and lowpass filter designs can be used.

Figure 2.6 shows 2 designs which are designed in FILPRO tools By Built-in LC Prototypes and By Prototype with Inverter as distributed bandstop filters which are distributed versions of the circuits in Figure 2.5. Both designs are equivalent of each other, so frequency responses are the same and given in Figure 2.6.c.

Built-in LC Prototypes	Distr, BSF, Cheby
Ripple (dB)	0.01
Passband Corners (MHz)	9800-10200
Proto. Degree	3
f_q (MHz)	20000

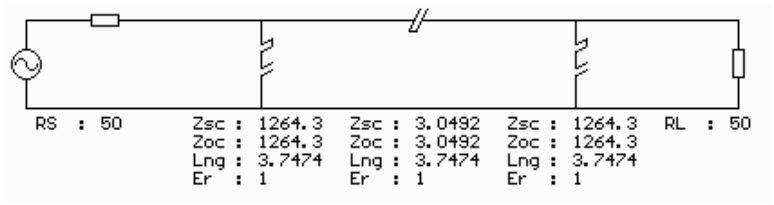

(a)

By Prototype with Inverters	Distr, BSF, Cheby, Shunt Caps+ Inverters
Ripple (dB)	0.01
Passband Corners (MHz)	9800-10200
Proto. Degree	3
f_q (MHz)	20000

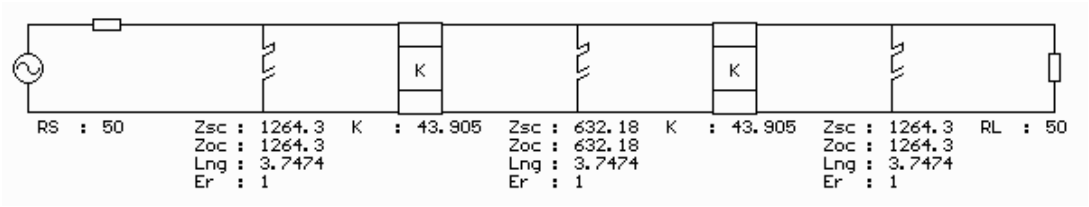

(b)

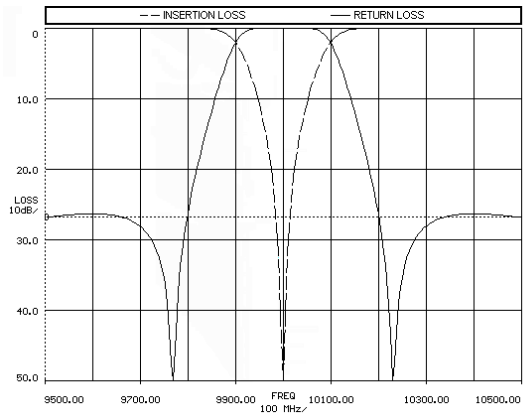

(c)

Figure 2.6 FILPRO Standard Distributed Designs from BSF. (a) By Built-in LC Prototypes. (b) By Prototype with Inverters. (c) Frequency Responses.

In Figure 2.6, it is seen that impedances of OC and SC stubs are either too high or too low. So at these values, both circuits are not realizable similar to the lumped case. But using various circuit transformations, element values in these circuits can be transformed to realizable ones.

Figure 2.7 shows 2 designs which are designed in FILPRO tools By Built-in LC Prototypes and By Prototype with Inverters as distributed lowpass filters. Both designs are equivalent of each other, so frequency responses are the same and given in Figure 2.7.c.

Built-in LC Prototypes	Distr, LPF, Cheby
Ripple (dB)	0.01
Passband Corner (MHz)	9800
Proto. Degree	3
f_q (MHz)	10000

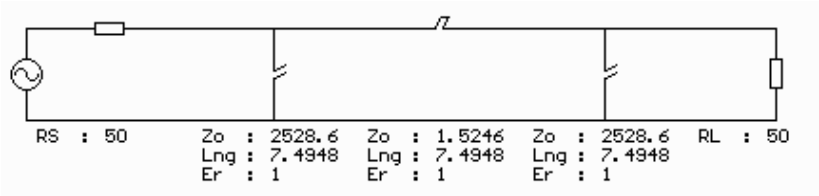

(a)

By Prototype with Inverters	Distr, LPF, Cheby, Shunt Caps+ Inverters
Ripple (dB)	0.01
Passband Corner (MHz)	9800
Proto. Degree	3
f_q (MHz)	10000

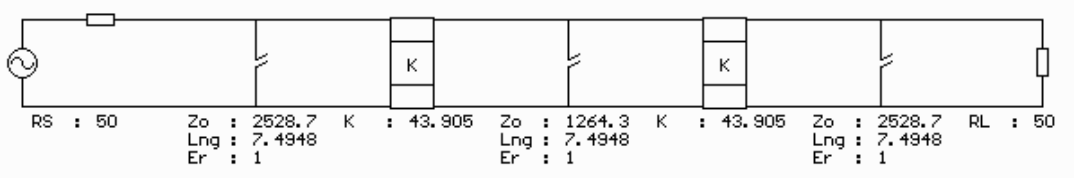

(b)

Figure 2.7 FILPRO Standard Distributed Designs from LPF. (a) By Built-in LC Prototypes. (b) By Prototype with Inverters.

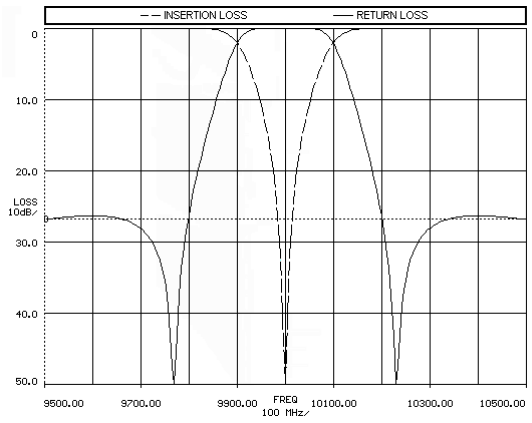

(c)

Figure 2.7 (continued) (c) Frequency Responses.

The stubs in these designs have unrealizable values as expected. But again these circuits can be realized using certain transformations and approximations.

In the following sections of this chapter, the realization ways for the distributed bandstop and lowpass filters with unrealizable element values are introduced and their performances with lossy resonators and under tuning are investigated. In all approaches, one example filter circuit with two resonators is given. Using this example circuit, performances of the topology is investigated. In all these circuits, resonator elements are mainly OC stubs. So tuning property is achieved by using the approximation in Figure 2.8, in which a capacitor is attached to the open end of OC stub and length of OC stub is shortened so that resonance frequency is adjusted to the initial value. When the capacitance of tuning capacitor C_p is changed, the resonance frequency of the element also changes. By tuning all the resonators center frequency of the filter is changed. The initial value of tuning capacitor for example circuits is chosen as 0.2pF or 0.5pF and is tuned between 0pF to 1pF. These capacitance values can be achieved by commercially available varactor diodes. For microwave frequencies (especially above 8GHz), Q of varactor diodes is very poor. In the following example circuits, loss of tuning capacitors are taken into account and Q of these capacitors is chosen as 50, which is in fact an optimistic value for practical implementations containing varactors in X-Band (8-12GHz).

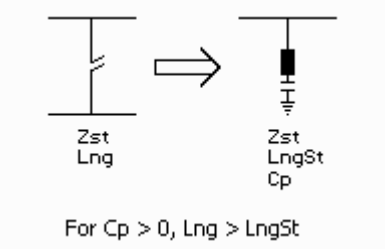

Figure 2.8 OC Stub to Capacitor Loaded OC Stub.

2.4.1 Distributed BSF with PCL scOS-L Resonators

In this approach, first a distributed bandstop filter with inverters is synthesized. Inverters are realized by quarter wavelength transmission lines (TL). TL + parallel SC-OC stubs in series arm pair is realized by parallel coupled line (PCL) configuration in which coupled and isolation ports are loaded with ground and an OC stub. The transformation is shown in Figure 2.9.

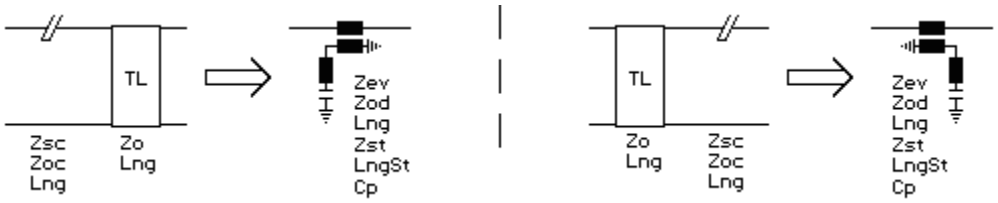

Figure 2.9 PCL scOS-L Resonator Transformation.

Using this equivalence, Z_{sc} and Z_{oc} stubs with very low impedances are transformed to a PCL configuration with realizable element values. In Figure 2.9, the resonators are the OC stub + tuning capacitor pairs connected to the isolation and coupled ports of the PCL. When $C_p = 0$, meaning only OC stub is connected as the resonator, this transformation is exact equivalent of the initial TL + parallel SC-OC stubs in series arm pair. Using Z_{sc}, Z_{oc}, Lng and Z_o parameters, all elements of equivalent PCL configuration except C_p are calculated. According to the chosen C_p, LngSt is shortened to give the initial resonant frequency.

In this approach, f_0 (notch center frequency) and f_q (quarter wavelength frequency) are specified independently, so nearest spurious frequency can be located away from $3f_0$, which is $3f_0$ when BSF is designed from LPF. The design steps are as follows:

1) The initial circuit (Figure 2.10) is synthesized using FILPRO By Prototype with Inverters with the following specifications:

By Prototype with Inverters	Distr, BSF, Cheby
Ripple (dB)	0.01
Passband Corners (MHz)	9800-10200
Proto. Degree	2
f_q (MHz)	20000

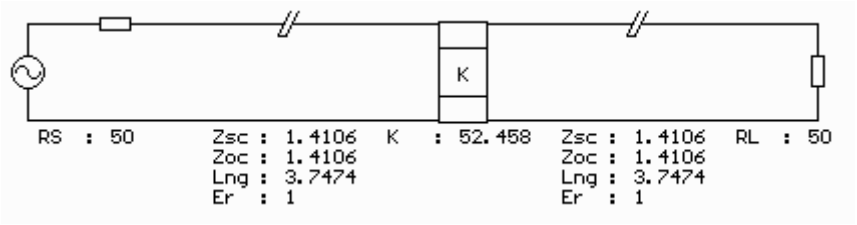

Figure 2.10 Initially Synthesized Circuit.

2) Redundant 50Ω TL pieces are inserted to input & output of the circuit

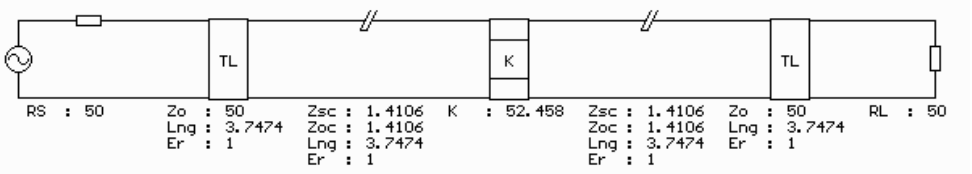

Figure 2.11 Redundant Element Insertion.

3) Inverter K is realized by quarter wavelength TL piece with $f_0 = f_q$

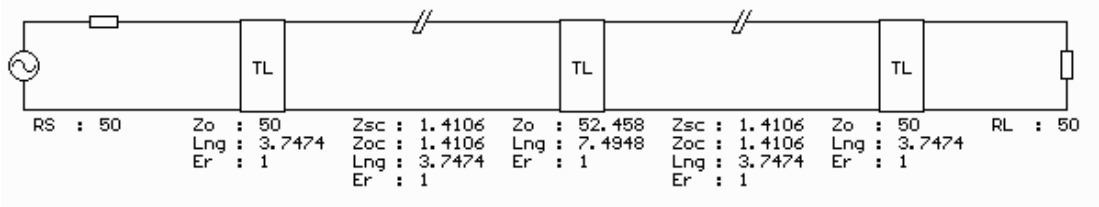

Figure 2.12 Inverter Realization.

4) Using transformation given in Figure 2.9, TL + parallel SC-OC stubs in series pairs are transformed to give components with realizable element values.

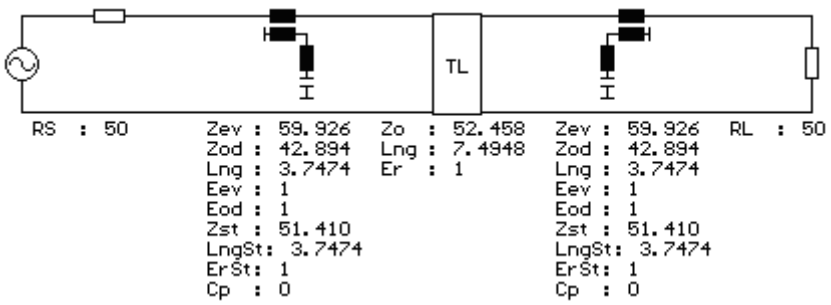

Figure 2.13 Final Circuit.

The frequency responses of the resultant circuit in Figure 2.13 are given in Figure 2.14.

Notch Property	Value
Notch Depth	-142.809dB
3dBc Stopband BW	120 MHz
20dBc Stopband BW	40 MHz
30dBc Stopband BW	20 MHz

(a)

Figure 2.14 Frequency Responses of Final Circuit. (a) Notch Characteristics.

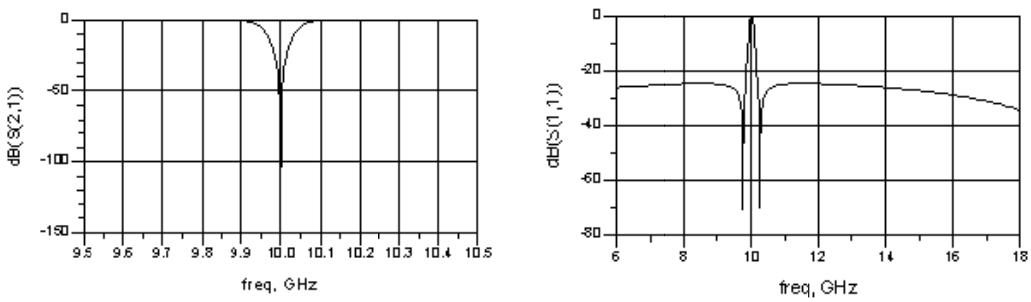

(b)

Figure 2.14 (continued) (b) Frequency Responses.

This topology is flexible for modifying some notch characteristics. By manually adjusting parameters Z_{ev} and Z_{od} of PCL, stopband bandwidth of the filter can be modified. Also, when Z_{st} is changed, center frequency changes but by adjusting LngSt it can be restored.

In Figure 2.13, C_p is zero. When C_p is taken as 0.2pF, length of the OC stub (LgnSt) should be decreased in order to adjust the center frequency of the notch filter back to initial resonance frequency. The frequency responses of this modified circuit when C_p = 0.2pF and for different values of C_p are given in Figure 2.15.

Notch Property	Value
Notch Depth	-121.194dB
3dBc Stopband BW	134 MHz
20dBc Stopband BW	40 MHz
30dBc Stopband BW	22 MHz

(a)

Figure 2.15 Frequency Responses of the Circuit During Tuning.
(a) Center Notch Characteristics.

Tuning Capacitor (C_p) Value (pF)	Center Frequency of Notch Filter (MHz)
0.05	13584
0.1	12032
0.2	10000
0.3	8720
0.4	7826

(b)

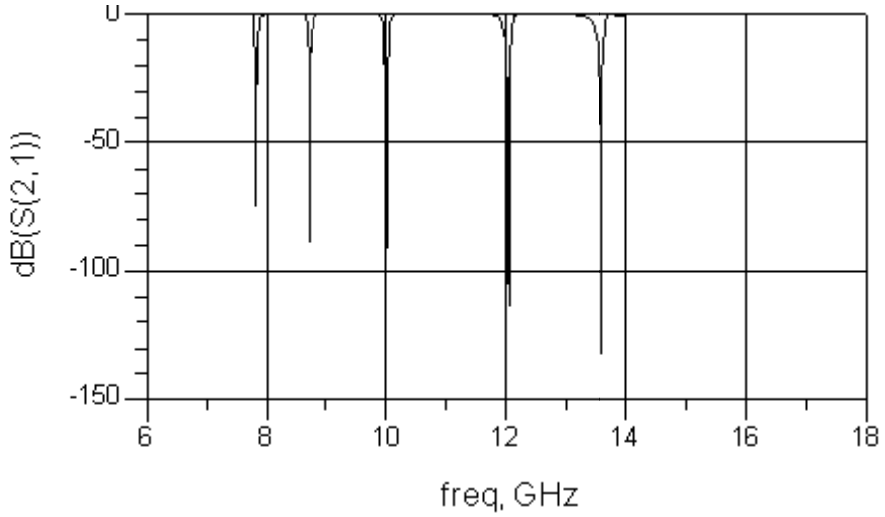

(c)

Figure 2.15 (continued) (b) Table of Results. (c) Tuning Responses.

The capacitance change of 0.05pF to 0.4pF moves the center frequency in a quite wide frequency range (~5.8GHz). For lossless case, the notch depths in tuned frequencies are very deep. But when losses of tuning capacitors are considered, notch depth is severely degraded. With the tuning capacitors of Q = 50, the notch depths for the values of C_p in Figure 2.15.c are given in Figure 2.16.

Tuning Capacitor (C_p) Value (pF)	Notch Depth (dB)	3dBc Stopband BW (MHz)
0.05	-28.534	320
0.1	-19.068	294
0.2	-11.168	244
0.3	-7.644	200
0.4	-5.717	162

(a)

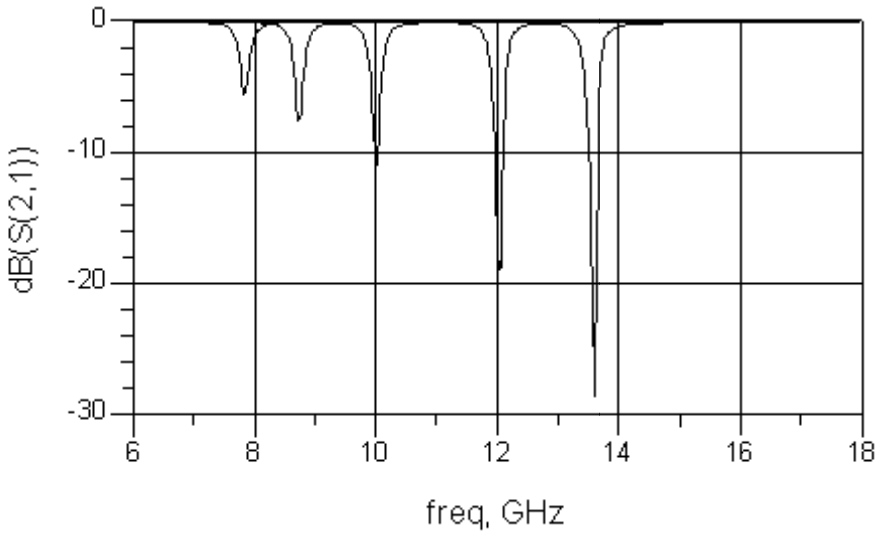

(b)

Figure 2.16 Frequency Responses of Lossy Circuit During Tuning.
(a) Table of Tuning Results. (b) Tuning Responses.

The effect of lossy resonators can be seen in two notch parameters. Firstly, notch depths at the initial center frequency and other tuned frequencies are severely degraded compared to lossless case and notch depths get very different values during tuning. Secondly, at the initial center frequency (10GHz), 3dBc stopband bandwidth (BW) is 134MHz (Figure 2.15.a) for lossless case and 244MHz (Figure 2.16.a) for lossy case. So stopband BW is also degraded and when the center frequency is tuned to a different frequency, stopband BW also changes considerably. This stopband BW increase gets even worse when the degree of the filter is increased. Hence, this filter topology suffers greatly from losses.

2.4.2 Distributed LPF with PCL L-Resonators

Distributed lowpass filters whose corner frequency is close to the quarter wavelength frequency f_q have a response of a notch filter around f_q. Since f_0 (notch center frequency) and f_q are equal to each other, nearest spurious frequency is located at $3f_0$. The design procedure begins with a distributed LPF design in FILPRO. But there are several ways to design a distributed LPF. With the tools By Built-in LC Prototypes and By Prototype with Inverters, the initial circuit can easily be synthesized in FILPRO. But instead of these redundant filter synthesis methods, the Synthesis tool of FILPRO can be used to design nonreduntant filters. So by Synthesis approach, the initial circuit in Figure 2.17 is synthesized with the following specifications.

By Synthesis	Distr, LPF, Cheby
Ripple (dB)	0.01
Passband Corner (MHz)	9800
Transmission Zeros	2 Ninf, 3 NUE
Degree	5
f_q (MHz)	10000

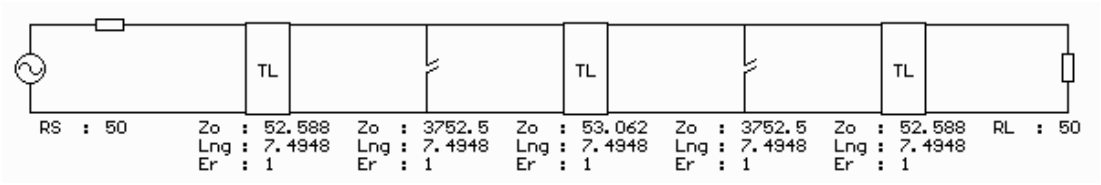

Figure 2.17 Initially Synthesized Circuit.

In Figure 2.17, OC stub impedances are extremely high. There are three ways to realize these high impedance stubs. First way is by using a PCL configuration similar to the one in the previous distributed BSF case. The other two ways are explained in the following sections. TL + OC stub in shunt pair can realized by parallel coupled line (PCL) configuration in which one of the coupled and isolation ports is loaded with an OC stub and the other port is remained open. The transformation is shown in Figure 2.18.

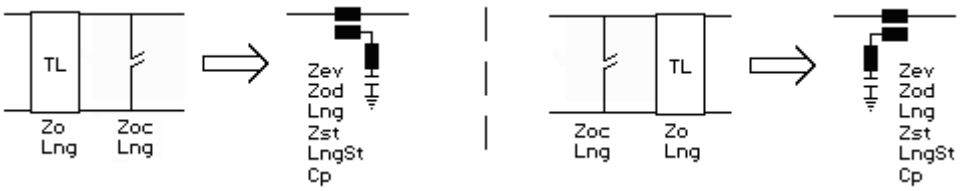

Figure 2.18 PCL L-Resonator Transformation.

Using this equivalence, shunt Z_{oc} stub with very high impedance is transformed to a PCL configuration with realizable element values. In Figure 2.18, the resonators are the OC stub + tuning capacitor pairs connected to the isolation and coupled ports of the PCL. When $C_p = 0$, meaning only OC stub is connected as the resonator, this transformation is exact equivalent of the initial TL + OC stub in shunt arm pair. Using Z_o, Lng and Z_{oc} parameters, all elements of equivalent PCL configuration except C_p are calculated according to a chosen Z_{ev} (or Z_{od}) or Z_{st} value. For different values of Z_{st}, different Z_{ev}, Z_{od} values are found and vice versa. Hence this transformation gives flexibility in specifying the parameters of PCL and the resonator OC stub. Once PCL and OC stub parameters are specified, according to the chosen C_p, LngSt is shortened to give the initial resonant frequency.

The design is completed by applying transformations in Figure 2.18 to the initial circuit in Figure 2.17. Z_{ev} is chosen as 62 Ω. The resultant circuit is in Figure 2.19.

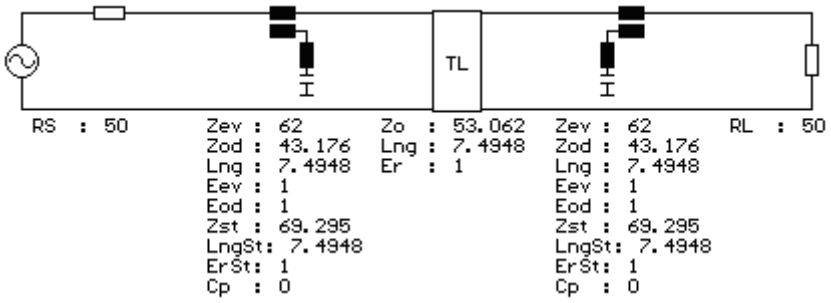

Figure 2.19 Final Circuit.

The frequency responses of the resultant circuit in Figure 2.19 are given in Figure 2.20.

Notch Property	Value
Notch Depth	-143.628dB
3dB Stopband BW	126 MHz
20dB Stopband BW	42 MHz
30dB Stopband BW	24 MHz

(a)

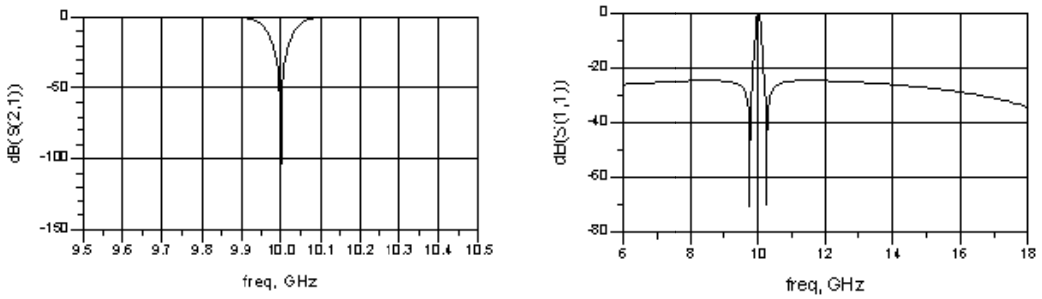

(b)

Figure 2.20 Frequency Responses of Final Circuit.
(a) Notch Characteristics. (b) Frequency Responses.

Similar to the previous BSF topology in 2.4.1, this topology is flexible for adjusting some parameters. By manually adjusting parameters Z_{ev} and Z_{od} of PCL, stopband bandwidth of the filter can be modified. Also, when Z_{st} is changed, center frequency changes but by adjusting LngSt it can be restored.

In Figure 2.19, C_p is zero. When C_p is taken as 0.5pF, length of the OC stub (LgnSt) should be decreased in order to adjust the center frequency of the notch filter back to the beginning value, which is 10 GHz. The frequency responses of this modified circuit when C_p = 0.5pF and for different values of C_p are given in Figure 2.21.

Notch Property	Value
Notch Depth	-144.714dB
3dB Stopband BW	134 MHz
20dB Stopband BW	40 MHz
30dB Stopband BW	22 MHz

(a)

Tuning Capacitor (C_p) Value (pF)	Center Frequency of Notch Filter (MHz)
0.1	13665
0.3	11090
0.5	10000
0.7	9402
0.9	9025

(b)

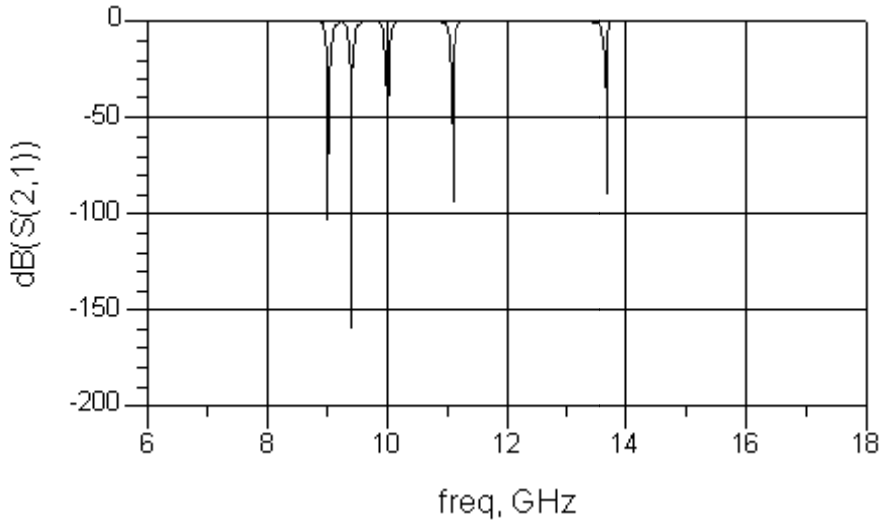

(c)

Figure 2.21 Frequency Responses of the Circuit During Tuning.
(a) Center Notch Characteristics. (b) Table of Tuning Results. (c) Tuning Responses.

The capacitance change of 0.1pF to 0.9pF moves the center frequency in a quite wide frequency range (~4.6GHz). For lossless case, the notch depths are very deep. But

when loss of tuning capacitor is considered, notch depth is severely degraded. With the tuning capacitors of Q = 50, the resultant frequency responses when C_p = 0.5pF and for different values of C_p are given in Figure 2.22.

Tuning Capacitor (C_p) Value (pF)	Notch Depth (dB)	3dB Stopband BW (MHz)
0.1	-18.034	210
0.3	-18.11	261
0.5	-19.721	263
0.7	-21.395	259
0.9	-22.986	254

(a)

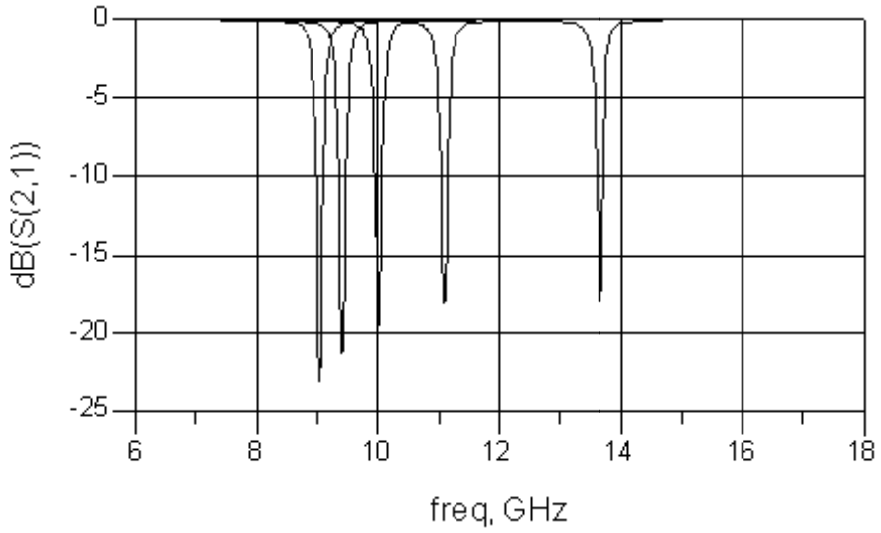

(b)

Figure 2.22 Frequency Responses of Lossy Circuit During Tuning.
(a) Table of Tuning Results. (b) Tuning Responses.

Notch depths are severely degraded by lossy resonators. But comparing to the previous BSF design, notch depths in tuned frequencies are close to each other. At the initial center frequency (10GHz), 3dBc stopband bandwidth (BW) is 134MHz

(Figure 2.21.a) for lossless case and 263MHz (Figure 2.22.a) for lossy case. So stopband BW is also degraded and when the center frequency is tuned to a different frequency, stopband BW also changes. But changes in stopband bandwidth are small considering the previous BSF design.

2.4.3 Distributed LPF with PCL Gap Coupled Resonators

A simple approach for realization of the very high impedance shunt OC stubs of narrowband BSF's is to use gap coupled stubs. In this case, a stub is coupled to the main line with a gap capacitance. This transformation is an approximation and gives good results around the center frequency. The approximation is shown in Figure 2.23.

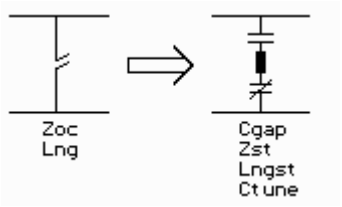

Figure 2.23 Gap Coupled Resonator Transformation.

In this transformation, C_{gap}, C_{tune} and Z_{st} parameters are specified and Lngst is calculated to preserve the resonance frequency. There is great flexibility in choosing parameters of the gap coupled resonators at the expense of great changes in stopband bandwidth and passband return loss responses. Therefore, some trials should be made to shape the desired response. C_{gap} is the primary parameter for stopband bandwidth and should be low (generally below 0.1pF) for narrow stopband bandwidth responses.

The design is completed by applying the approximation in Figure 2.23 to the initial circuit in Figure 2.17. After a few trials, C_{gap} is chosen as 0.045pF and Z_{st} is chosen

as 68 Ω to obtain close 3dBc bandwidth value with the example lossless design in previous PCL L-resonator case. The resultant circuit is in Figure 2.24.

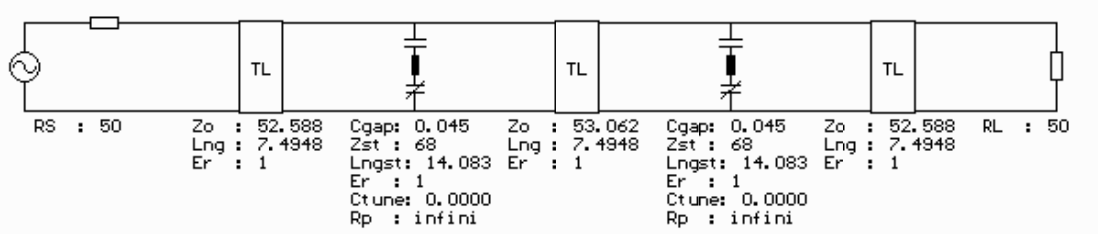

Figure 2.24 Final Circuit.

The frequency responses of the resultant circuit in Figure 2.24 are shown in Figure 2.25.

Notch Property	Value
Notch Depth	-98.088dB
3dB Stopband BW	125 MHz
20dB Stopband BW	41 MHz
30dB Stopband BW	23 MHz

(a)

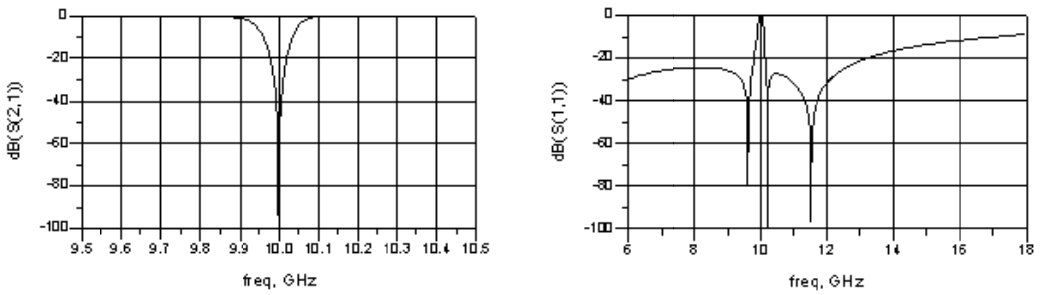

(b)

Figure 2.25 Frequency Responses of Final Circuit.
(a) Notch Characteristics. (b) Frequency Responses.

In Figure 2.25.b, it is seen that filter response starts to degrade after 13GHz. This is because gap coupled stub is an approximation for high impedance shunt OC stubs and gives good results only around the center frequency. Away from the center frequency in upper passband, spurious stopband starts to appear. Location of this spurious stopband depends on gap coupled stub parameters C_{gap}, Z_{st} and C_{tune}.

In Figure 2.24, C_{tune} is zero. When C_{tune} is taken as 0.5pF, length of the stub (LgnSt) should be decreased in order to adjust the center frequency of the notch filter back to the beginning value. Frequency responses of the modified circuit when C_{tune} = 0.5pF and for different values of C_{tune} are given in Figure 2.26.

Notch Property	Value
Notch Depth	-93.935dB
3dB Stopband BW	164 MHz
20dB Stopband BW	53 MHz
30dB Stopband BW	30 MHz

(a)

Tuning Capacitor (C_p) Value (pF)	Center Frequency of Notch Filter (MHz)
0.1	13110
0.3	10910
0.5	10000
0.7	9504
0.9	9192

(b)

Figure 2.26 Frequency Responses of the Circuit During Tuning.
(a) Center Notch Characteristics. (b) Table of Tuning Results.

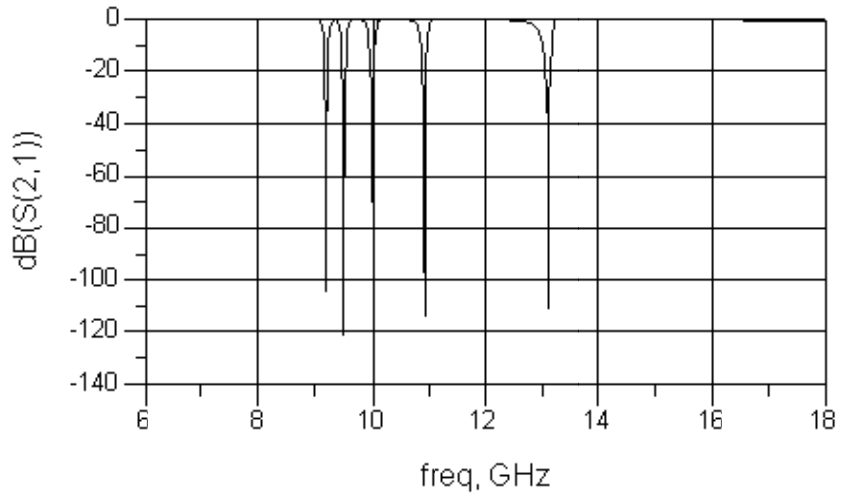

(c)

Figure 2.26 (continued) (c) Tuning Responses.

The capacitance change of 0.1pF to 0.9pF moves the center frequency in a quite wide frequency range (~3.9GHz) close to the frequency range of the previous LPF design. For lossless case, the notch depths are very deep. But when loss of tuning capacitor is considered, notch depth is severely degraded. With the tuning capacitors of Q = 50, the resultant frequency responses when C_{tune} = 0.5pF and for different values of C_{tune} are given in Figure 2.27.

Tuning Capacitor (C_p) Value (pF)	Notch Depth (dB)	3dB Stopband BW (MHz)
0.1	-29.734	384
0.3	-21.735	279
0.5	-21.194	240
0.7	-21.883	218
0.9	-22.916	203

(a)

Figure 2.27 Frequency Responses of Lossy Circuit During Tuning.
(a) Table of Tuning Results.

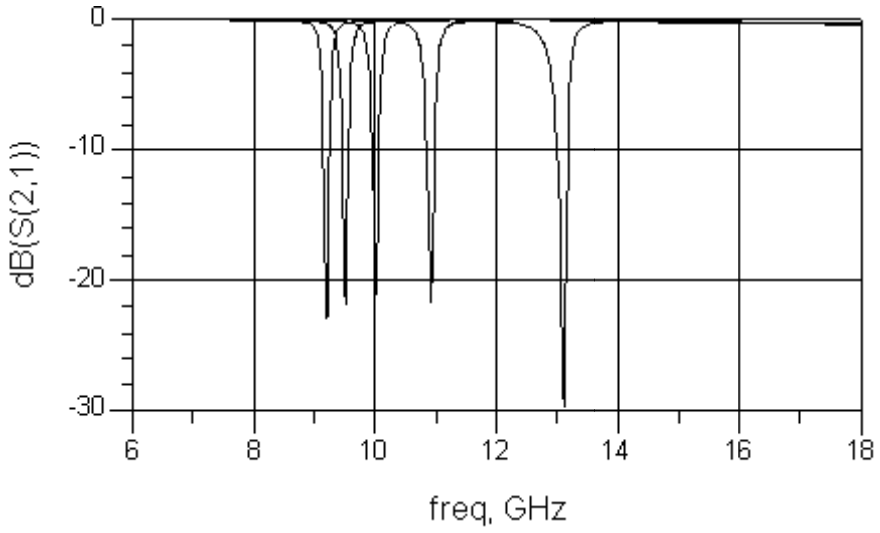

(b)

Figure 2.27 (continued) (b) Tuning Responses.

As in previous designs, notch depths are severely degraded compared to lossless case. However similar to the previous LPF design, notch depths in tuned frequencies are close to each other. At the initial center frequency (10GHz), 3dBc stopband bandwidth (BW) is 164 MHz (Figure 2.26.a) for lossless case and 240 MHz (Figure 2.27.a) for lossy case. So stopband BW is also degraded and when the center frequency is tuned to a different frequency, stopband BW also changes. As in the first BSF design, changes in stopband bandwidth are high.

2.4.4 Distributed BSF/LPF with Off-Line Resonators

An off-line resonator is either a lumped element parallel LC resonator or parallel combination of OC and SC stubs coupled to the main line through an inverter. The OC stub may also be a lumped capacitor. Figure 2.28 shows an off-line resonator in between two TL pieces.

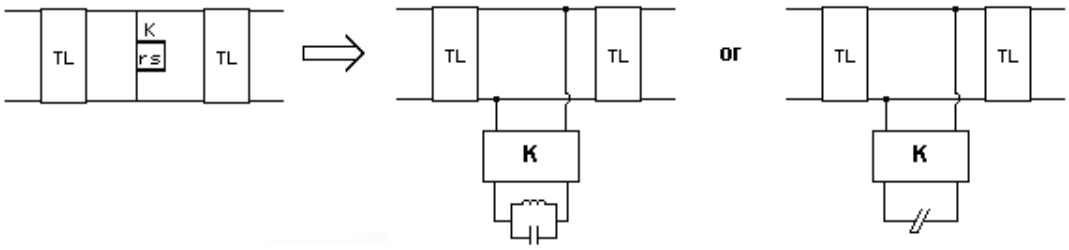

Figure 2.28 Off-Line Resonator Transformations.

Off-line resonators may be used to convert the series resonators in shunt arms with unrealizable element values into parallel resonators in shunt arm with realizable element values. The element value adjustment is possible by assigning proper impedance to the inverters. The inverters may then be converted into proper forms consistent with the topology of the circuit and type of the elements. Due to inverter realization this transformation is an approximation and gives good results around the center frequency only. Off-line resonator conversions are shown in Figure 2.29.

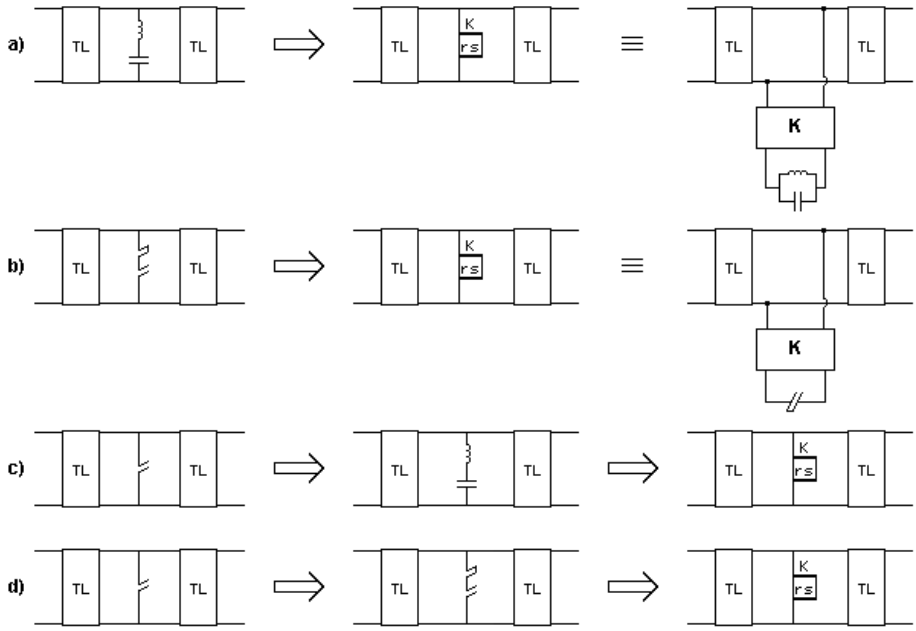

Figure 2.29 Off-Line Resonator Conversions.

Note that both series resonator formed by a SC and OC stub in shunt arm (Figure 2.29.b) and a shunt OC stub (Figure 2.29.c,d) can be transformed to off-line resonators. So this method can be used in realization of both distributed BSF designs (Figure 2.10) and distributed LPF designs (Figure 2.17). However since only shunt arm elements can be converted to off-line resonators, dual of the circuit in BSF design in Figure 2.10 (with series SC and OC stubs in shunt arm) should be used.

As an example design consider the dual of the circuit in Figure 2.10, which is shown in Figure 2.30.

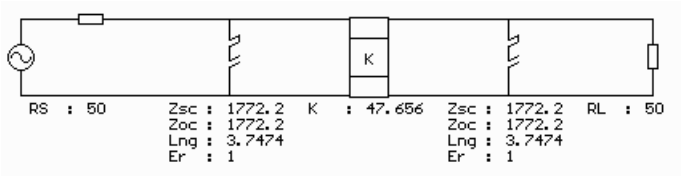

Figure 2.30 Initial Circuit.

The resonator stubs can be converted into tee-resonators which is a special case of off-line resonators in which the inverter is converted into a quarter wavelength TL with a desired impedance. Choosing the off-line resonator inverter impedance as 120Ω, the circuit in Figure 2.30 is converted to the following circuit in Figure 2.31 with tee-resonators.

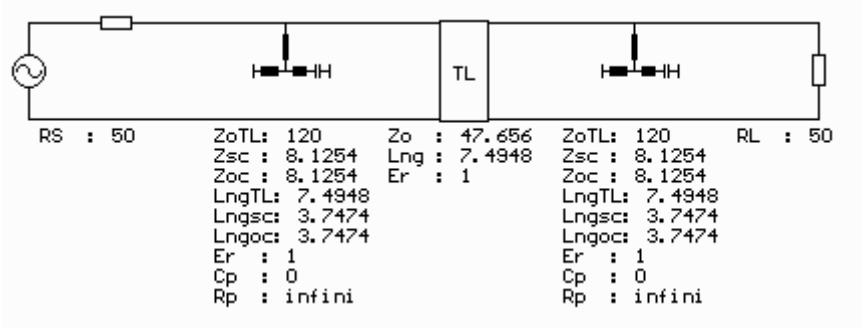

Figure 2.31 Final Circuit.

In Figure 2.31, SC and OC stubs in parallel are connected to the main line with a quarter wavelength TL piece which acts as inverter. When impedance of the quarter wavelength TL piece is 120Ω which is a high value considering practically realizable values, the impedance of SC and OC stubs in parallel are very low. As impedance of quarter wavelength TL piece increases, impedance of these stubs also increases. But in this case impedance of quarter wavelength TL may exceed the realizable values. For better impedance values, stopband bandwidth of the filter should be increased, which is usually not desired for a notch filter.

The frequency responses of the resultant circuit are shown in Figure 2.32.

Notch Property	Value
Notch Depth	-143.064dB
3dB Stopband BW	128 MHz
20dB Stopband BW	40 MHz
30dB Stopband BW	22 MHz

(a)

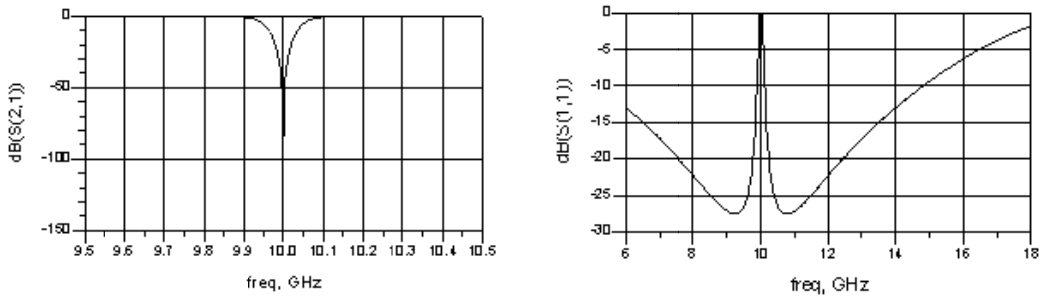

(b)

Figure 2.32 Frequency Responses of Final Circuit.
(a) Notch Characteristics. (b) Frequency Responses.

In Figure 2.32.b, it is seen that filter response starts to degrade outside the frequency range 8GHz and 12GHz. This is because tee-resonator is an approximation for high

impedance shunt OC stubs and gives good results only around the center frequency. Away from the center frequency, both lower and upper passband starts to decline.

The center frequency can be tuned by connecting a capacitor to the OC stubs of the tee-resonators and shortening the lengths of the OC stubs to accommodate a tuning capacitor. In Figure 2.31, C_{tune} is zero. When C_{tune} is taken as 0.5pF, length of the stub (LgnSt) should be decreased in order to adjust the center frequency of the notch filter back to the beginning value, which is 10 GHz. The modified circuit, its frequency responses when C_{tune} = 0.5pF and for different values of C_{tune} are given in Figure 2.33.

Notch Property	Value
Notch Depth	-149.903dB
3dB Stopband BW	164 MHz
20dB Stopband BW	53 MHz
30dB Stopband BW	22 MHz

(a)

Tuning Capacitor (C_p) Value (pF)	Center Frequency of Notch Filter (MHz)
0.1	11383
0.3	10641
0.5	10000
0.7	9447
0.9	8968

(b)

Figure 2.33 Frequency Responses of the Circuit During Tuning.
(a) Center Notch Characteristics. (b) Table of Tuning Results.

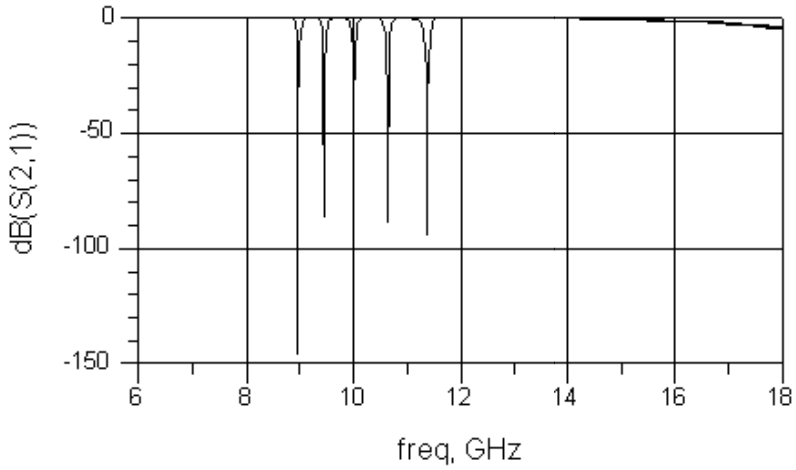

(c)

Figure 2.33 (continued) (c) Tuning Responses.

The capacitance change of 0.1pF to 0.9pF moves the center frequency in a wide frequency range (~2.4GHz) narrower than the frequency range of the previous designs. For lossless case, the notch depths are very deep. But when loss of tuning capacitor is considered, notch depth is severely degraded. With the tuning capacitors of Q = 50, the resultant frequency responses when C_{tune} = 0.5pF and for different values of C_{tune} are given in Figure 2.34.

Tuning Capacitor (C_p) Value (pF)	Notch Depth (dB)	3dB Stopband BW (MHz)
0.1	-45.289	208
0.3	-26.494	201
0.5	-18.723	197
0.7	-14.354	192
0.9	-11.625	188

(a)
Figure 2.34 Frequency Responses of Lossy Circuit During Tuning.
(a) Table of Tuning Results.

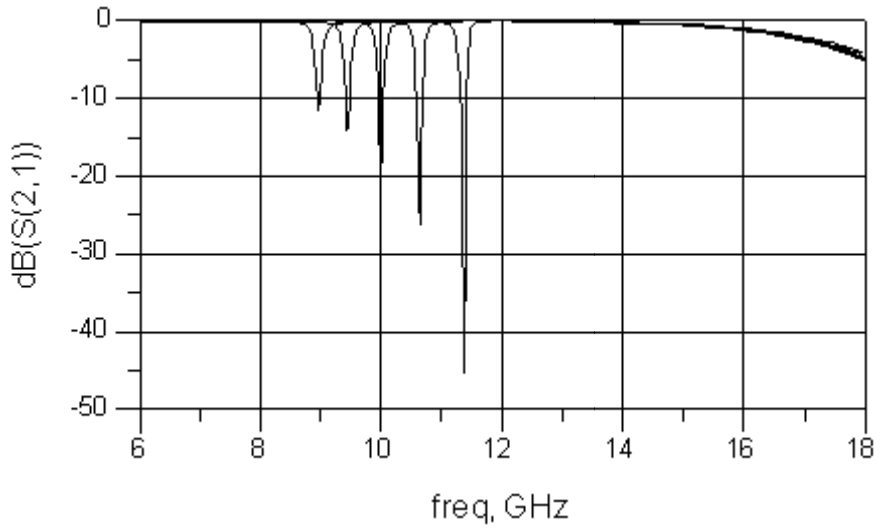

(b)

Figure 2.34 (continued) (b) Tuning Responses.

Similar to the first BSF design, notch depths in tuned frequencies differs too much. At the initial center frequency (10GHz), 3dBc stopband bandwidth (BW) is 164MHz (Figure 2.33.a) for lossless case and 197MHz (Figure 2.34.a) for lossy case. So stopband BW is also degraded but considering the previous designs this filter has the minimum stopband BW degradation. When the center frequency is tuned to a different frequency, stopband BW also changes. But this change is very small compared to the other designs.

2.5 Comparisons / Comments on Direct Bandstop Filters

To sum up, using distributed filter design approach, there are 4 ways to design a narrowband bandstop filter (or notch filter). Based on the frequency responses of example designs, the following results are observed:

- In all these designs, when lossless resonators are used, notch depths are very deep not only at center frequency, but also in other tuned frequencies. When a fixed-Q lossy capacitor is used, notch depths in all designs are severely degraded. This is the main disadvantage of these topologies. In order to increase notch depth performances, either high Q resonators should be used,

which may not be possible in practice for microwave frequencies, or degree of the filter should be increased. The increase in degree of the filter increases the notch depth, but also increases stopband bandwidth and average insertion loss, which are not desired.

- In all these designs, notch depths differ in other tuned frequencies. These differences can be very severe as in the designs given in sections 2.4.1 and 2.4.4. This is also a disadvantage since when the degree of these filters are increased for deeper notches, notch depth differences during tuning of center frequency also increase further.

- In all these designs, the stopband bandwidths (3dBc, 20dBc, 30dBc) change by tuning the center frequency. This change is small for 2.4.2 and 2.4.4 and high for 2.4.1 and 2.4.3 when fixed-Q lossy capacitors are used.

- In the first two methods in 2.4.1 and 2.4.2, exact transformation techniques are used. So the filters designed with these methods have a wide upper passband bandwidth. But in the last two methods, approximations are used. Hence their performances are good around center frequency but distorted away from the center frequency.

- The tuning range of the filter in 2.4.1 is the maximum among all designs even for less capacitance tuning range (0.05pF-0.4pF) and the tuning range of 2.4.4 is the minimum one.

- The element values of the example filter in section 2.4.4 are still not realizable in practice because of very low stub impedances. The impedance of stubs can be increased by increasing the impedance of quarter wavelength TL piece but this time impedance of quarter wavelength TL gets too high value. So only if the stopband bandwidth of the filter is increased, then realizable values of this filter can be achieved which is not desired for a narrowband notch filter.

2.6 Remarks

In this chapter, after a brief introduction of bandstop and notch filters, direct narrowband bandstop filter synthesis methods (lumped and distributed) are introduced. 2^{nd} order example filters are designed and frequency responses under lossless and lossy conditions are presented. The main point of this chapter is to demonstrate that design of notch filters from direct bandstop filters does not give satisfactory results. Even only tuning capacitor loss is considered (all the other elements are assumed lossless), the notch depths are very poor. Higher degree filters can be used to increase notch depth but this also increases stopband bandwidth and average passband insertion loss. Also notch depth differences in different tuned frequencies may limit the tuning range. In the following two chapters, methods to increase the poor performances of these direct bandstop filters are introduced.

CHAPTER 3

PHASE CANCELLATION APPROACH

3.1 Phase Cancellation

Rejection levels of narrowband bandstop/notch filters are severely limited by the losses of the resonators. Therefore when high rejection is needed either degree of the filter need be increased or special precautions are taken to improve rejection levels. For the latter case, an effective way of improving rejection levels is the amplitude balanced phase cancellation approach. In this approach, one or more extra paths are introduced between input and output ports in parallel with the main filter and the signals are enforced to cancel each other at the output port by proper adjustment of amplitudes and phases [11]. By this way, very deep notches can be achieved at a specific center frequency with low order main filter regardless of resonator losses. This approach is shown in Figure 3.1.

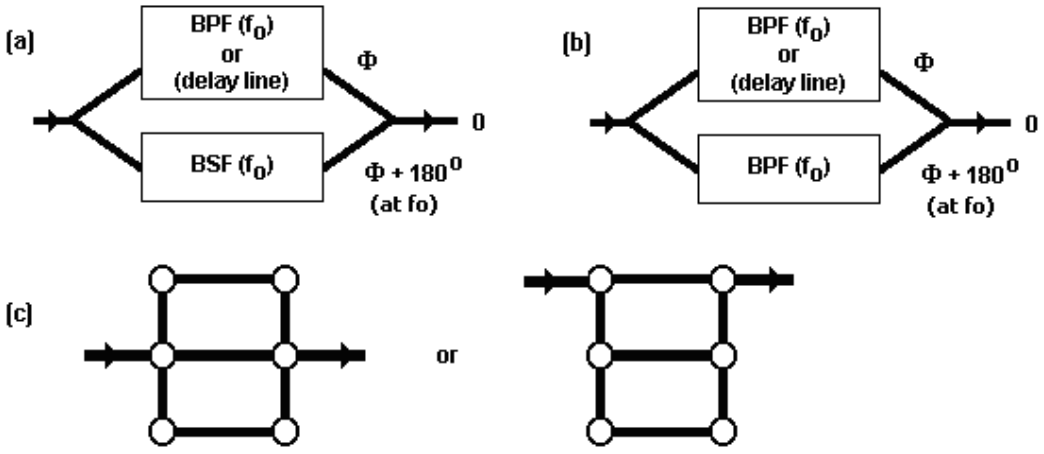

Figure 3.1 Bandstop Filtering by Phase Cancellation.
(a) Bandstop Main Filter. (b) Bandpass Main Filter.
(c) More than Two Paths.

The main filter can be a bandstop filter (BSF) (Figure 3.1.a) or a bandpass filter (BPF) (Figure 3.1.b) and the bridge can be a BPF or a simple phase shifting delay line. If the signals at the output of the paths can be made equal in amplitude with 180^0 phase difference then they will cancel each other when combined. More than two paths can also be used as shown in Figure 3.1.c and d.

When the main filter is a narrowband BSF, the input signal is already rejected by a certain level around the center frequency. However the rejection level is not satisfactory for most cases. In order to increase the rejection level, one can get a small sample of the input signal and add that sample to the output signal of the BSF filter. If amplitudes of both signals are equal at the output and have 180^0 phase shift, then a deep notch is obtained. This approach is shown in Figure 3.2.

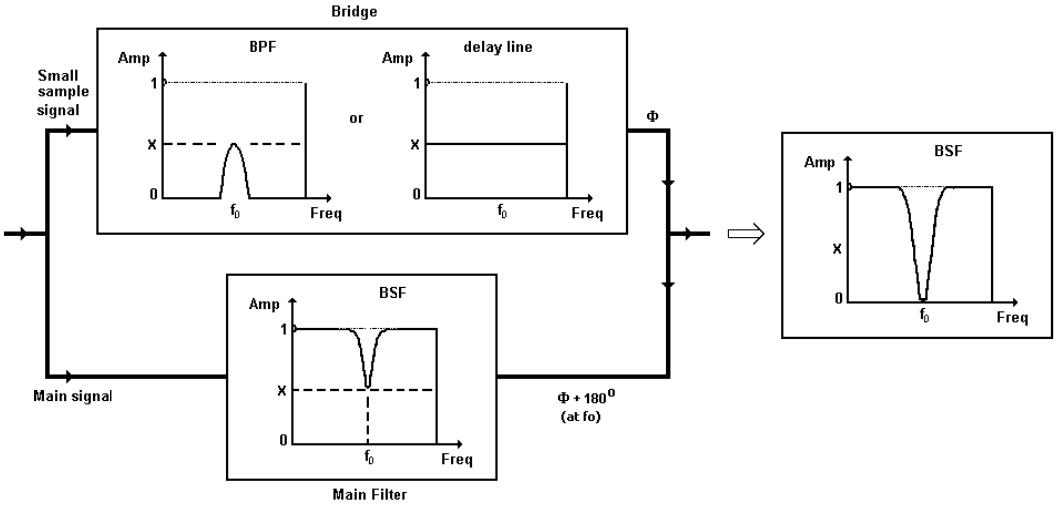

Figure 3.2 Phase Cancellation Approach When Main Filter is a BSF.

In Figure 3.2, the main filter and the bridge attenuates the input signal by X value at the center frequency f_0. When a signal with a frequency away from f_0 passes through this structure, since attenuation at the bridge is much higher than the main bandstop filter, most of the signal passes through the main filter. However, when a signal around center frequency passes through the structure, a sample signal close to half of

the input signal (exactly half of the input signal at f_0) passes through the bridge and since the phases of bridge and main signals are close to opposite (exactly opposite at f_0), the output signal becomes very low (0 at f_0). The resultant notch characteristic of this structure is better when a narrowband BPF is used in the bridge. This is because narrowband BPF allows signals only around the center frequency and attenuation increases quickly when frequency is away from the center frequency so the input signal only passes through BSF away from the center frequency. However, the passband loss of this BPF should be equal to the notch depth of BSF at f_0. Also for tunable notches, bridge BPF should also be tunable. Because of the difficulties of a narrowband and tunable BPF design with a desired extra passband loss, especially at high frequencies like X-Band, BPF filter is not preferred for the bridge. Instead a simple phase shifting transmission line piece can also be used for the bridge with impedance which gives passband loss equal to the notch depth of main filter. In this case, small amount of input signal always passes through the bridge. Hence average passband loss of the overall structure is higher than the case when BPF bridge is used and also return loss performance is poorer. If the notch depth of main BS filter is very low (ex. 3dB), then impedance of the delay line gets closer to the system impedance. In this case the signal flowing through the bridge increases, average passband loss increases and proper notch characteristics can not be obtained. Hence when a delay line is used as the bridge path, the main filter notch depth should not be too low. As notch depth of BSF increases, the small sample signal passing through the delay line bridge decreases and so passband response of the overall structure approaches to passband response of main filter. Also return loss response in passband gets closer to the return loss response of main filter. But as the notch depth of BSF increases, the impedance of delay line should also be increased further which can get unrealizable values. In fact direct connection of delay line to input and output of a BSF is limited due to either poor filter performances or unrealizable delay line impedances. In order to overcome the problems when a directly connected delay line is used, parallel coupled line splitters and combiners can be used. Also there are branch line like topologies which creates notches due to phase cancellation. Details of bridged BSF approaches will be introduced in section 3.3.

When the main filter is a narrowband BPF, main flow path of the input signals outside the passband is not the main filter because of mismatch. Instead the input

signal passes through the bridge, which can be a simple phase shifting transmission line piece or a wideband bandpass filter. This is because the main filter only allows the input signal to pass around the center frequency. In this case, around the center frequency, a signal close to the half of the input signal (exactly half of the input signal at f_0) passes through the bridge and the rest of it passes through the main narrowband BPF filter. Since the amplitudes of both paths are close to each other (equal at f_0) and phases are close to opposite of each other (exactly opposite at f_0), the output signal becomes very low (0 at f_0). This approach is shown in Figure 3.3.

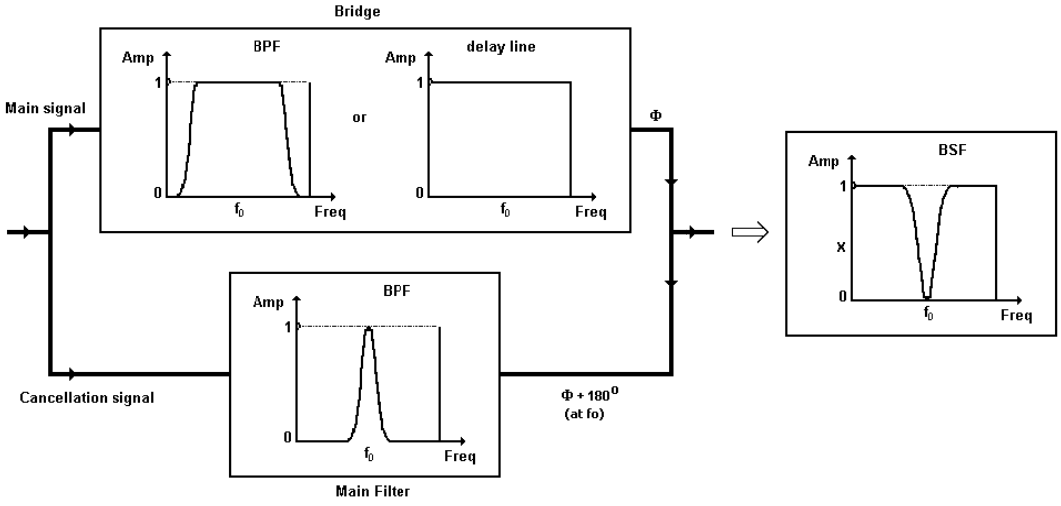

Figure 3.3 Phase Cancellation Approach When Main Filter is a BPF.

When a wideband bandpass filter is used as the bridge, operating frequency range of the system is limited to the passband of the wideband BPF, which is mostly not desired. Wideband BPF bridge also increases the complexity of the overall structure. So when the main filter is a narrowband BPF, the bridge always becomes a delay line. At passband, the input signal passes through the bridge. So when a delay line is used, the impedance of the line should be around the system impedance (50Ω normally). At stopband, the input signal passes through both paths nearly equally. So 3dB power division and combining occurs at input and output of the structure around

center frequency. There are various ways to implement this approach. The details of these ways are introduced in section 3.4.

The amplitude balanced phase cancellation approach works perfectly for designing notch filters with fixed center frequency. This approach also produce tunable notch filters with better notch depths than direct bandstop methods given in Chapter 2. However the tuning ranges of all phase cancellation methods are limited because of the phase and amplitude differences occurring when frequency gets away from the center frequency. The tuning is achieved by only tuning of main filter in almost all cases. This is because the bridge is almost always a delay line or a combination of transmission lines and PCL's which have no tunable elements. When a BSF or a BPF is tuned by using its resonators, its notch depth or passband loss also changes so that the amplitudes at the outputs of both paths are not exactly equivalent any more. Moreover, as the center frequency changes, the phase differences are no more exactly opposite of each other. As a result, as the notch frequency is tuned away from the initial center frequency, proper amplitude balanced phase cancellation does not occur and notch depths decreases. This limits the frequency tuning range of phase cancellation approaches.

3.2 Bridged Topologies with Bandstop Main Filter

The phase cancellation approach can be easily applied to any bandstop filter topology. Some low order notch filter topologies are given in Figure 3.4.

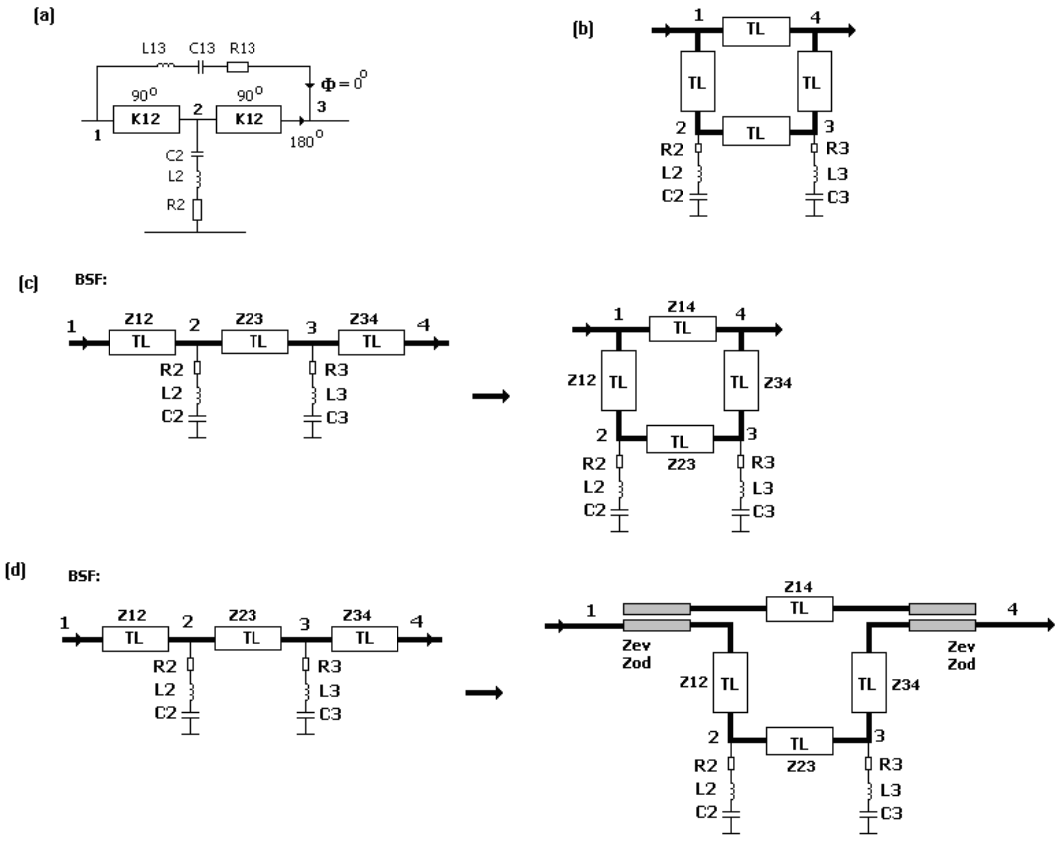

Figure 3.4 Low Order BSF Topologies.
(a) Lumped BS Bridged-Tee. (b) BLC with BS Resonators.
(c) Delay Line Bridged BSF. (d) PCL S/C Bridged BSF.

Figure 3.4.a shows a simple bridged BSF which is composed of single lumped BS resonator, inverters and a bridging BP resonator. The simplest way for bridge path is to connect a delay line in parallel with the main BSF filter as shown in Figure 3.4.c. In this case, power is split and combined using Tee junctions. Another way of bridging is to connect the delay line to BSF by using a PCL splitter/combiner as shown in Figure 3.4.d. In this case, power is split and combined using PCL's. There is also another design method that inherently using phase cancellation which is called as branch line coupler (BLC) two resonator notch filter as shown in Figure 3.4.b. The details of all these are introduced in the following subsections.

3.2.1 Lumped BS Bridge Tee with Inverters

In order to get some insight on limitations of stopband rejection level and improvement of rejection level by phase cancellation approach, a simple lumped element notch filter with single shunt BS resonator can be used as shown in Figure 3.4.a. Main limitation on the stopband rejection levels of BSF's come from the finite Q of the resonators. In order to increase rejection level the degree of BSF need be increased. However when a low degree BSF is to be used then one way to get around low Q problem is to use a delay line or a BPF as bridging element of the BSF.

The simplest version of this structure is formed by a degree one BSF bridged by a degree one BPF as shown in Figure 3.5.

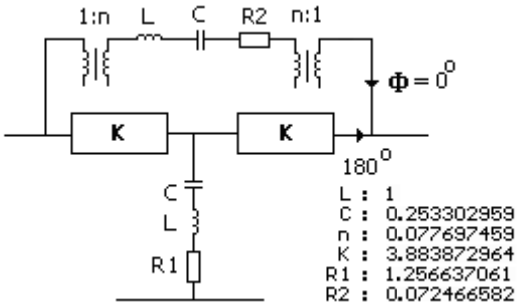

(a)

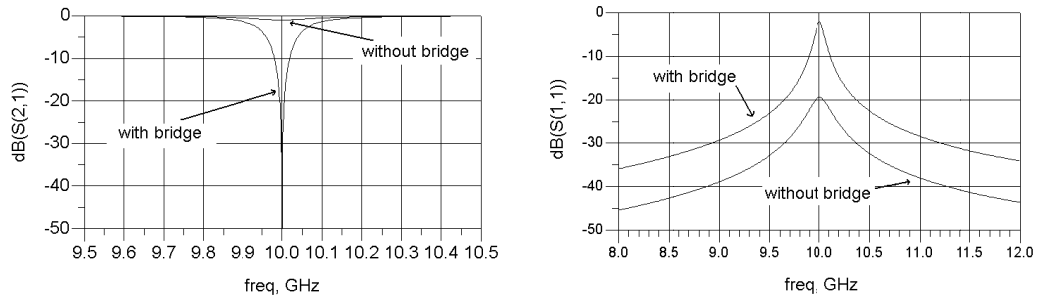

(b)

Figure 3.5 Lumped BS Bridged Tee.
(a) Circuit. (b) Frequency Responses.

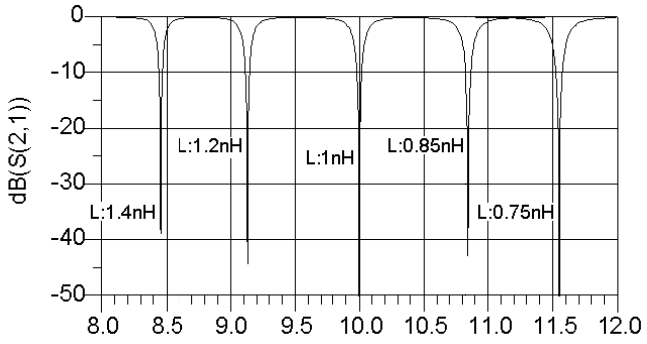

(c)

Figure 3.5 (continued) (c) Tuning Responses.

The BSF is formed by a shunt arm series RLC resonator in between two inverters which are used to scale the resonator elements. Each inverter provide 90^0 phase shift so that in total 180^0 phase shift is provided. The resistor R1 represent the resistance of the bandstop LC resonator, whose value is constant and equal to the resistance when Q=50 at 10GHz. In Figure 3.5.a, the bridging arm is a single series resonator forming a BPF with passband center at the same center frequency as the BSF. In this structure, delay line bridge can not be used since notch depth of the main BSF is too low (around -1 dB). The bridging arm L and C are made identical to the shunt resonator element by introducing transformers of turns ratio n. The bridge provides 0^0 phase shift. Amplitude equalization is carried out by adjusting the bridge resistor R2. The bridging elements become effective only when lossy resonators are used. Thus a high Q notch filter action is obtained by using lossy resonators.

In Figure 3.5.b, it is seen that using two resonators, very deep notches can be obtained even with low Q resonators. Also when the resonators are tuned, high notch depths are observed over a wide range (Figure 3.5.c). The transformers in the bridge path and the element values of the lumped BS bridge tee filters are not realizable because of narrowband resonator components. Instead of lumped filters, distributed direct bandstop filters given in Chapter 2 can be used as the main BS filter.

3.2.2 Delay Line Bridging with BSFs

This is the most primitive form of bridging. The delay line is directly connected to input and output ports of a BSF as shown in Figure 3.4.c. Consider the distributed LPF with PCL L-resonator bandstop filter topology in section 2.4.2. Using the same circuit with capacitors having Q factor of 50 in Figure 2.19, the addition of delay line creates a deep notch as shown in Figure 3.6.

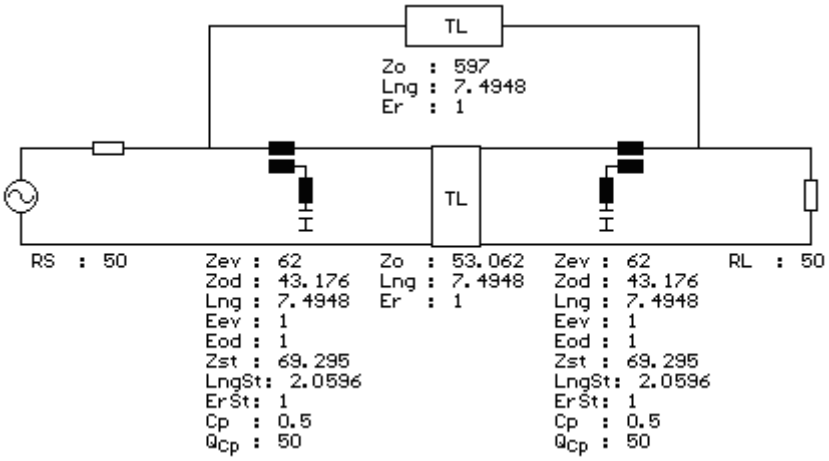

(a)

Notch Property	Value
Notch Depth	-55.655dB
Average PB Insertion Loss	0.25dB
3dBc Stopband BW	261 MHz
20dBc Stopband BW	42 MHz
30dBc Stopband BW	12 MHz

(b)

Figure 3.6 Delay Line Bridged BSF with Q of 50.
(a) Circuit. (b) Notch Characteristics.

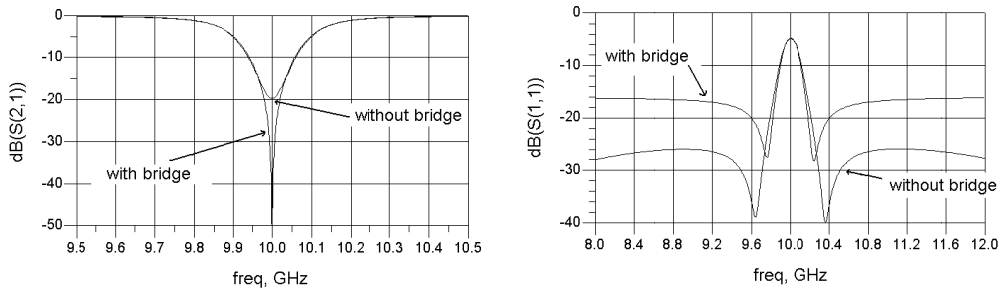

(c)

Figure 3.6 (continued) (c) Frequency Responses.

The impedance of the delay line is found by manual optimization using the EDA tool ADS. Exact theoretical calculations can be found, but due to their complexity manual trials are preferred. Addition of the bridge improves notch depth by approximately 35dB. The notch depth of the main BSF filter is around 20dB which is a very high value for proper impedance values of bridging delay lines. Hence the impedance of the delay line (597Ω) becomes unrealizable. Outside the stopband, insertion loss responses of both filters are close to each other. This is because impedance of the delay line is too high (597Ω) so that very weak signal passes through the bridge. However, return loss of the bridged circuit in passband is decreased to about 10dB, which is a serious distortion compared to non-bridged case. Note that in the example filters with lossy resonators given in Chapter 2, average passband insertion loss parameter is not given since it has a very small value (smaller than 0.1dB) so neglected. However in bridged filters average passband insertion loss can not be neglected. In this example, passband insertion loss changes around 0.25dB outside the stopband. In bridged BSF filters, delay line impedance is very effective over passband insertion loss besides circuit losses.

Consider the case when Q of the capacitors has less value. In this case, the notch depth of the main filter BSF decreases, so impedance of the delay line also decreases. For Q = 20, the following notch responses are obtained as shown in Figure 3.7.

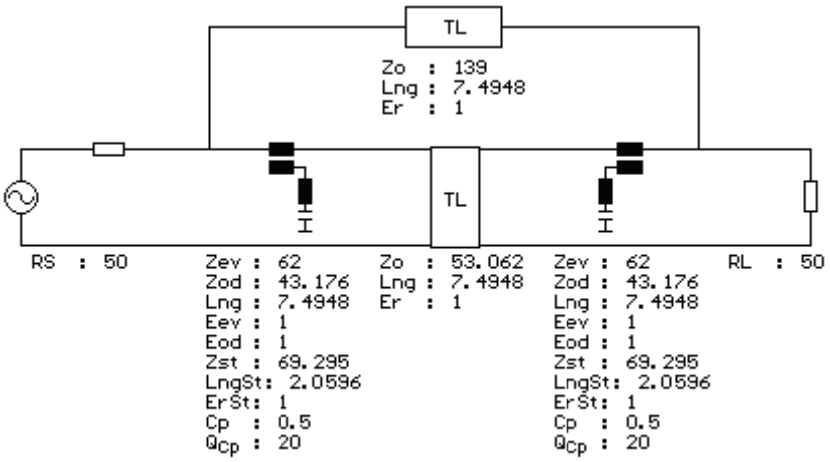

(a)

Notch Property	Value
Notch Depth	-58.240dB
Average PB Insertion Loss	1.4dB
3dBc Stopband BW	345 MHz
20dBc Stopband BW	40 MHz
30dBc Stopband BW	12 MHz

(b)

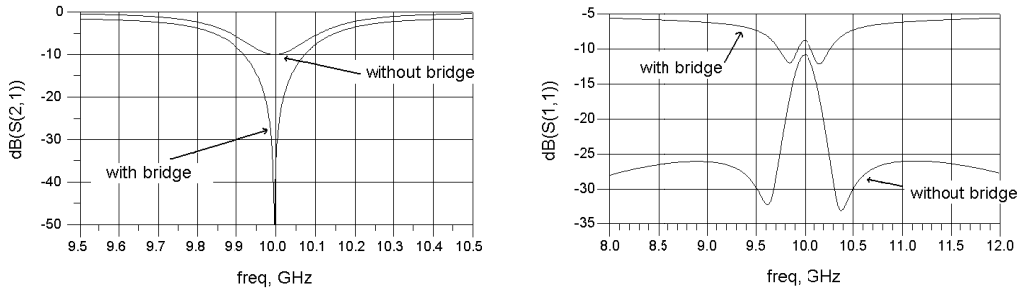

(c)

Figure 3.7 Delay Line Bridged BSF with Q of 20.
(a) Circuit. (b) Notch Characteristics. (c) Frequency Responses.

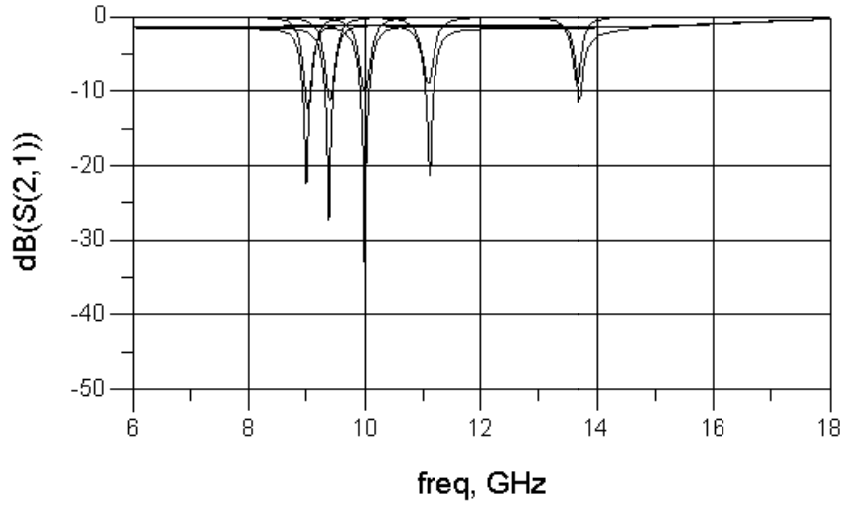

(d)

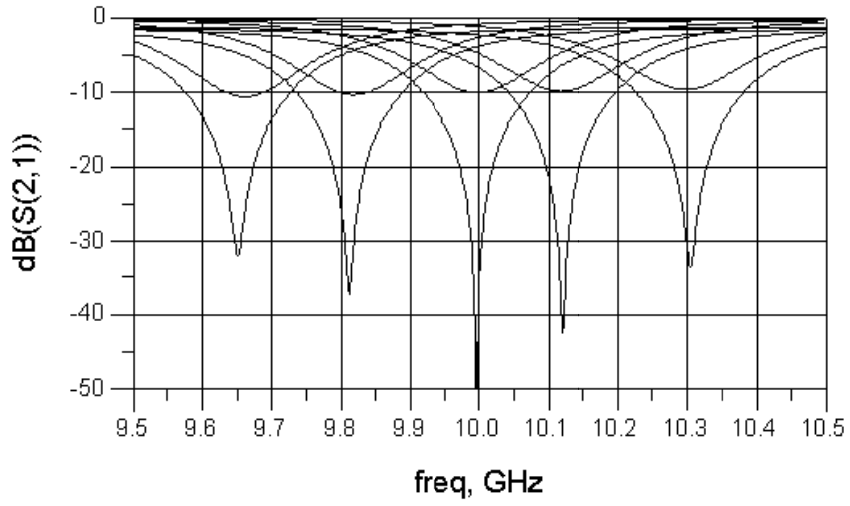

(e)

Figure 3.7 (continued)
(d) Wideband Tuning Responses. (e) Narrowband Tuning Responses.

Again impedance of the delay line is found by manual optimization and the center frequency of the filter is slightly shifted due to the reason explained in the previous note. Addition of the bridge improves notch depth by approximately 48dB. The frequency responses of both filters are not close to each other as in the previous case. This is because impedance of the delay line is now not very high (139Ω) relative to the system impedance (50Ω) so that a relatively strong signal always passes through the bridge. This increases the insertion loss and decreases the return loss of the bridged circuit outside the stopband as shown in Figure 3.7.c Average passband

insertion loss is considerably high compared to the previous case. Return loss of the passband also severely distorted, which is close to 5dB outside the stopband. This return loss level is not a satisfactory value in practice. When the capacitor values are tuned as in Chapter 2.4.2 (0.1pF, 0.3pF, 0.5pF, 0.7p.F, 0.9p.F), the results of both bridged and non-bridged filters are shown in Figure 3.7.d. The notch depths of all bridged filters are deeper than the non-bridged filters. But for the bridged filters notch depth quickly decreases below 30dB as capacitor value moves away from the initial center frequency. This is because of the amplitude variations and deviations from opposite phase occurring when the center frequency is changed. When the tuning capacitor values are chosen in a narrower range as 0.43pF, 0.47pF, 0.5pF, 0.55pF and 0.6pF, the notch depth does not drop below 30dB as shown in Figure 3.7.e.

To sum up, in directly connected delay line bridged BSF's, average passband insertion loss gets high value which can not to be neglected for delay lines with realizable impedances and more importantly the return loss performance is poor even with delay lines which have high impedance that can not be realized. Hence, direct connection of delay line can improve notch depth significantly at center frequency and other tuned frequencies but degrades average passband loss and return loss performances of main BSF filter. Also in most cases delay line impedance values can be too high to be realized. So this approach can have very limited practical application. Instead of directly connecting, the delay lines can be connected to BSF by using PCL power splitter and combiners by which the average insertion loss and return loss performances can be significantly improved.

3.2.3 Delay Line Bridging using PCL Power Splitting/Combiners

When delay line is directly connected to the main filter, power is split into two paths at input port and combined at output port using Tee-junctions. This type of connection may interact heavily degrading performance of devices as seen in the previous section. Also at microwave frequencies, power splitting and combining is problematic because of unavoidable junction discontinuities leading to mismatches, hence multiple reflections degrading the performance of devices. Also when a BSF is

to be bridged, the output signal of the BSF path is weak at stopband center because of the high rejection at this frequency. Therefore, to get equal amplitude the bridging path signal must also be weak. This condition can be satisfied by a PCL with light coupling between bridging path and main BSF path as shown in Figure 3.4.d. Therefore, in microwave applications PCL type splitter and combiners can be preferred in expectation of less problems at the expense of some new problems like spurious notches. Figure 3.8 shows the equivalent circuit of a PCL splitter and usage of PCL splitter/combiners.

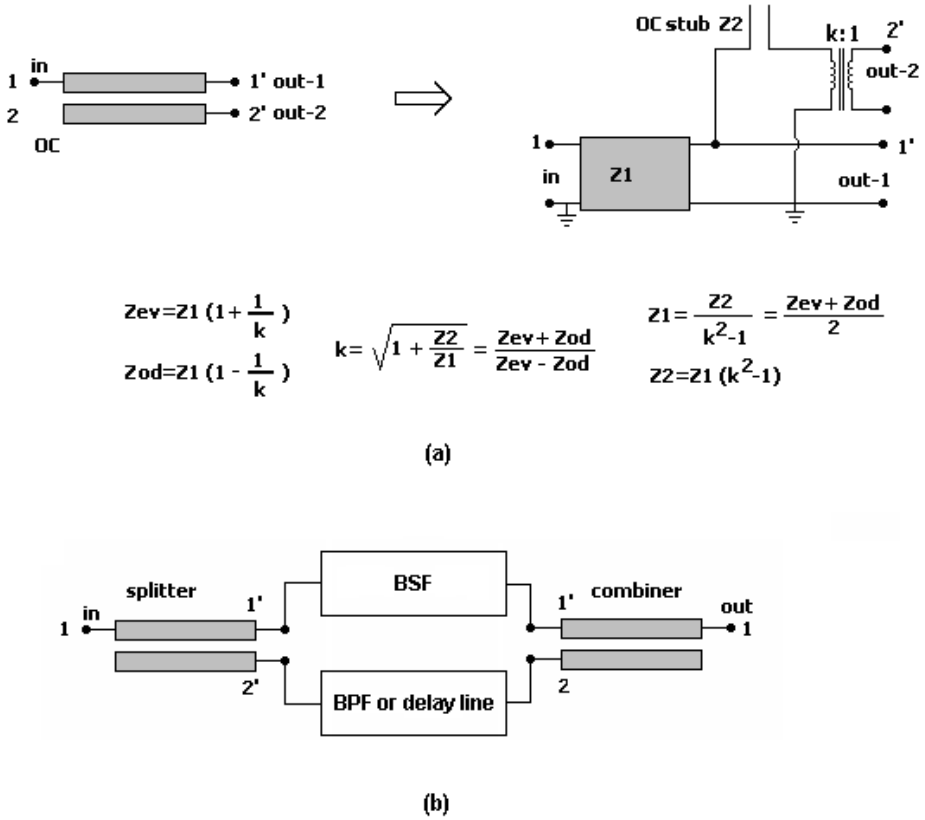

Figure 3.8 Equivalent Circuit and Usage of PCL Splitter/Combiners.
(a) Equivalent Circuit. (b) Usage of PCL S/C.

A PCL splitter is a 3-port device in which Port-1 is input and Port-1' and Port-2' are outputs. Port-2 of the PCL is left as OC. When Port-1' and Port-2' are used as inputs and Port-1 as output, the device becomes a combiner. Figure 3.8.a shows the

complete equivalent circuit on which port conditions can be imposed. PCL parameters Z_{ev}, Z_{od} (or Z1, Z2, k) determine the power division between ports of PCL splitters and combiners. The connection of these components to the main filter and bridge are shown in Figure 3.8.b. The function of power splitter/combiners is to equalize the amplitudes of both paths at the output. While doing this, unrealizable delay line impedances are avoided and return loss/average insertion loss degradations are minimized. The parameters of PCL's are determined from the notch depth of the main filter at center frequency. Although exact theoretical values can be calculated for PCL parameters, best way of finding proper PCL parameters is to use manual optimization starting from initial PCL parameters using a CAD tool since exact calculations are complicated. Z_{ev}, Z_{od} (or Z1, Z2, k) parameters of PCL also affects 3dBc, 20dBc and 30dBc bandwidth parameters and return loss response besides the notch depth. The impedance of the bridge delay line also affects the performance of the overall structure and it is also another parameter to be adjusted. Hence PCL and delay line impedance parameters can be calculated by trial and error until to achieve desired notch depth, 3dBc, 20dBc and 30dBc bandwidth parameters and return loss response. The electrical length of the PCL is taken as 90^0 at center frequency. A PCL splitter/combiner example is shown in Figure 3.9 for the same filter in the previous section with Q = 50 capacitors. PCL splitter/combiner and delay line impedance parameters are found by manual optimization using the design program ADS.

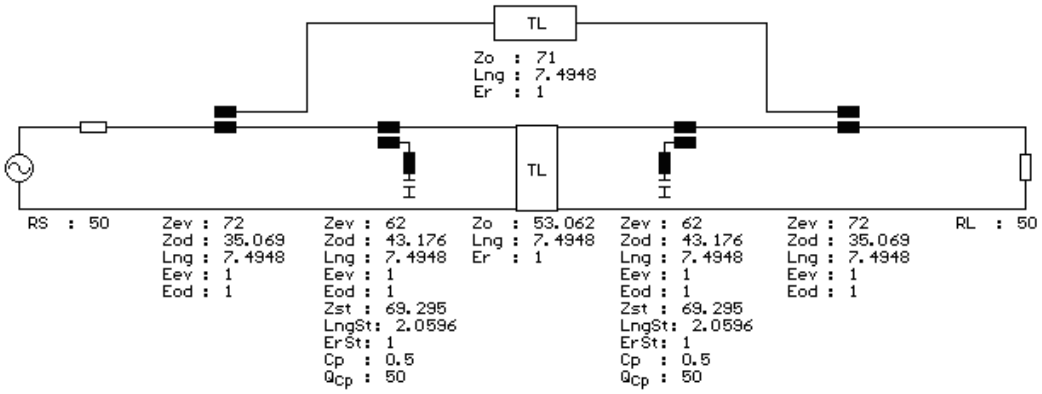

(a)

Figure 3.9 PCL Splitter/Combiner Bridged BSF with Q of 50. (a) Circuit.

Notch Property	Value
Notch Depth	-55.997dB
Average PB Insertion Loss	Below 0.1dB
3dBc Stopband BW	261 MHz
20dBc Stopband BW	37 MHz
30dBc Stopband BW	12 MHz

(b)

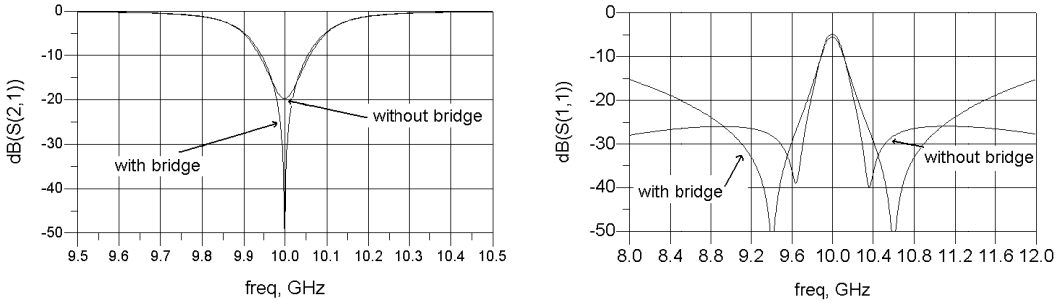

(c)

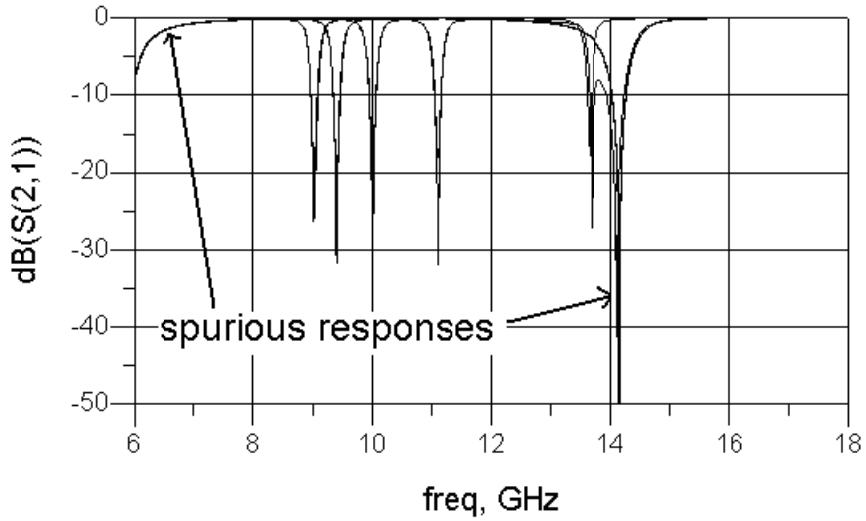

(d)

Figure 3.9 (continued) (b) Notch Characteristics.
(c) Frequency Responses. (d) Wideband Tuning Responses.

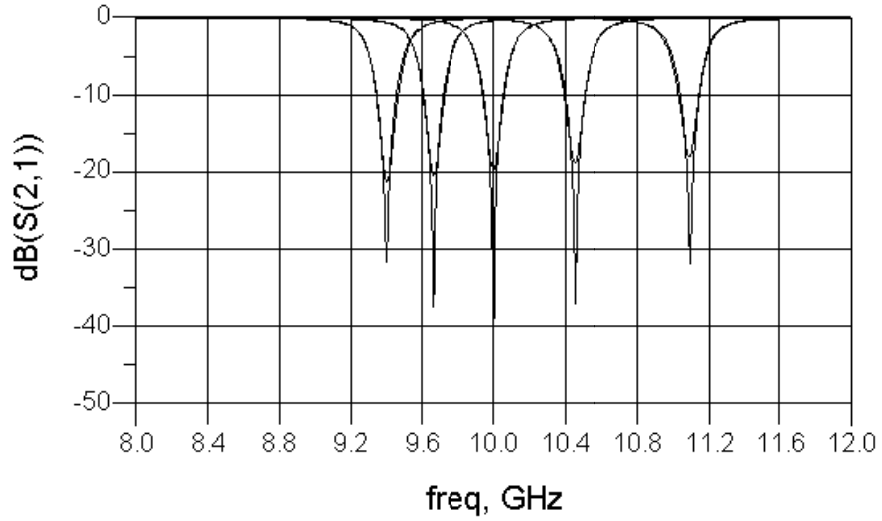

(e)

Figure 3.9 (continued) (e) Narrowband Tuning Results.

PCL parameters Z_{ev}, Z_{od} and impedance of the delay line are found by manual optimization and the center frequency of the filter is slightly shifted similar to the previous bridged BSF cases.

Addition of PCL splitter/combiner and delay line bridge improves the notch depth by approximately 35dB. Outside the stopband, the responses of both filters are close to each other as in the case with very high impedance delay line in Figure 3.6. Since the signal in bridge path is very weak, the average insertion loss is also very low (below 0.1dB) so that it can be neglected. When return losses are considered, it is seen in Figure 3.9.c that return loss gets distorted as the frequency gets away from the center frequency. However, return loss values are in acceptable levels in a wide frequency range (8-12GHz in the example) unlike directly connected case. This distortion arises from PCL splitter and combiners. PCL splitter/combiner + delay line bridge works as desired in a limited frequency band, which depends on parameters of the bridge. Beyond that frequency band, return loss performance degrades and spurious responses start to occur. When the capacitor values are tuned as in Chapter 2.4.2, the results of both bridged and non-bridged filters are shown in Figure 3.9.d. The notch depths of all bridged filters are deeper than the non-bridged filters. But for the

bridged filters notch depth quickly decreases below 30dB as capacitor value moves away from the initial center frequency due to the amplitude variations and deviations from opposite phase occurring when the center frequency is changed. Note that spurious responses are seen in Figure 3.9.d. When the tuning capacitor values are chosen in a narrower range as 0.3pF, 0.4pF, 0.5pF, 0.6pF and 0.7pF, the notch depth does not drop below 30dB as shown in Figure 3.9.e.

Consider the case when Q of the capacitors is lower than the previous example. For Q=20, the following notch responses are obtained as shown in Figure 3.10.

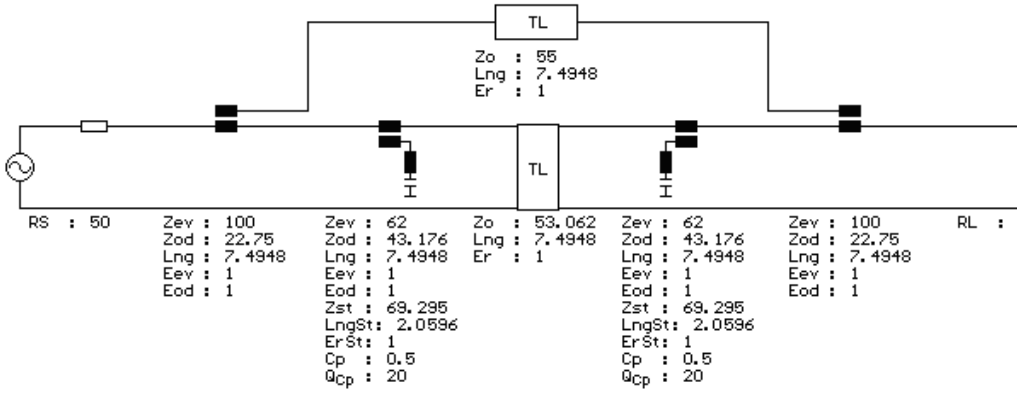

(a)

Notch Property	Value
Notch Depth	-55.377dB
Average PB Insertion Loss	0.5dB
3dBc Stopband BW	373 MHz
20dBc Stopband BW	40 MHz
30dBc Stopband BW	12 MHz

(b)

Figure 3.10 PCL Splitter/Combiner Bridged BSF with Q of 20.
(a) Circuit. (b) Notch Characteristics.

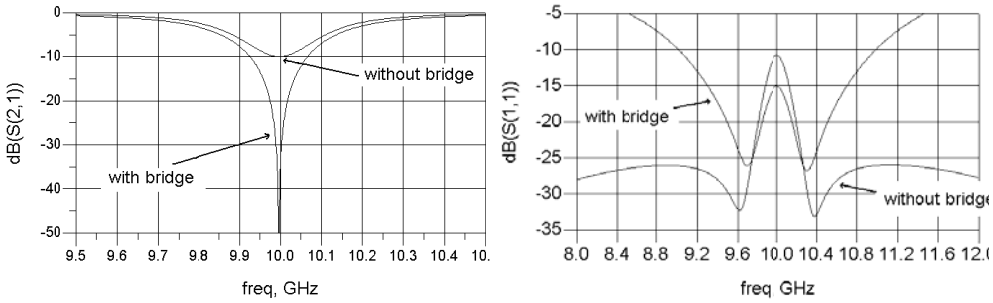

(c)

Figure 3.10 (continued) (c) Frequency Responses.

When Q=20, the signal passing through the bridge also increases as in the previous delay line bridged BSF case with the same Q value. Hence the coupling of the splitter and combiner PCL's should be increased. However coupling of splitter/combiner becomes very high which is hard to realize in practice as seen from the impedance values of PCL's in Figure 3.10.a. The average insertion loss is increased compared to the case with Q=50 but still lower than directly connected delay line case in previous example.

In summary, PCL power splitter/combiners used in bridge path improves average passband loss and return loss responses of directly delay line bridged bandstop filter designs. They avoid tee-junctions which creates discontinuities and hence multiple reflections degrading the filter performance. Unless notch depth of the main BSF is too low, PCL parameters get realizable values. Hence delay line with very high impedance bridge problem when main BSF has moderately high notch depth can be overcome using PCL splitter/combiners. If the main filter notch depth is very low, then element values of PCL can be unrealizable. In directly connected delay line bridge case, impedance of delay line gets better realizable values as notch depth of main BS filter decreases. However, in this case overall passband loss and return loss performances are severely degraded. Hence, in both bridging approach, phase cancellation method does not give satisfactory results when the main BSF filter notch depth is too low.

3.2.4 BSF Design Using BLC

Another way of designing notch filters is the use of branch line coupler and two identical bandstop resonators as shown in Figure 3.4.b. This approach inherently uses phase cancellation. Before going into further details, a brief description about a BLC is given in Figure 3.11.

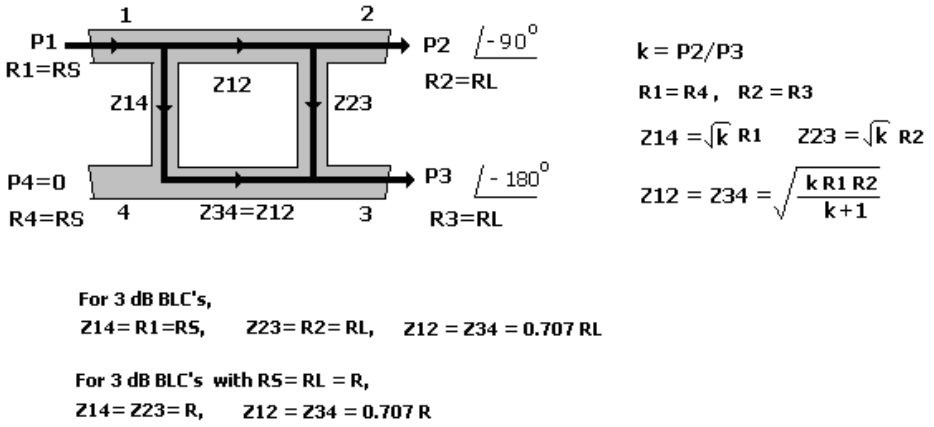

Figure 3.11 Definitions for BCL Parameters.

The convention used for BLC port numbering is shown in Figure 3.11. If Port-1 is taken as input, then Port-2 is the direct port and Port-3 is the coupled port while Port-4 is the isolated port. With proper termination resistors, the two port circuit between Port-1 and Port-4 has a notch at the quarter wavelength frequency. At this frequency there is a 180^0 phase difference between the paths 1-4 and 1-2-3-4, leading to phase cancellation. In most cases, 3dB BLCs are used and termination resistors RS and RL are 50Ω. However, in some cases 3dB BLCs with different RS and RL values can be used. This type of BLC is called as impedance transforming BLC.

When all 4 ports of BLC are terminated by proper impedances, at center frequency of BLC input signal at Port-1 passes through Port-2 and Port-3. There is a natural isolation between Port-1 and Port-4. This property of BLC can be used to form a notch filter. For this purpose, consider a conventional 3dB BLC with RS=RL=50Ω. When two identical bandstop resonators with series resistance equal to RL=50Ω are

connected to Port-2 and Port-3, a notch around the center frequency of BLC is created. Bandwidth of this notch depends on the bandstop resonators. Figure 3.12 shows an example of this approach by using lumped RLC resonators.

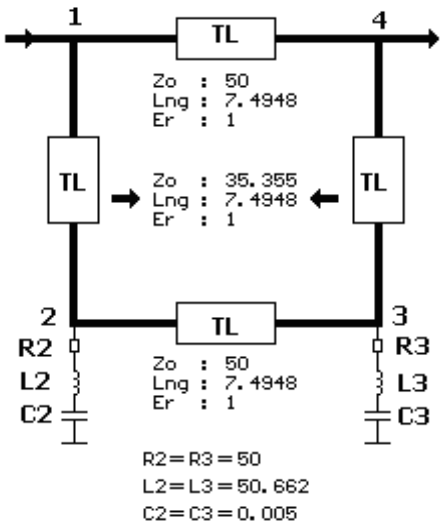

(a)

Notch Property	Value
Notch Depth	-61.063dB
Average PB Insertion Loss	0.25dB
3dBc Stopband BW	308 MHz
20dBc Stopband BW	31 MHz
30dBc Stopband BW	10 MHz

(b)

Figure 3.12 BS Resonators Connected BLC.
(a) Circuit. (b) Notch Characteristics.

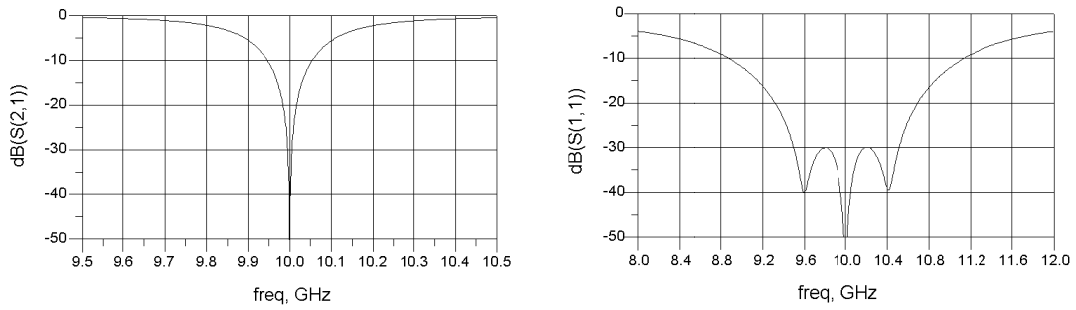

(c)

Figure 3.12 (continued) (c) Frequency Responses.

In Figure 3.12, it is seen that although series resistors of BS resonators are very high, a good notch characteristics are achieved. Also note that at notch center, return loss is very high which means there is no reflection to input. So this filter behaves as absorptive filter. However, this filter works properly approximately in 9.2-10.8GHz frequency band when return loss response below -15dB is considered. This passband distortion is due to the narrowband coupler response of BLC. Since bandwidth of the notch is very narrow, LC values of resonators get extreme values. This case is similar to direct BSF designs in Chapter 2 with very high shunt OC stubs. When OC stub is used as bandstop resonators in this topology, by using the realization methods given in Chapter 2 BS resonators with extreme values can be realized. An example application of this is given in Figure 3.13 in which series LC resonators are realized by gap coupled resonators using the approximation shown in Figure 3.13.a. Gap capacitor is chosen to make 3dB bandwidth close to initial case and series resistors are tuned to obtain proper notch characteristics since now series resistors are connected to BLC via gap capacitors.

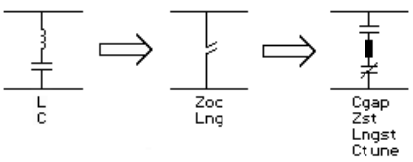

(a)

Figure 3.13 Gap Coupled Resonators Connected BLC. (a) Approximation.

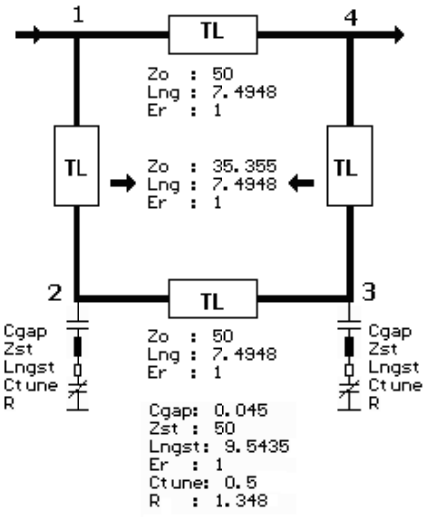

(b)

Notch Property	Value
Notch Depth	-59.069dB
Average PB Insertion Loss	0.166dB
3dBc Stopband BW	296 MHz
20dBc Stopband BW	30 MHz
30dBc Stopband BW	10 MHz

(c)

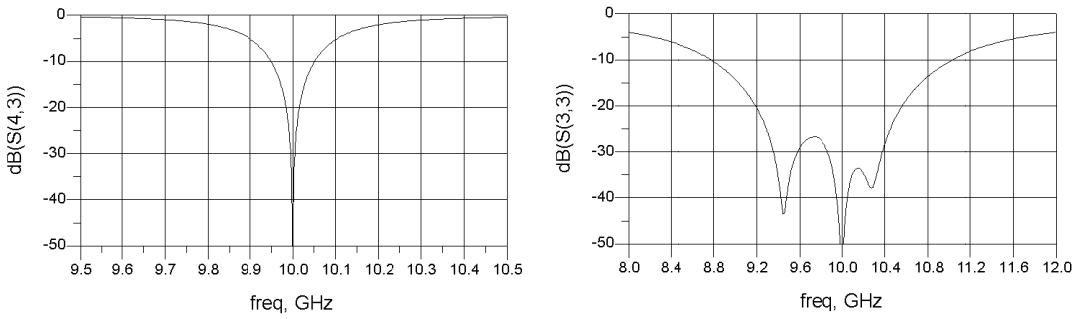

(d)

Figure 3.13 (continued) (b) Circuit. (c) Notch Characteristics. (d) Frequency Responses.

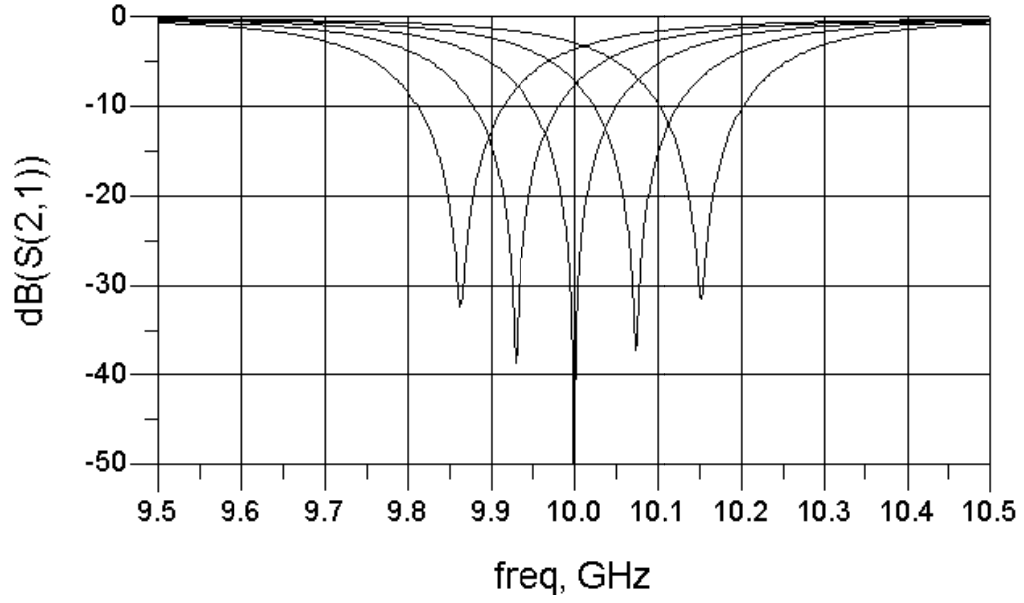

(e)

Figure 3.13 (continued) (e) Tuning Responses.

A good absorptive notch characteristics is obtained by using a BLC and two gap coupled resonators with realizable values. Value of loss resistors are found by manual optimization. Notch depth depends on value of loss resistors which act as termination resistors of BLC at these ports. So in practice their values should be as close to design value as possible for deep notch response. The given value in Figure 3.13.b is close to series resistance of a lossy capacitor with value of 0.5pF and Q of 24. Hence by using very low Q capacitors, a good notch characteristic is obtained. Center frequency of this notch filter can also be tuned by tuning capacitors of gap coupled resonator. However tuning range is very limited due to narrowband coupler performance of BLC. When tuning capacitors are tuned between 4.6pF to 5.4pF, notch depths do not fall below 30dB and center frequency changes between 9.85GHz and 10.15GHz as shown in Figure 3.13.e. Notch depth goes below 30dB beyond this capacitance range quickly. Impedance transforming 3dB BLC can also be used in this filter topology with the same notch performances.

In summary, this topology can be used in a narrow frequency band. However, it allows obtaining good notch characteristic by using low Q resonators and it has absorptive response which may be useful in some applications.

3.3 Bridged Topologies with Bandpass Main Filter

Phase cancellation approach allows additional design methods using BPFs for fixed and tunable bandstop filters besides direct bandstop designs. As shown in Figure 3.3, to obtain a notch filter, a narrowband BPF is bridged with a delay line or a wideband BPF with proper amplitude and phase characteristics. In this approach, narrowband bandpass filter is the problematic element at high frequencies due to lossy elements and unrealizable element values. This narrowband BPF should be tunable for tunable notch filter designs. There are a few ways to implement notch filters using bandpass main filter. These approaches can be divided into two categories which are branch line coupler (BLC) like topologies and PCL splitter/combiner containing topologies.

3.3.1 BLC like Topologies

There are various techniques for the formation of BSF's from a BPF by using BLC like topologies.

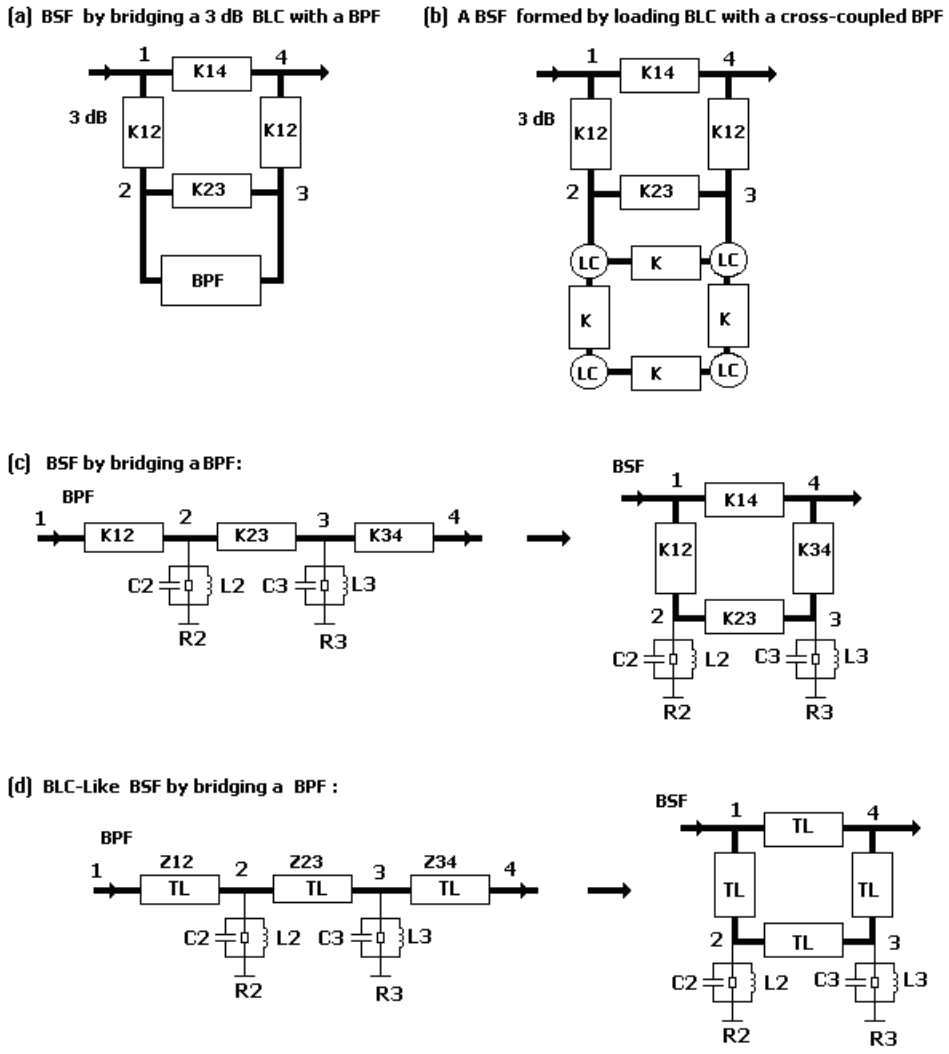

Figure 3.14 BLC like BSF Topologies.

Figure 3.14.a describes the well known topology where a symmetric BPF is placed between the output ports (Port-2 and Port-3) of a 3 dB BLC. The two port circuit between Port-1 and Port-4 acts as a BSF. The insertion loss response of BPF appears as return loss of BSF while the return loss of BPF appears as insertion loss of BSF. Hence, any symmetric BPF can be converted into a BSF using this general and systematic approach. For example in Figure 3.14.b, a cross-coupled BPF is placed between ports 2 and 3. In this circuit the circles are denoting resonators coupled by ideal inverters. The cross-coupling inverter of the BPF may be combined with the inverter K23 of the BLC. This topology is a generic topology. It is seen that there are more than one path between input (Port-1) and output (Port-4). The signals flowing

along these paths cancel each other when combined at the output port. It can be used to get insight into the operation of the BSF's formed by phase cancellation. We can generate many variations from this general topology. In this section, we will concentrate on simpler versions of such structures, formed only by two resonators.

The simplest version of the above described topologies is shown in Figure 3.14.c. A BSF is formed by introducing a cross-coupling inverter to bridge a BPF by brute force. Although exact designs are possible, a brute force introduction of the bridging inverter may also yield useful results simply by tuning or optimization. If the inverters of the circuit of Figure 3.14.c are converted into quarter wavelength TL's then we get a BLC-like topology as shown in Figure 3.14.d. The impedances of the BLC-like topology usually does not satisfy the constraints of a BLC, hence the name BLC-like is used.

3.3.1.1 BSF from BPF Connected BLC

An example design of the topology in Figure 3.14.a is shown in Figure 3.15.

By Prototype with Inverters	Distr, BPF, Cheby
Ripple (dB)	0.001
Passband Corners (MHz)	9975-10025
Proto. Degree	2
f_q (MHz)	20000

(a)

Figure 3.15 BSF from 3dB BLC with BPF Connected.
(a) Design Specifications.

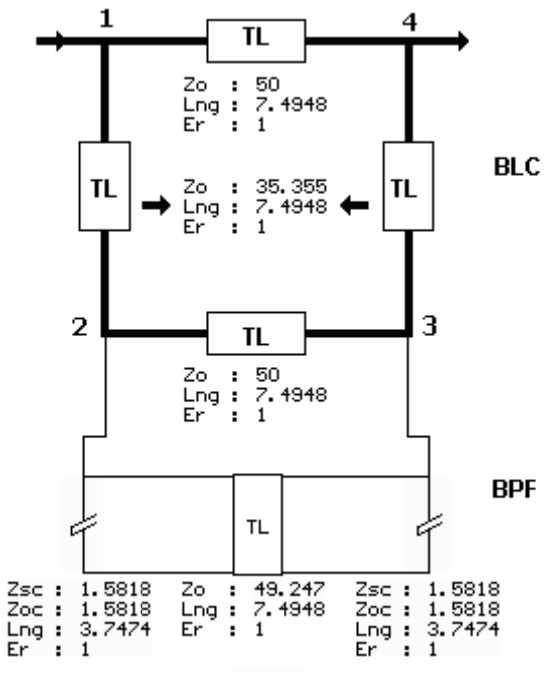

(b)

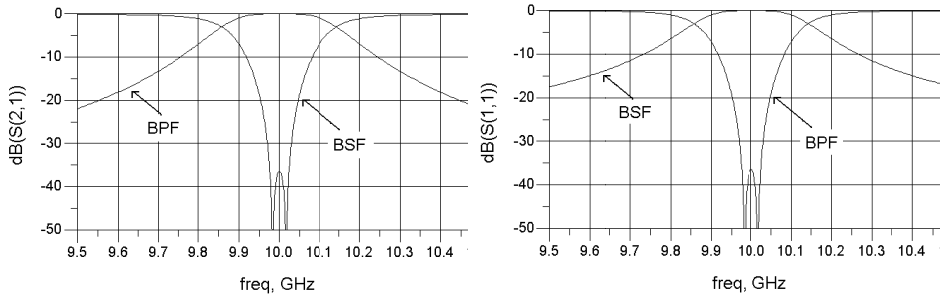

(c)

Figure 3.15 (continued) (b) Circuit. (c) Frequency Responses.

Main BPF in Figure 3.15.b is designed by By Prototype with Inverters tool of FILPRO with specifications given in Figure 3.15.a. Note that passband ripple is chosen as 0.001dB. This is because return loss response of BPF appears as insertion loss of BSF. Therefore it should be very low to get deeper notch depth in bridged circuit. It is composed of two SC resonators and one inverter which is realized by a quarter-wave TL. Passband bandwidth of symmetric BPF is chosen as 50 MHz in order to make 3dB bandwidth of BSF close to 300MHZ. Note that in Figure 3.15.c, the return loss of BPF appears to be insertion loss of BSF and insertion loss of BPF

appears to be return loss of BSF. So a BLC can be used to obtain bandstop filter characteristics by connecting a symmetric BPF to direct and coupled ports. Center frequency of this notch filter can be tuned by using the following elements instead of SC + OC stubs pair in Figure 3.16 in which shunt connected OC stub is replaced by either a single capacitor or a capacitor loaded OC stub.

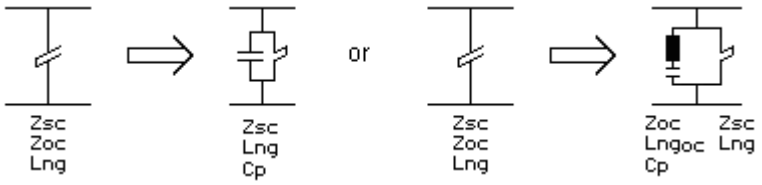

Figure 3.16 Tuning Capacitor Addition to Shunt SC+OC Stubs Pair.

Shunt OC stub in bandpass resonator is either interchanged with a capacitor or its length is decreased and it is loaded with a lower capacitance. By changing value of this capacitor, center frequency of notch filter can be changed. Due to narrowband coupler performance of BLC, filter characteristics get degraded as frequency gets away from center frequency. Since BW of BPF is very small relative to center frequency, impedance values of SC stubs become very low to be realizable. This filter can not be realized with these element values. However there is a way to obtain realizable circuit elements when design starts from generic models of BLC and BPF with inverters. In this case impedance transforming 3dB BLC is used. Impedance transforming BLC is a type of 3dB BLC in which RL value in Figure 3.11 is different from RS which is almost always 50Ω. Design parameters of BLCs are given in Figure 3.11. A design method for this case is shown in Figure 3.17. The design steps are as follows:

- A symmetric BPF is designed with regular source and load resistors (RS=RL=50Ω), filter resonator parameters (impedance of SC stubs in this case) are scaled to the desired realization level by inserting inverters at source and load ends. (Figure 3.17.a)

- Inverters at ports are absorbed into source and load resistances so that BPF now wants to see new terminating impedance RS'. (Figure 3.17.b)

- This BPF is connected to an impedance transforming BLC with RL=RS' (Figure 3.17.c) with proper connection of ports (Figure 3.17.d).

- Finally K23 and K23' inverters are paralleled to form one inverter K23'' (Figure 3.17.e).

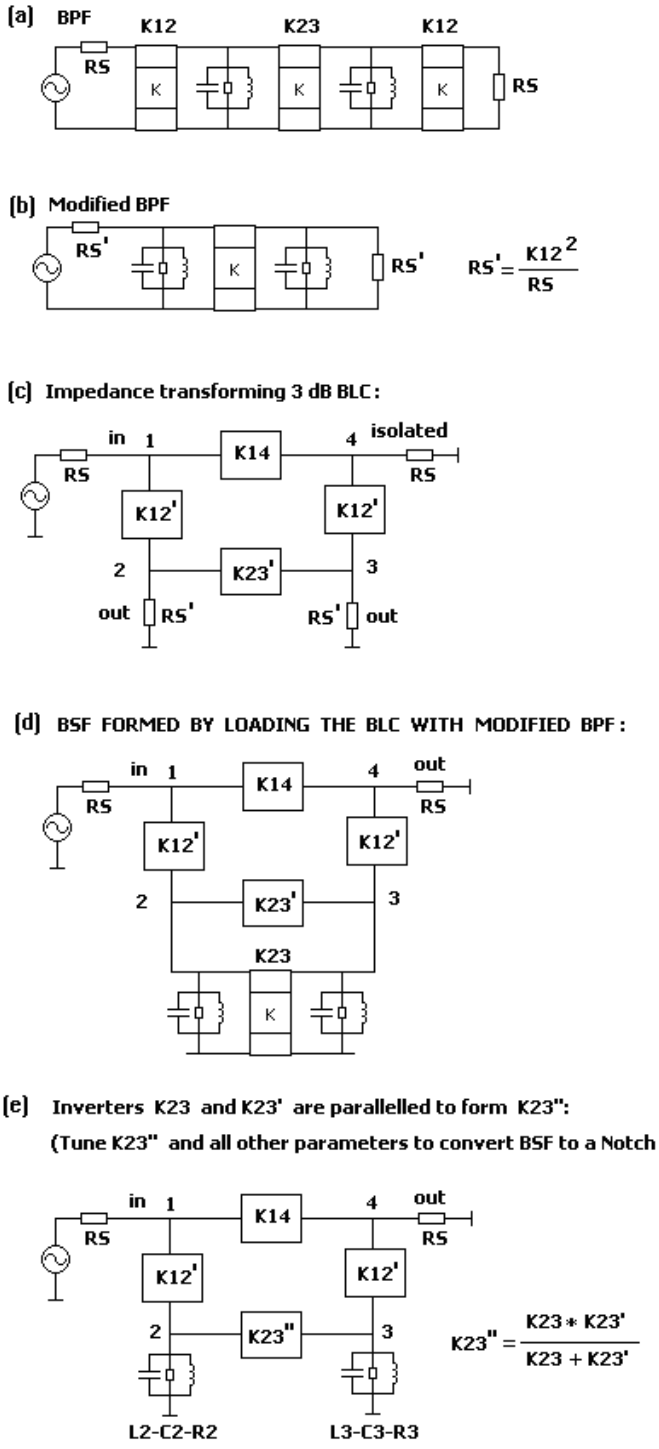

Figure 3.17 Formation of a BSF from BPF Using Impedance Transformating BLC.

An example design of a BSF with the given design method in Figure 3.17 using the same BPF design in Figure 3.15.b is shown in Figure 3.18. SC and OC stub impedances are chosen as 50Ω.

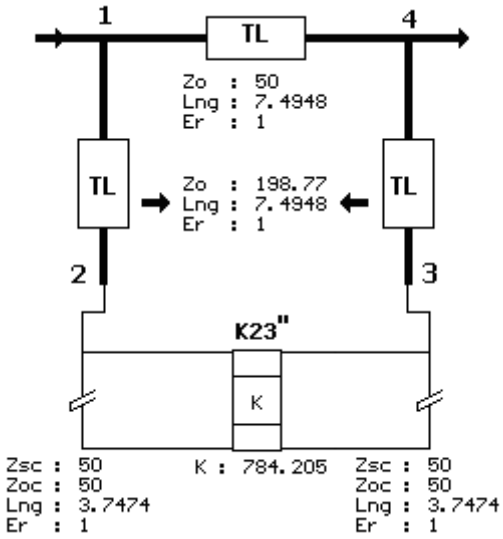

Figure 3.18 BSF from Impedance Transforming BLC with BPF Connected.

Note that after all design steps in Figure 3.17 are applied, K14 and K12' inverters are realized by quarter-wave TLs since there are no transformations or approximations that can be applied for these inverters. Frequency response of this structure is close to the initial case in Figure 3.15. The impedance of SC stubs have realizable levels at the expense of higher impedance values of BLC lines except Z14. However in this case K23'' gets too high values for narrowband designs. This very high value K23'' can be realized by using pi-section SC stub approximation of the inverter and filter resonator shunt SC stubs. This is shown in Figure 3.19.

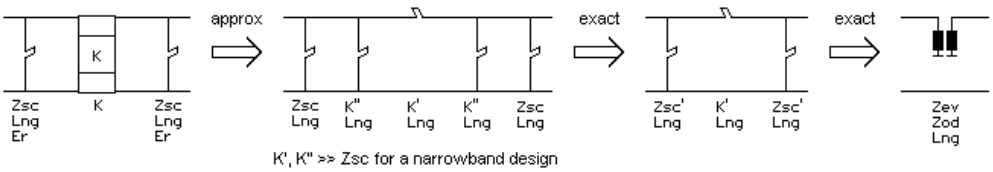

Figure 3.19 Transformation of High Value K23'' to Comb Type PCL.

In Figure 3.19, resonator shunt SC stubs are combined with pi-section SC stubs approximation of the inverter and the resultant pi-section SC stubs are transformed to an equivalent comb type PCL configuration which have realizable element values. After applying these transformations, tuning capacitors are added by loading OC stub and tunable BSF design is finished.

In Figure 3.15.c it is seen in insertion loss response that there is a ripple in stopband of notch response which makes notch depth around 30dB at center frequency. Before applying inverter realization and capacitor addition, manual optimization of Z14 (=Z34) and K23'' can be performed to improve this notch response. After manual optimization, inverter realization and capacitor addition, the resultant circuit and frequency responses together with the initial design in Figure 3.18 are shown in Figure 3.20.

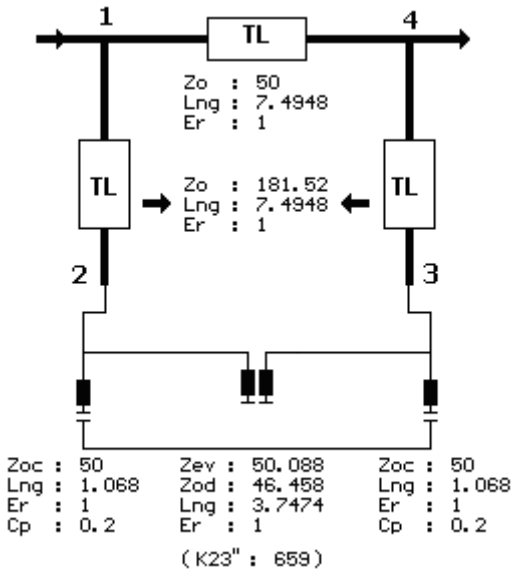

(a)

Figure 3.20 A Realizable BSF Design from BLC with BPF Connected.
(a) Circuit.

Notch Property	Value
Notch Depth	-99.137dB
3dBc Stopband BW	327 MHz
20dBc Stopband BW	102 MHz
30dBc Stopband BW	57 MHz

(b)

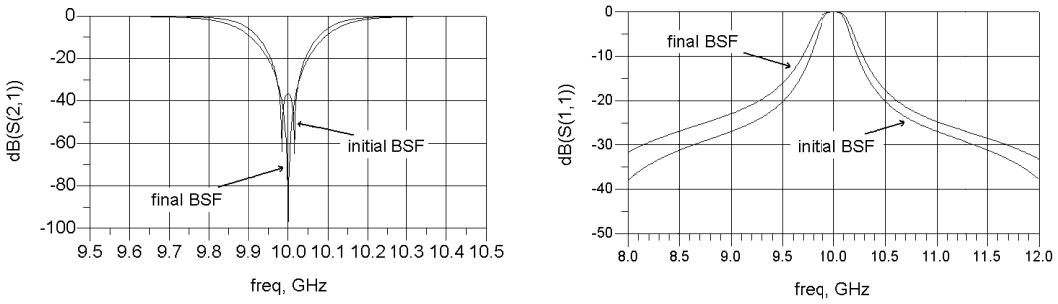

(c)

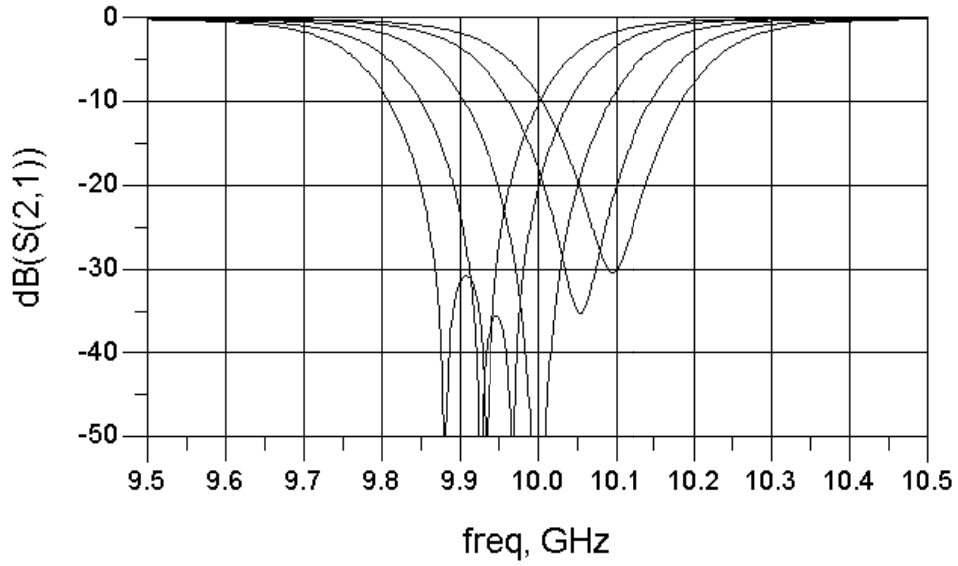

(d)

Figure 3.20 (continued) (b) Notch Characteristics.
(c) Frequency Responses. (d) Lossless Tuning Responses.

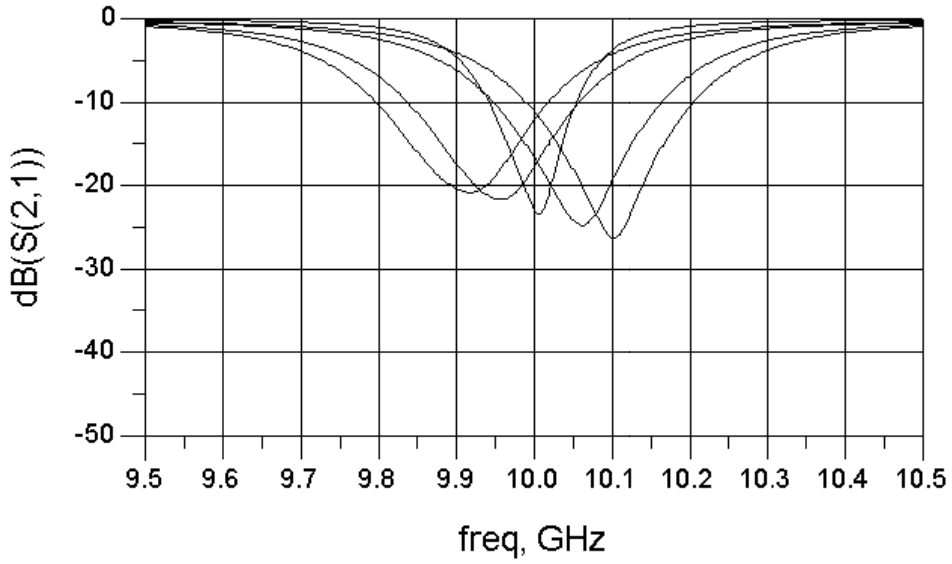

(e)

Figure 3.20 (continued) (e) Lossy Tuning Responses.

For lossless case, a deep notch response from BPF is obtained. Circuit elements have realizable values except maybe Z12 (=Z34) which can be high for some transmission mediums. Z12 (and so Z34) can be decreased by choosing wider 3dBc bandwidth. Note that in Figure 3.20.c, although 3dBc bandwidth is close to previous designs, 20dBc and 30dBc bandwidths are wider than all the previous designs. This property may be desired for some applications or vice versa. However tuning characteristics are very poor. When tuning capacitor is changed slightly, notch depth goes quickly below satisfactory values. The center frequency is changed between 9.9 GHz - 10.1 GHz with capacitor values 0.193pF, 0.196pF, 0.2pF, 0.204pF and 0.207pF for notch depth minimum of 30dB as shown in Figure 3.20.d which is a very narrow tuning range. When loss of resonators is includes, notch depth becomes severely degraded. For example for tuning capacitors with Q = 50, notch depth at center frequency goes below 25dB and 3dBc bandwidth also increases considerably as shown in Figure 3.20.e. It is possible to improve notch depth to some extent under lossy conditions by manual tuning of Z12 (=Z34) impedance value and comb PCL parameters but increase in 3dBc bandwidth can not be improved.

A simple modification for this filter can be to connect quarter-wave OC stub to ground ports of comb PCL configuration as shown in Figure 3.21.a. In this case virtual ground is formed at input of OC stub at center frequency and notch depth in initial case is conserved. However notch bandwidths (3dBc, 20dBc, 30dBc) decreases considerably and according to the chosen impedance of OC stub, bandwidth can be adjusted (as impedance of OC stub increases, notch bandwidths decreases). So increase in notch bandwidths when lossy resonators are used can be prevented by adding OC stubs to ground ports of comb PCL configuration. In addition to this, instead of tuning the filter by using OC stub of BPF, these added OC stubs can be capacitor loaded and be used to tune the center frequency as shown in Figure 3.21.b. However, these modifications do not improve tuning characteristics of this filter topology.

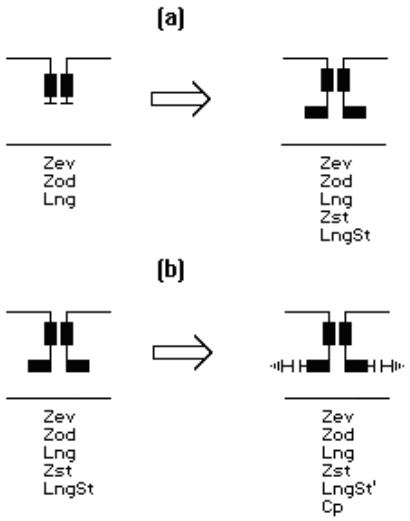

Figure 3.21 Tuning Capacitor Addition to Comb Type PCL.
(a) OC Stub Addition. (b) Capacitor Addition.

In order to decrease 3dBc in lossy case addition of OC stubs to comb PCL is a good solution rather than increasing Z12 (=Z34) which becomes too high to be realized. So applying the modification in Figure 3.21.a to the filter in Figure 3.20 and tuning Z12(=Z34) for proper notch depth the following responses in Figure 3.22 are obtained.

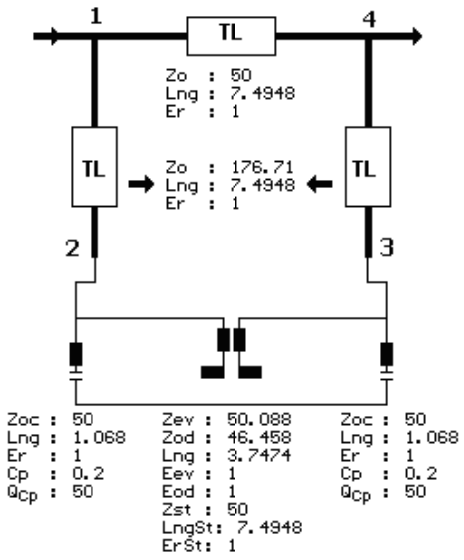

(a)

Notch Property	Value
Notch Depth	-54.338dB
3dBc Stopband BW	231 MHz
20dBc Stopband BW	38 MHz
30dBc Stopband BW	12 MHz

(b)

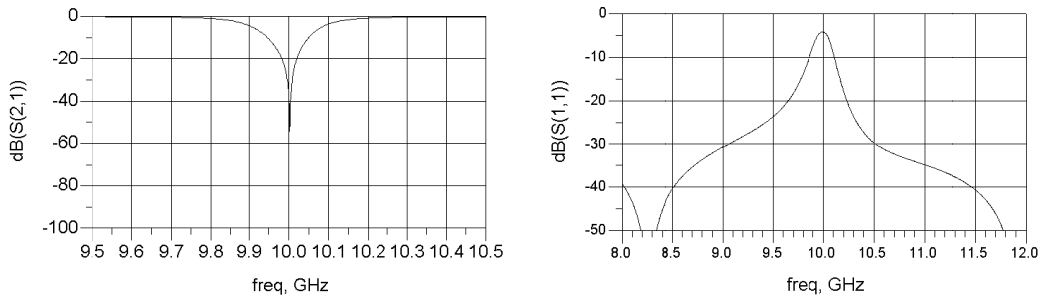

(c)

Figure 3.22 BSF Design with OC Stubs Connected to Short Ends of Comb PCL. (a) Circuit. (b) Notch Characteristics. (c) Frequency Responses.

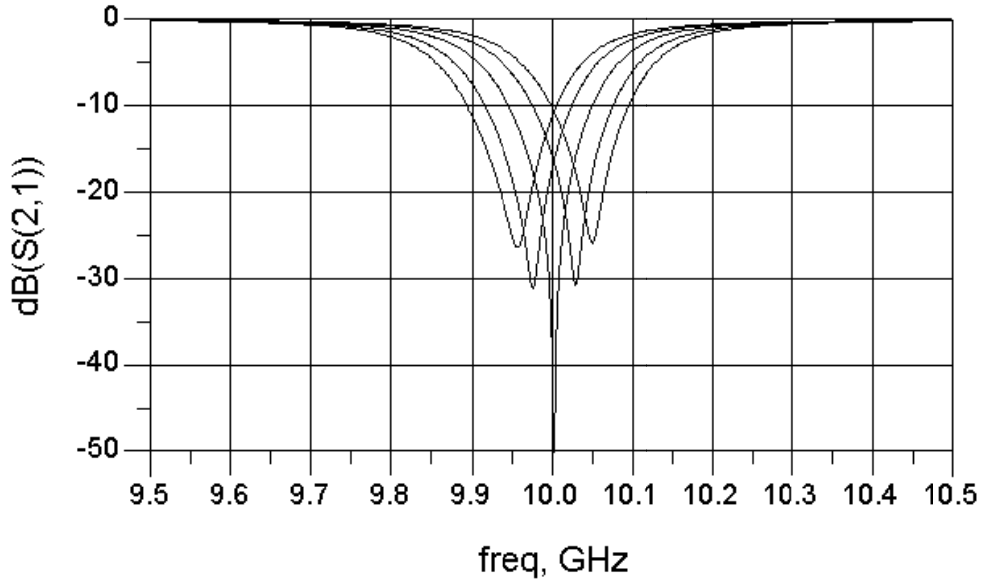

(d)

Figure 3.22 (continued) (d) Tuning Responses.

As seen in Figure 3.22, a deep notch under lossy is obtained with realizable element values. Also notch bandwidths (3dBc, 20dBc, 30dBc) are considerably narrower than the previous case. So bandwidths of the notch filter can easily be readjusted using this modification. However tuning characteristics are worse than the previous case. When capacitors are tuned with the same values of previous case, notch depth drops below 30dB at maximum and minimum values of capacitors. Hence, improvement on notch depth and bandwidth is obtained at the expense of more limited tuning range.

Instead of connecting a symmetric BPF to 3dB BLC, two identical bandpass resonators can also be connected to couple and direct ports of BLC to get a bandstop response. Frequency response of this structure is close to BPF connected case and same transformation and approximation techniques can be applied for better circuit elements.

To sum up, a bandstop filter response can be obtained by connecting a symmetric BPF or two identical bandpass resonators with proper connections to BLC. This

structure is best useful when a fixed notch is desired. Tuning characteristics are very poor. With lossy resonators deep notches can be obtained after some manual optimizations. However this topology can be used to obtain good quality tunable notch filter designing when all-pass filter approach in Chapter 4 is used.

3.3.1.2 BSF from Brute Force Delay Line Bridged BPF

An easier way of obtaining bandstop response from BPF is to connect a delay line as a phase shifter to input and output of a BPF as shown in Figure 3.14.c and d. This is similar to directly connected delay line bridging of BSFs in section 3.2. However this time impedance of delay line is always around 50Ω since at center frequency BPF is matched to 50Ω. Consider a narrowband BPF design with low impedance resonators are scaled to 50Ω by using impedance inverters in Figure 3.23 with additional inverter as bridge component.

By Prototype with Inverters	Distr, BPF, Cheby
Ripple (dB)	0.001
Passband Corners (MHz)	9975-10025
Proto. Degree	2
f_q (MHz)	20000

(a)

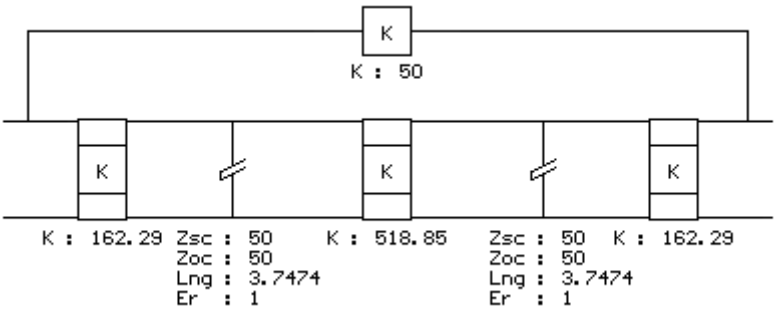

(b)

Figure 3.23 Inverter Bridged Narrowband BPF Design.
(a) Design Specifications. (b) Circuit.

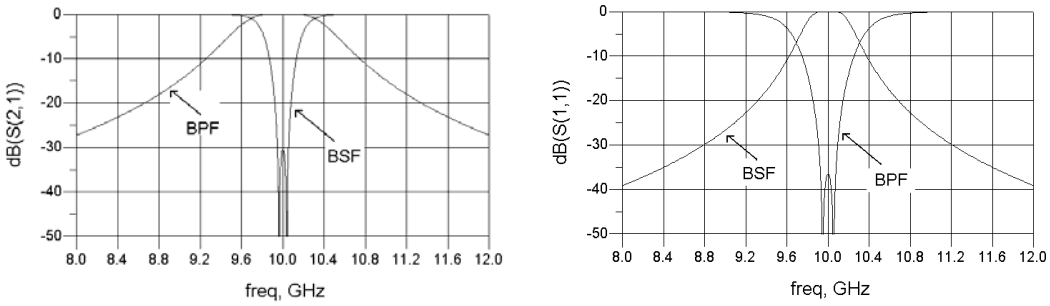

(c)

Figure 3.23 (continued) (c) Frequency Responses.

Addition of the bridge to BPF creates frequency response similar to the previous addition of BPF to BLC case. Insertion loss of BPF resembles return loss of BSF and vice versa. Note that circuit of this topology is exactly the same with the previous BLC case when K23 and K23' inverters are combined. So approximation and transformation techniques that are used in previous case like realization of high value inverter with comb type PCL configuration and tuning capacitor addition can also be used here. The inverters except the one with high value are realized by quarter wavelength TLs. To get a better notch response (elimination of ripple in stopband) manual optimization over inverter values should be performed. By this way stopband bandwidths can also be readjusted. Further modifications given in Figure 3.21 can be applied to decrease notch bandwidths. This approach in fact a short-cut way for the previous case and if resonator impedances are chosen the same, the same circuit with BLC case can be reached during manual optimization. Hence this topology shares the same advantage and disadvantages with the previous case.

3.3.2 PCL Power Splitter/Combiner Containing Topology

PCL splitter/combiners can also be used in BSF designing with BPF main filter. They enable alternative design method to branch line like topologies besides avoiding tee-junctions formed by direct connection of delay lines. In previous BSF main filter case, PCL splitter and combiner is added to input and output of a predesigned BSF filter to adjust the proper amplitude of the signal passing through

the bridge. In BPF main filter case, besides the same function of adjusting bridge signal level, they are also integral part of BPF. The design of PCL splitter/combiner containing topology starts with BPF design. Then a delay line is added and BSF is formed . The design steps are as follows:

5) The initial circuit (Figure 3.24) is synthesized using FILPRO Synthesis tool with the following specifications:

Syntesis	Distr, BPF, Cheby
Ripple (dB)	0.001
Passband Corners (MHz)	9950-10050
Degree	4 (3Nzero, 1Ninf)
f_q (MHz)	20000

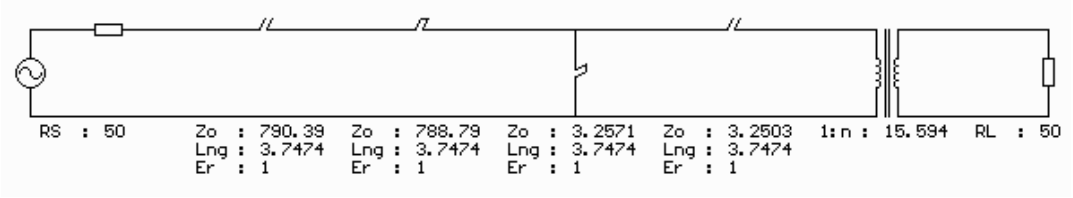

Figure 3.24 Initial Circuit.

6) L-section SC stubs in the middle of initial circuit are transformed to Symmetric Pi-section SC stubs, transformer formed by this transformation cancels transformer in initial design and quarter-wave 50Ω TLs are inserted to input and output of the circuit (Figure 3.25).

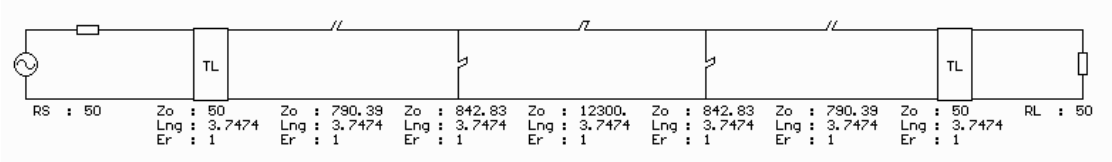

Figure 3.25 L-Section SC Stubs to Pi-Section Stubs with Additional 50Ω TLs.

7) 50Ω TL and series OC stub pair in input and output of the circuit are transformed to interdigital type PCL equivalent as shown in Figure 3.26.

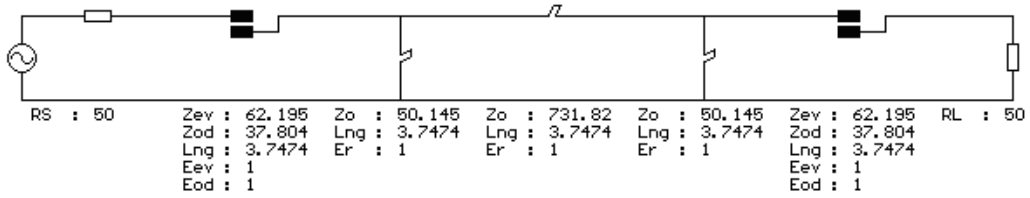

Figure 3.26 Introduction of Edge Coupled PCLs.

8) Pi-section SC stubs in the middle of the circuit are transformed to comb type PCL equivalent and BPF design is finished (Figure 3.27).

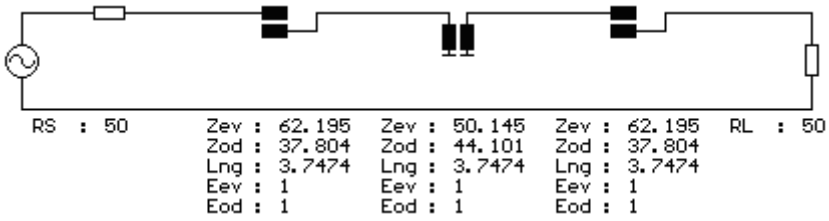

Figure 3.27 Pi-Section SC Stubs Transformed to Comb Type PCL.

9) Finally 50Ω quarter wavelength delay line is connected to PCL splitter/combiners and design stage is finished (Figure 3.28).

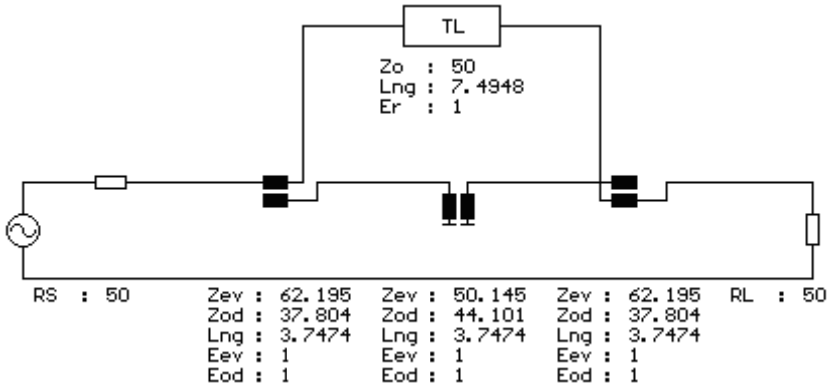

Figure 3.28 Final Circuit After Addition of Bridge line.

The frequency responses of the resultant circuit Figure 3.28 are shown in Figure 3.29.

Notch Property	Value
Notch Depth	-30.687dB
3dBc Stopband BW	300 MHz
20dBc Stopband BW	104 MHz
30dBc Stopband BW	71 MHz

(a)

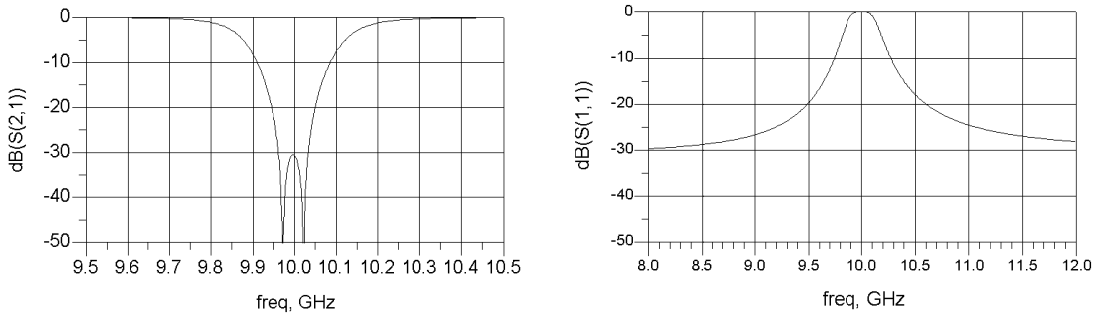

(b)

Figure 3.29 Frequency Responses of Final Circuit.
(a) Notch Characteristics. (b) Frequency Responses.

Similar to previous BPF cases, when delay line with proper electrical length is added, bandpass response transforms to bandstop response and there is a ripple in bandstop stopband response which is not desired for a notch filter. As in previous cases this ripple can be removed by manual optimization. However before fixing the ripple, tuning capacitors should be added to the design. This can be done by using the modifications in Figure 3.21. Ground connections of comb type PCL are done by addition of quarter wavelength OC stubs and capacitor loading of these OC stubs enables tuning of center frequency. Note that addition of OC stubs decreases notch bandwidths and this decrease depends on impedance of OC stub. So bandwidth characteristics of this filter can be adjusted by using impedances of these OC stubs. When impedance of OC stub is chosen as 50Ω and tuning capacitor is chosen as 0.5pF for initial value the resultant filter and frequency responses are as shown in Figure 3.30. Q of capacitors are taken as 50Ω and impedance value of delay line is tuned manually to improve notch characteristics.

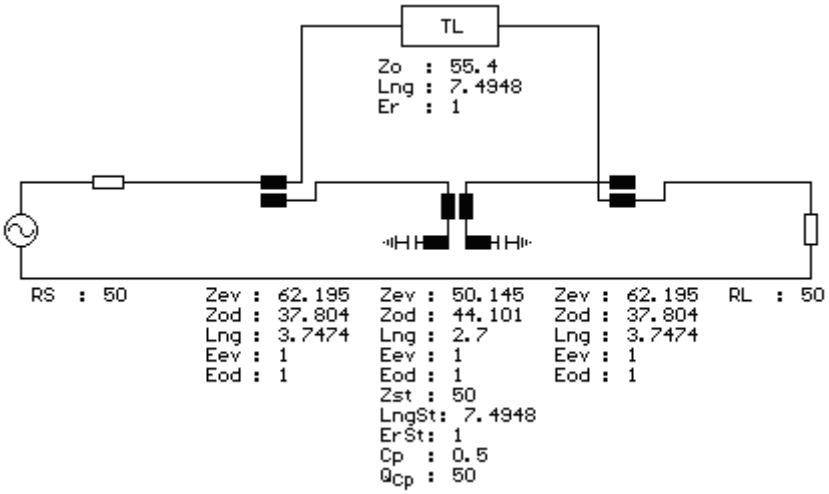

(a)

Figure 3.30 Final Circuit with Tuning Capacitors Added.
(a) Circuit.

Notch Property	Value
Notch Depth	-59.531dB
3dBc Stopband BW	251 MHz
20dBc Stopband BW	38 MHz
30dBc Stopband BW	12 MHz

(b)

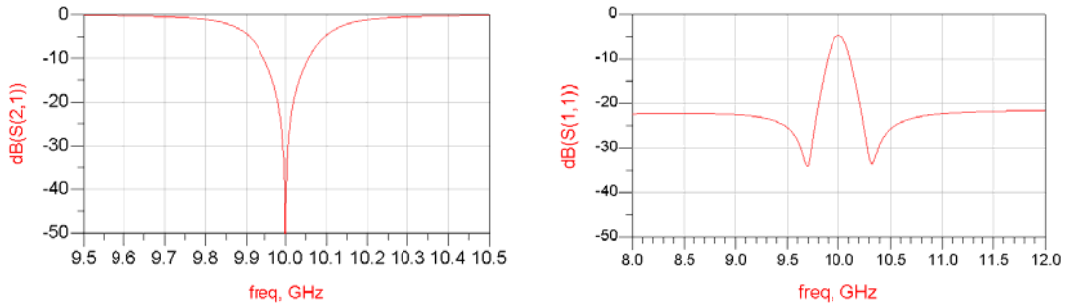

(c)

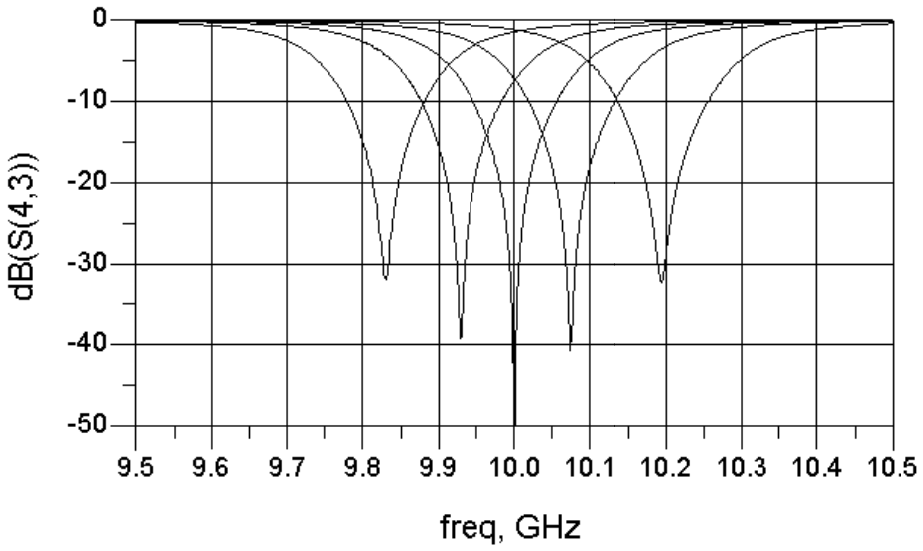

(d)

Figure 3.30 (continued) (b) Notch Characteristics.
(c) Frequency Responses. (d) Tuning Responses.

As seen in Figure 3.30, a good notch response is obtained from BPF with realizable element values. Notch bandwidths are narrow and notch bandwidths can be

readjusted by changing the impedance of capacitor loaded OC stub connected to comb PCL configuration. When capacitors are tuned to 0.45pF, 0.48pF, 0.5pF, 0.52pF and 0.55pF, notch depth does not drops below 30dB and center frequency changes between 9.8GHz-10.2GHz. Tuning range of this filter is still very limited but better than BSF from BPF connected BLC case.

In summary, PCL splitter/combiner containing topology can better be used for fixed notch filter like BSF from BPF connected BLC case due to limited frequency range for lossy resonators. However this topology can also be used to obtain good quality notch filter designing when when all-pass filter approach in Chapter 4 is used.

3.4 Comparison/Comments on Bridged Bandstop Filters

To sum up, phase cancellation approach can be useful in designing tunable notch filters. Based on the frequency responses of example designs, the following results are observed:

- Phase cancellation approach is very useful for fixed notch filters since very deep notches can be obtained using a low order main filter (BSF or BPF) with low-Q resonators.
- Phase cancellation approach can also be useful for tunable notch filters. Deep notch depths obtained by phase cancellation is conserved for a limited tuning frequency range. However this frequency range is very narrow for most cases. Directly connected or PCL splitter/combiner connected BSF filters have better tuning range than rest of the design methods which are BSF from BLC design and BSF designs obtained from BPF.
- Return loss performances are better for notch designs with BPF main filter than designs with BSF main filter. When delay line is directly connected to BSF main filter, according to impedance of delay line return loss in passband becomes distorted severely which also increases passband insertion loss. When delay line is connected by PCL splitter/combiner, return loss performance becomes better but due to degradation in coupler performance, passband bandwidth is limited. When main filter is a BPF, return loss and so

passband insertion loss are better since outside stopband the signal passes through the bridge which is a TL with impedance around 50Ω.

- BSF design from BLC with BS resonators has absorptive response. So both return loss and insertion loss of this filter at center frequency is very low. This property can be beneficial in some cases.
- Amplitude balance in main filter and bridge path is very important for deep notches. To maintain this balance, loss of circuit and resonators should be modeled carefully.
- Tuning performance of many phase cancellation topologies is not satisfactory. However, using all-pass filter approach in Chapter 4 these topologies can be used in designing high quality tunable notch filters.

3.5 Remarks

In this chapter, amplitude balanced phase cancellation approach is introduced and bandstop filter topologies using this approach are given. Example filters with 2 resonators are designed and frequency responses under lossless and lossy conditions are presented. The main point of this chapter is to demonstrate the properties and performances of this approach, which is basically suitable for fixed low order notch filters. Considering the results of example filters, this approach provides limited improvements. However in the following chapter, an approach to increase performance of phase cancellation is introduced.

CHAPTER 4

ALL-PASS FILTER APPROACH

4.1 All-Pass Filter Approach

All-pass filter approach is a special case of phase cancellation approach which deserves separate treatment. This is because it allows systematic design with controllable parameters of notch filters and it produces better tunable notch filter characteristics than the methods given so far in Chapter 2 and Chapter 3. In this approach first a bridged all-pass filter is designed by using either readily available all-pass topologies or by bridging a BPF or a BSF. Then it is converted into a notch filter by detuning some elements of the all-pass filter until phase difference between the signal along the bridge path and main filter path becomes 180^0 and hence cancel each other at desired frequencies.

Design stages of this approach are as follows:

1) Design stage begins with designing of a low order all-pass filter. All-pass filters are mainly used for phase or delay adjustment purposes. In order to design notch filters, bridged type all-pass filters are necessary. As bridged type all-pass filters, readily available all-pass topologies can be used as well as bridged BSF or BPF filter topologies given in Chapter 3. It should be noted that in all-pass designing stage, circuit losses are not considered. There are two classical lumped bridged all-pass structures called as bridge tee all-pass sections that find usage for tunable notch filter designing. Details of these structures are given in section 4.2. However they can have little usage at microwave frequencies since they are composed of lumped elements. Instead of readily available filters, bridged BSF or BPF filters given in Chapter 3 can be used to design bridged all-pass filters

with good filter characteristics and realizable element values. Details of these are given in section 4.3.

2) When a bridged all-pass filter is designed, tuning elements are added if not present in the initial all-pass design. In bridge tee all-pass filter case, since elements are lumped, tuning capacitors or inductors are inherently present. However in distributed BSF or BPF filters, mostly capacitor loaded OC stubs or SC stubs with capacitor in parallel are added to the circuit. Finally circuit losses (loss of resonators, TLs, stubs etc.) are added to the design.

3) When some elements of all-pass filter are detuned, phase difference between the signal along the bridge path and main filter path becomes 180^0. Since amplitude of the signals in two paths already have a balanced distribution due to all-pass filter response, 180^0 phase difference between two paths maintained by detuning of some elements creates a deep notch response. When a bridged BSF or BPF with two resonators is used as all-pass filter, two resonators are detuned to get a notch response. In this case to get a notch at center frequency, one resonator is tuned below center frequency and the other resonator is tuned above center frequency by manual tuning. Note that in all of the designs so far in Chapter 2 and Chapter 3, all the resonators in a design are identical and so tuned to the same center frequency. In all-pass filter approach, resonators are tuned to different frequencies.

4) Center frequency of this notch filter can be tuned by changing center frequency of resonators. All-pass notch filter approach yield notch filters which are tunable over broad bandwidths and with notch depths much higher than the previous BSF design methods.

In the rest of this chapter, the topologies that can be used for this approach are given.

4.2 Bridged Tee All-Pass Section

Figure 4.1 shows two classical lumped element bridged tee all-pass sections named as L13-C-C and C13-L-L.

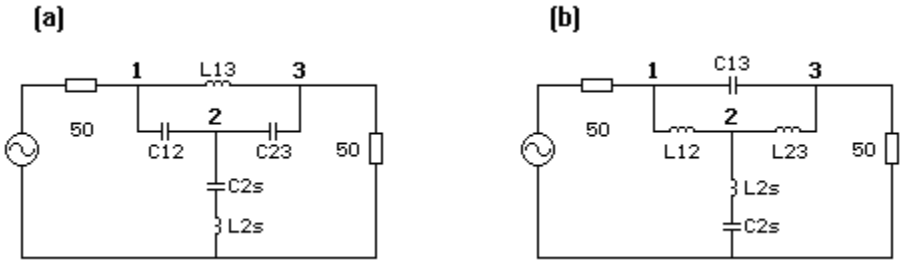

Figure 4.1 Lumped Bridged Tee All-Pass Sections.
(a) L13-C-C. (b) C13-L-L.

In all-pass applications, the arms of the tee section are formed by identical C12 and C23 or identical L12 and L23. In L13-C-C all-pass section the bridging element is the inductor L13 while in C13-L-L all-pass section the bridging element is the capacitor C13. It is possible to convert these all-pass sections into fixed or tunable notch filters by setting the elements properly.

An example design stage for L13-C-C all-pass section is as follows:

1) First a default L13-C-C type bridge tee element is inserted in FILPRO and its parameters are changed for f_0=10GHz, RS=RL=50 and k=0.95. "k" is a parameter that can be set between 0 and 1 to produce infinitely many alternative all-pass sections with different phase shifting properties and different element values. In notch filter applications this parameter sets the stopband bandwidth of the resulting notch filter with k closer to 1 giving narrower stopband bandwidths. The initial circuit is in Figure 4.2.

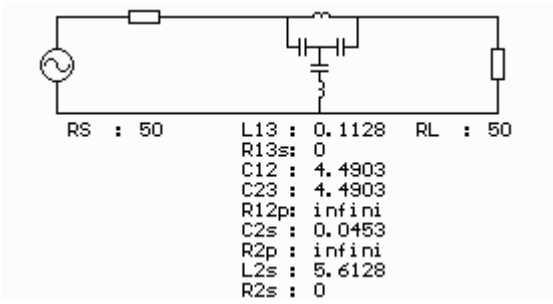

Figure 4.2 Initial Circuit.

As k gets closer to unity, L13 gets smaller, C12=C23 get higher, L2s gets higher and C2 gets smaller. L13 and C12+C23 form a parallel resonance circuit in series arm while L2s and C2s form a series resonance circuit in shunt arm.

2) After all-pass filter is formed, a notch response can be formed by tuning one or more elements. Before that it is better to add circuit losses. In the example circuit, inductor and capacitor Q's are taken as 50. Many different notch characteristics can be obtained by changing some of the element values. In Figure 4.3, notch response is obtained by tuning the cross-coupling inductor L13.

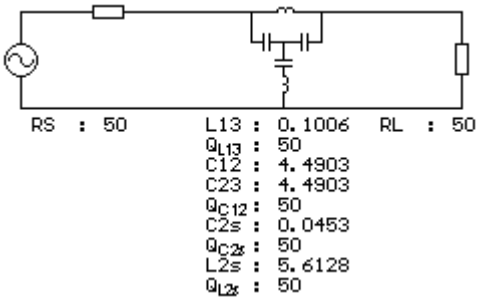

Figure 4.3 Circuit with Detuned L13.

The element L13 forms a parallel resonator with C12 and C23. When L13 is changed, if the resonance frequency is desired to remain the same then C12 and/or

C23 should also be changed. In the example design C12 and C23 are left unchanged and the resonance frequency is allowed to change. If L13 is increased then a notch appears below the center frequency while a notch appears above the center frequency if L13 is decreased. Note that as shown in Figure 4.4, a deep notch is obtained in spite of lossy elements. It is also possible to obtain a notch response by tuning C12 or C23 or both.

Notch Property	Value
Notch Depth	-59.021dB (at 10292MHz)
Average Passband Insertion Loss	0.2dB
3dBc Stopband BW	1310 MHz
20dBc Stopband BW	188 MHz
30dBc Stopband BW	59 MHz

(a)

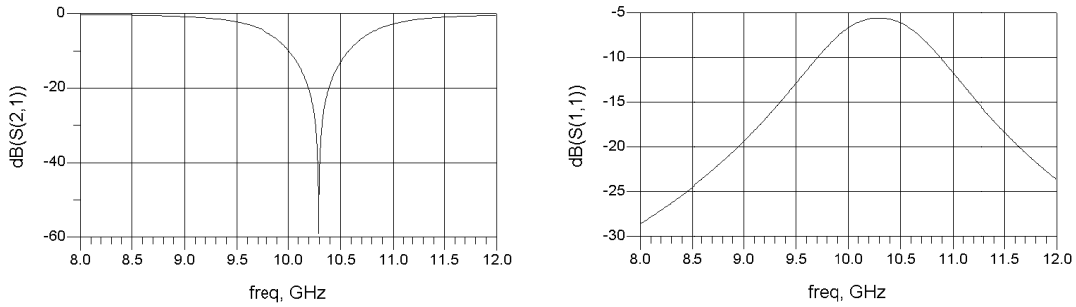

(b)

Figure 4.4 Frequency Responses of the Filter with Detuned L13.
(a) Notch Characteristics. (b) Frequency Responses.

3) Experimentation shows that the same notch response can be obtained by tuning L2s instead of L13 or by tuning both L13 and L2s. Also the notch frequency can be shifted by tuning the capacitors C2s, C12 and C23. This result can be useful both for modifying element values to make too high or too low values better and for tuning the center frequency. For the latter

case, either tuning of L13-L2s or C2s-C12-C23 can be used to change the center frequency. Figure 4.5 shows tuning results of the example filter by tuning of C2s and C12=C23.

Tuning Capacitor Values (pF)	Center Frequency (MHz)	3dBc Stopband BW (MHz)
C2s=0.0603 , C12=C23=6.0343	8899	1160
C2s=0.0503 , C12=C23=5.0003	9760	1252
C2s=0.0453 , C12=C23=4.4903	10292	1310
C2s=0.0363 , C12=C23=4.4923	10874	1311
C2s=0.033 , C12=C23=4.0933	11399	1368

(a)

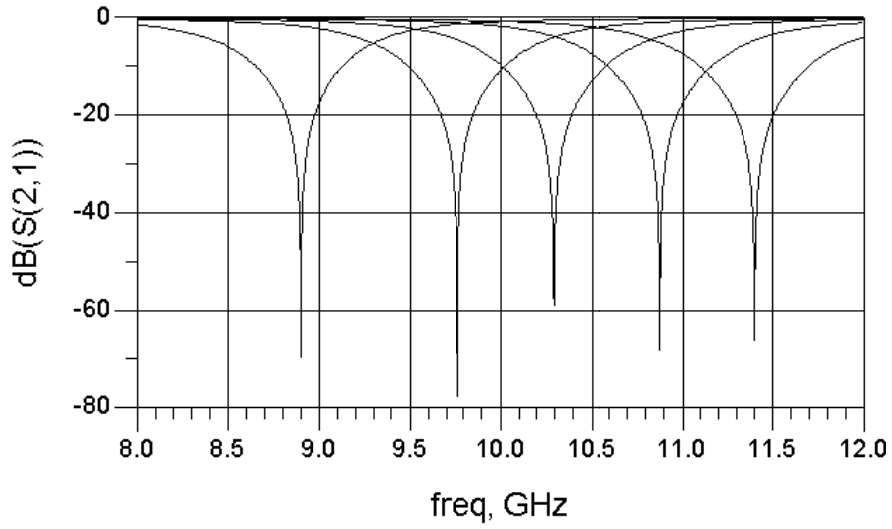

(b)

Figure 4.5 Frequency Responses of the Filter During Tuning.
(a) Table of Tuning Results. (b) Tuning Responses.

As seen in Figure 4.5, by tuning C2s and C12=C23 center frequency of the notch is tuned between 8.9GHz - 11.4GHz and deep notch depth is conserved during the tuning. Note that in previous designs in Chapter 2 and 3, as notch center frequency

gets away from initial center frequency, notch depth decreases and beyond a frequency band notch depth goes below satisfactory values. However, in this filter and also in all other all-pass filter approaches, deep notch depth can be conserved for a very large frequency bandwidth. This is the main advantage of all-pass filter approach. In this case the limiting factor for tuning range is generally 3dBc bandwidth which indicates the increase or decrease in stopband bandwidth during tuning of center frequency.

To sum up, bridged tee all-pass filter sections can be used to obtain good notch responses with lossy elements and center frequency of the notch can be tuned while deep notch depth conserved. The tuning range is determined not from notch depth degradation during tuning like the designs in previous chapters. Instead, changes in stopband bandwidth can get unsatisfactory values beyond a frequency band. This tuning range is much wider than the previous designs. The element values of the example filter have very small value elements like L13 and C2s and also this lumped topology is unrealizable for microwave frequencies. So this readily available all-pass topology is suitable for lower frequencies. For high frequency applications like X-Band, the following all-pass filters which are formed by bridging a BPF or a BSF are suitable.

4.3 Distributed Element All-Pass Filters

4.3.1 Introduction

A readily available distributed element all-pass filter topology which is suitable for conversion into notch filter is composed of a 3dB directional coupler (PCL or BLC) and two identical lossless resonators. The resonators are connected to direct and coupled ports of the directional coupler and isolated port is used as output. When the resonators are detuned a notch appears between input and output at a frequency within the passband of the directional coupler. This property of directional couplers is extended to other topologies which can present all-pass behavior. One novelty of this thesis is that it is demonstrated that a notch filter can be synthesized using

distributed BSF or BPF in a systematic way. The filters are first converted into an all-pass filter by introducing a quarter wavelength TL cross coupling the input and output which serves as phase shifter. If two lossless resonators are tuned to the same frequency we get a perfect all-pass filter by adjusting the signal levels of the path. After formation of the all-pass filter, resonance frequencies of the two resonators are detuned exposing a sharp and deep notch. Both approaches yield notch filters which are tunable over broad bandwidths and with notch depths much higher than the classical BSF's.

4.3.2 BLC Type All-Pass Topology

An all-pass filter can easily be created by using a 3dB directional coupler like a PCL or a BLC. A 3dB directional coupler works as an all-pass circuit if direct and coupled ports are loaded with identical lossless bandpass resonators. If the resonance frequencies of the two resonators are made different then a notch appears, converting the all-pass circuit into a notch filter. Note that for narrowband bandstop response, PCL directional couplers do not give satisfactory results. They are better useful for notches with wide stopband bandwidth. In this approach, BLCs, specifically impedance transforming 3dB BLCs, are more convenient since it allows realizable element values when narrowband notch response is desired. The design steps for an example filter are as follows:

1) Consider an impedance transforming 3dB BLC as shown in Figure 4.6.a. An all-pass response is obtained by addition of bandpass resonators (shunt parallel LC resonators) to ports 2 and 3. For realization in microwave frequencies, instead of lumped LC resonators, short circuit stubs can be used as bandpass resonator. Moreover, inverters except K23' can be realized by quarter wavelength TLs and tuning capacitors can be added in parallel with SC stubs for tuning center frequency as shown in Figure 4.6.b.

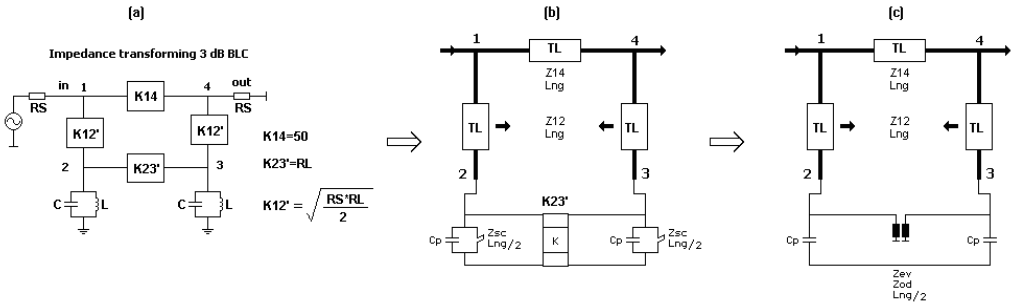

Figure 4.6 BLC Type All-Pass Filter Topology and Transformations.
(a) Full Inverter Topology. (b) TL Topology with only K23'' Inverter.
(c) Realizable Topology.

Note that to obtain realizable element values of C_p and Z_{sc}, value of K23' inverter should be very high for narrowband notch response. This inverter with very high value can be realized by using the transformations in Figure 3.19 of previous chapter and finally the schematic of the notch filter becomes as shown in Figure 4.6.c.

In the first design stage, circuit in Figure 4.6.b is used and the design stage starts with choosing initial values for Z_{sc}, C_p, Lng and K23'. The design of this topology is easier when circuit parameters RL (=K23'), tuning capacitor value (C_p), quarter wavelength (Lng) and impedance of SC stubs (Z_{sc}) are found manually instead of exact calculations. Value of Z14 is always 50Ω and Z12 depends on the chosen value of K23' and Z14 from BLC forming equations. K23' determines the notch bandwidths of the filter. As K23' increases notch bandwidth decreases. For a good notch filter, stopband bandwidth should be narrow, meaning high values for K23'. However K23' limits the minimum possible notch bandwidth due to realization problems occurring for too high values of K23'. Value of C_p depends on quarter wavelength (Lng) or in other words center frequency of the BLC. SC stub impedance determines input impedance of comb PCL configuration and also affects center frequency of the notch with chosen C_p values. Consider the following starting values: C_p=0.3pF, Lng=7.4948mm (f_0:10GHz), RL=K23'=1000 and Z_{sc}=50Ω. The initial all-pass circuit and its frequency responses are as shown in Figure 4.7.

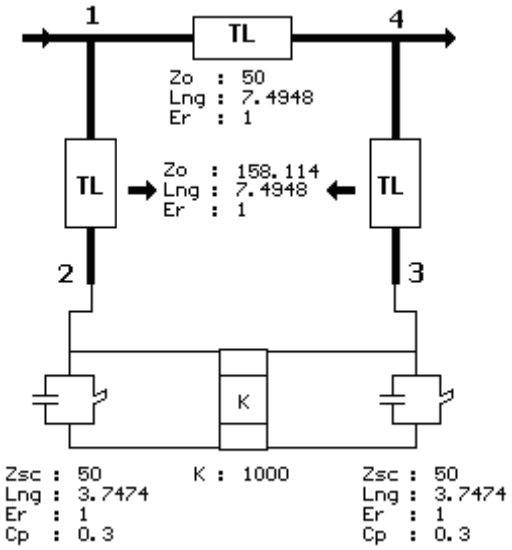

(a)

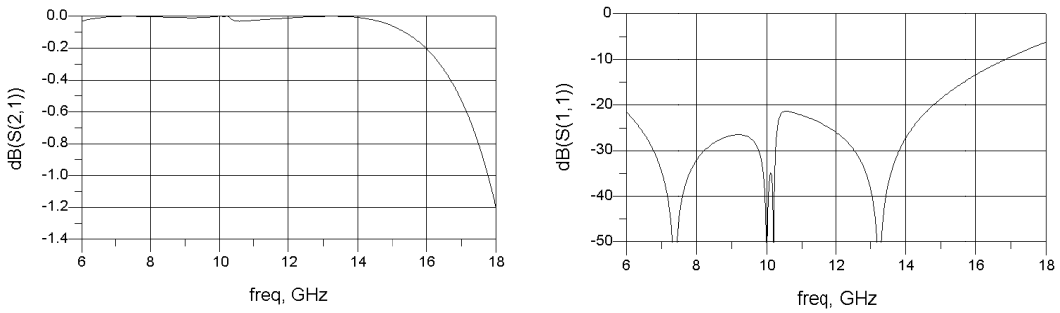

(b)

Figure 4.7 Initial All-Pass Design.
(a) Circuit. (b) Frequency Responses.

2) A wideband all-pass response is observed in Figure 4.7. However, for any chosen RL=K23' value, a wideband all-pass response can be obtained when identical lossless bandpass resonators are connected to ports 2 and 3. So the suitable value of K23', C_p and Lng which determine notch bandwidth and center frequency of the notch, can not be understood from this all-pass response. In this case, a notch response is obtained by detuning of one capacitor and then center frequency and notch bandwidths are checked. An appropriate response is tried to be reached by setting a trial value for K23' and C_p and checking the notch response for convenience. After a few trials, a

suitable response can be obtained. When one of the tuning capacitor is tuned to 0.3317pF to obtain a deep notch in the example circuit the following frequency responses in Figure 4.8 are obtained.

Notch Property	Value
Notch Depth	-56.532dB (at 10027MHz)
3dBc Stopband BW	462 MHz
20dBc Stopband BW	145 MHz
30dBc Stopband BW	80 MHz

(a)

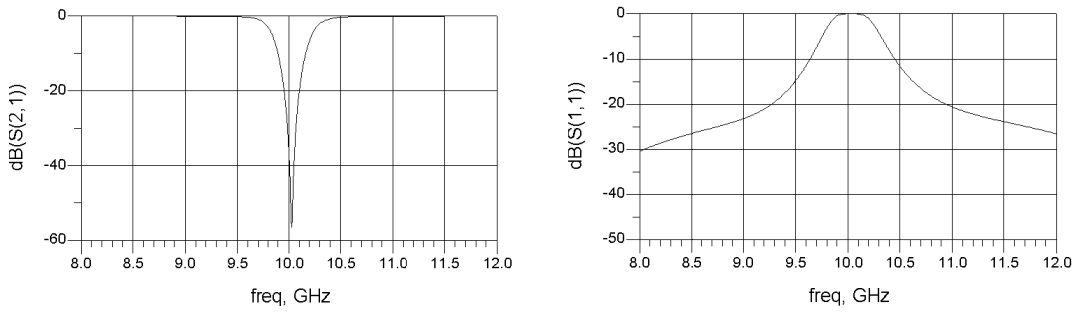

(b)

Figure 4.8 Checking of Notch Response.
(a) Notch Characteristics. (b) Frequency Responses.

For RL=K23'=1000, the given notch bandwidths in Figure 4.8.b are obtained. To decrease bandwidths, K23' should be increased. In the example circuit, K23' is renewed as 1200 for narrower bandwidths. Note that center frequency of the notch is very close to desired center frequency which is 10 GHz. So, C_p and Lng parameters have suitable values. If C_p is chosen higher than 0.3pF, center frequency of the notch when capacitor values are around initial chosen values become lower than the desired center frequency with the same Lng value. To compensate this, Lng value should be decreased meaning increasing center frequency of the notch filter.

With the new K23' and same C_p and Lng values, updated all-pass circuit is formed and then tuning capacitors are tuned to obtain a deep notch at center frequency (10GHz). The resultant filter and its frequency responses are as shown in Figure 4.9.

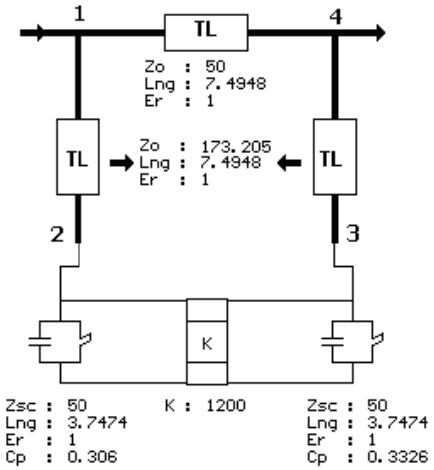

(a)

Notch Property	Value
Notch Depth	-59.752dB
3dBc Stopband BW	390 MHz
20dBc Stopband BW	122 MHz
30dBc Stopbband BW	67 MHz

(b)

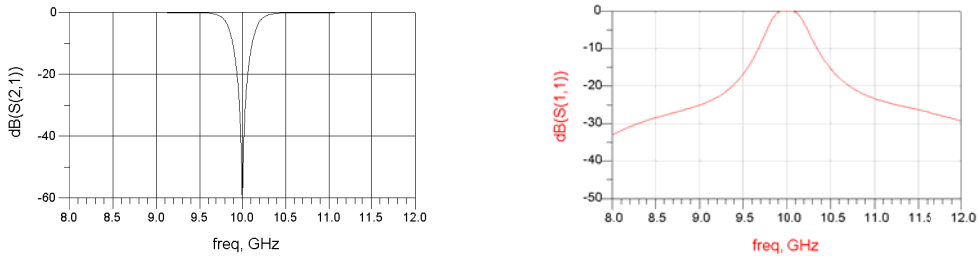

(c)

Figure 4.9 Circuit with Detuned K23' and Capacitors.
(a) Circuit. (b) Notch Characteristics. (c) Frequency Responses.

3) K23' inverter and two shunt SC stubs are transformed to comb type PCL by using the transformations given in Figure 3.19. Then circuit losses are added to the design. When losses are added, notch depth decreases. This can be compensated by slight tuning of both capacitors. In the example circuit, capacitor Q values are taken as 50 and capacitors are slightly tuned to achieve a deep notch. The resultant circuit and its frequency responses are shown in Figure 4.10.

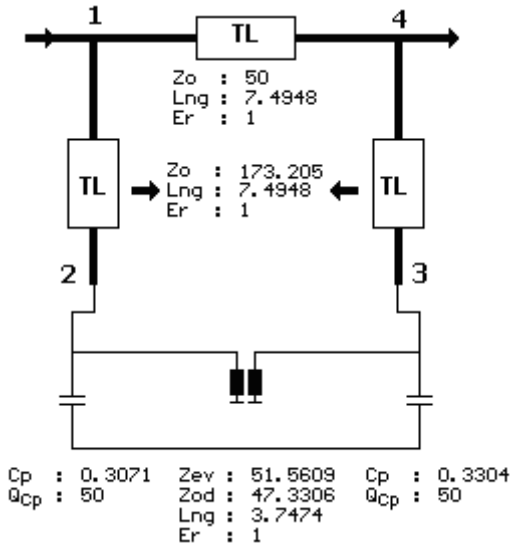

(a)

Notch Property	Value
Notch Depth	-61.442dB
3dBc Stopband BW	512 MHz
20dBc Stopband BW	79 MHz
30dBc Stopband BW	25 MHz

(b)

Figure 4.10 Frequency Responses of Final Circuit.
(a) Circuit. (b) Notch Characteristics.

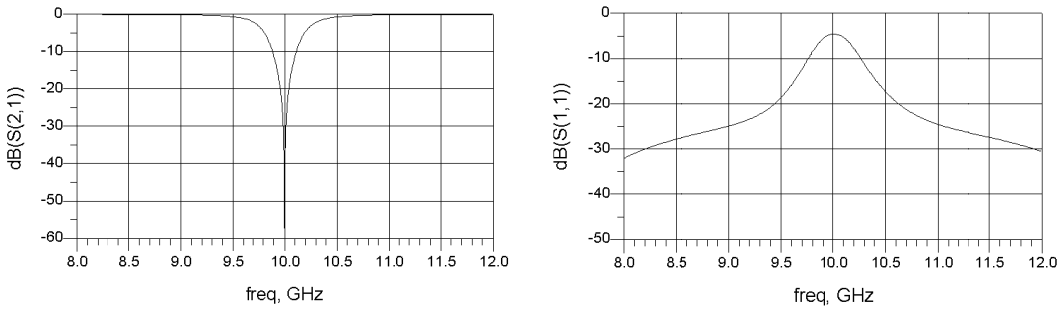

(c)

Figure 4.10 (continued) (c) Frequency Responses.

4) Notch center frequency can be changed by tuning of capacitors. When the capacitors are tuned between minimum of 0.1pF and maximum of 0.6pF, the results are as shown in Figure 4.11.

Tuning Capacitor Values (pF)	Center Frequency (MHz)	3dBc Stopband BW (MHz)
Cp1=0.5869 , Cp2=0.6	7993	408
Cp1=0.4282 , Cp2=0.45	8976	451
Cp1=0.3113 , Cp2=0.3345	10000	512
Cp1=0.2 , Cp2=0.2223	11371	626
Cp1=0.1 , Cp2=0.1203	13139	873

(a)

Figure 4.11 Tuning Results of Final Circuit.
(a) Table of Tuning Results.

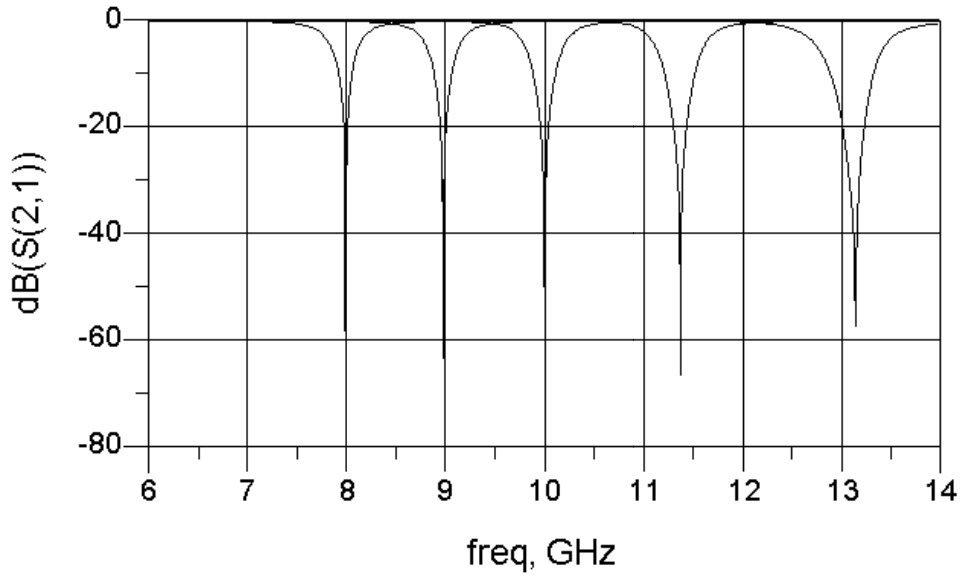

(b)

Figure 4.11 (continued) (b) Tuning Responses.

Deep notch depth is conserved during a wide tuning range over 5GHz as seen in Figure 4.11. As center frequency increases, notch bandwidths also increases and vice versa. This can be a limitation for determining the tuning range if notch bandwidths become too wide or too narrow after a frequency interval.

4.3.3 Bridged BPF type All-Pass Topology

An effective topology for designing an all-pass filter is the one given in section 3.3.2 in previous chapter namely PCL splitter/combiner containing topology. In the given section, a narrowband BPF is designed and bandpass response is transformed to bandstop response by addition of a bridge delay line. However in all-pass filter approach, the narrowband BPF is first transformed to an all-pass filter by tuning PCL splitter/combiner parameters and then all-pass filter is transformed to bandstop response by detuning of resonators. The design steps for an example design which uses the same initial design specification in Figure 3.19 are as follows:

1) An initial circuit is synthesized using FILPRO Synthesis tool with the following specifications in Figure 4.12.

Synthesis	Distr, BPF, Cheby
Ripple (dB)	0.001
Passband Corners (MHz)	9950-10050
Degree	4 (3Nzero, 1Ninf)
f_q (MHz)	20000

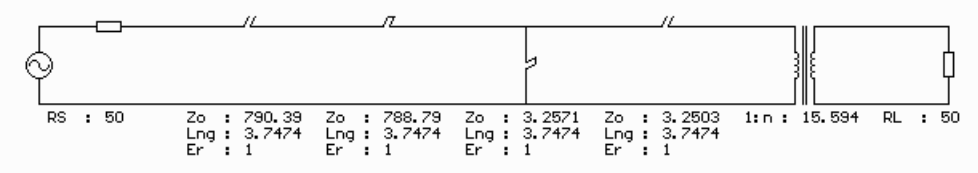

Figure 4.12 Initial Circuit.

2) L-section SC stubs in the middle of initial circuit are transformed to Symmetric Pi-section SC stubs and quarter-wave 50Ω TLs are inserted to input and output of the circuit. Then 50Ω TL and series OC stub pair in input and output of the circuit are transformed to interdigital type PCL equivalent as shown in Figure 4.13.

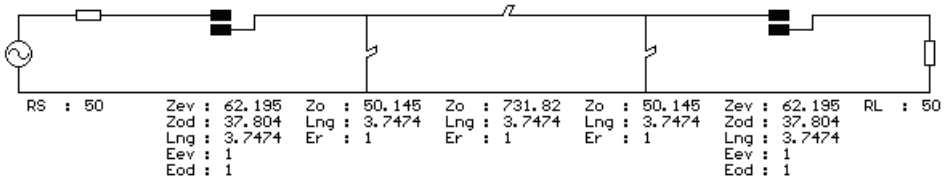

Figure 4.13 Addition of PCLs and Pi-Section SC Stubs.

3) Pi-section SC stubs in the middle of the circuit are transformed to comb type PCL equivalent and 50Ω quarter wavelength delay line is connected to PCL splitter/combiners as shown in Figure 4.14.

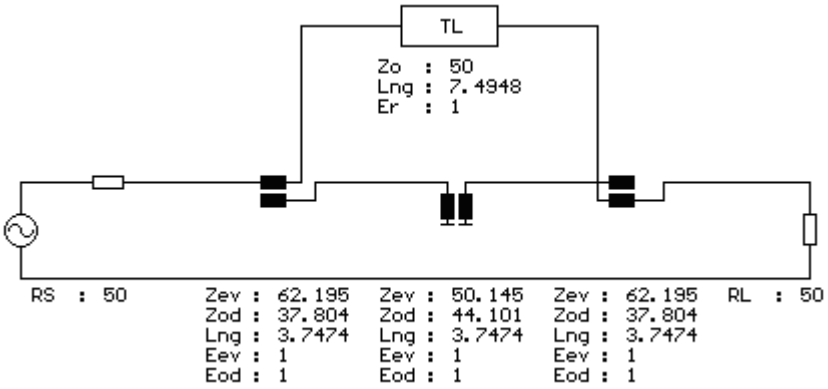

Figure 4.14 Addition of Comb type PCL and Delay Line Bridge.

4) Capacitor loaded OC stubs are added to ground connected ports of comb PCL configuration so that tunable resonators are added to the circuit. Then coupling characteristics of PCL splitter/combiners (Z_{ev}, Z_{od}) are changed manually until an all-pass response is obtained and all-pass design stage is completed. In this stage, circuit losses are not considered. The resultant all-pass filter and its frequency responses are shown in Figure 4.15. Impedance of capacitor loaded OC stubs are chosen as 50Ω and tuning capacitors are chosen as 0.5pF.

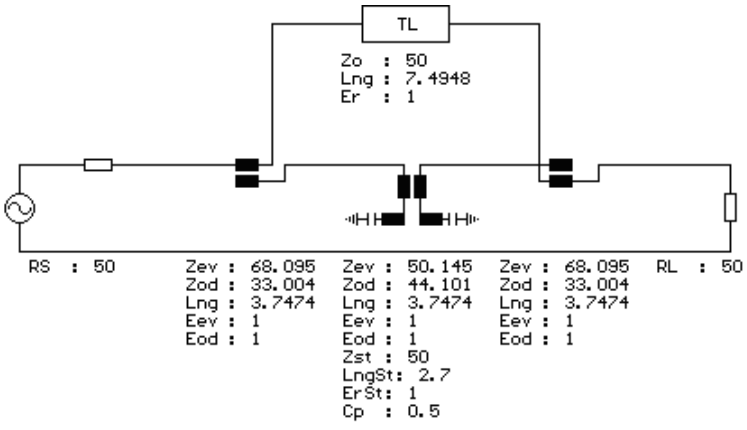

(a)

Figure 4.15 All-Pass Circuit.
(a) Circuit.

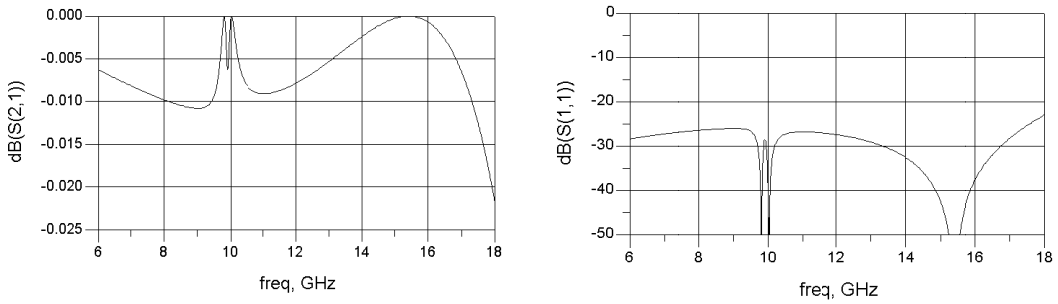

(b)

Figure 4.15 (continued) (b) Frequency Responses.

Note that all-pass response is observed for a wide frequency range (6-18GHz). In order to transform bandpass response to all-pass response, even mode impedance (Z_{ev}) of PCL splitter/combiners is increased and odd mode impedance (Z_{od}) is decreased until a proper all-pass response is obtained. In the example, these impedances are tuned until return loss is below 25dB around center frequency (10 GHz).

5) After all-pass response is obtained, circuit losses are added to the design and center frequencies of the resonators are detuned. Performing manual optimization of capacitors, a deep notch is obtained at the center frequency. Different from the topologies in previous chapters, center frequency of the resonators are not identical. Instead, center frequency of a resonator is below filter center frequency and center frequency of the other resonator is above filter center frequency. The resultant circuit and its frequency responses when this approach performed are shown in Figure 4.16. Lossy capacitors with Q=50 are used.

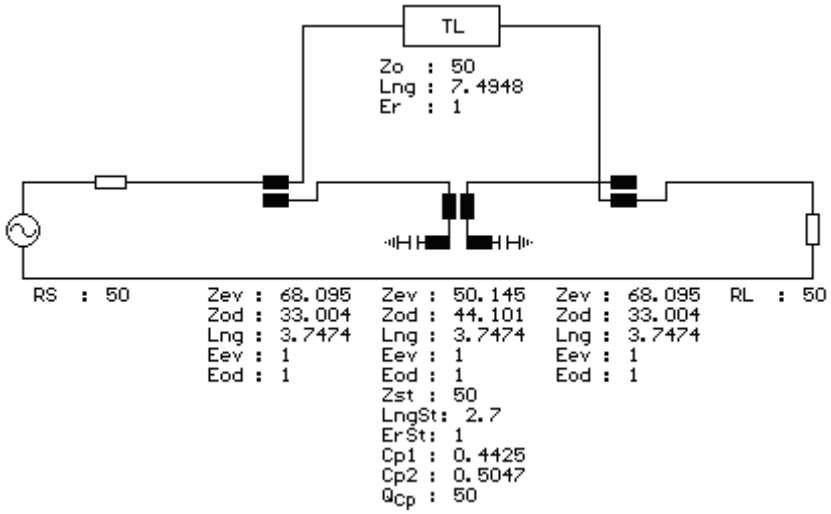

(a)

Notch Property	Value
Notch Depth	-67.933dB
3dBc Stopband BW	441 MHz
20dBc Stopband BW	93 MHz
30dBc Stopband BW	34 MHz

(b)

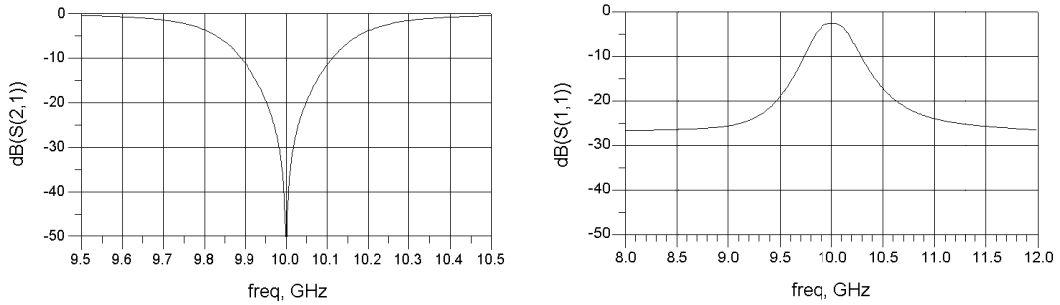

(c)

Figure 4.16 Notch Filter.
(a) Circuit. (b) Notch Characteristics. (c) Frequency Responses.

A deep notch is obtained as shown in Figure 4.16. Note that the capacitors should be adjusted preciously for a very deep notch.

6) Notch center frequency can be changed by tuning of capacitors. When the capacitors are tuned between minimum of 0.1pF and maximum of 1.5pF, the results are as shown in Figure 4.17.

Tuning Capacitor Values (pF)	Center Frequency (MHz)	3dBc Stopband BW (MHz)
Cp1=1.264 , Cp2=1.5	8415	352
Cp1=0.78 , Cp2=0.9	9045	388
Cp1=0.4425 , Cp2=0.5047	10000	441
Cp1=0.25 , Cp2=0.2879	11107	511
Cp1=0.1 , Cp2=0.1235	12740	637

(a)

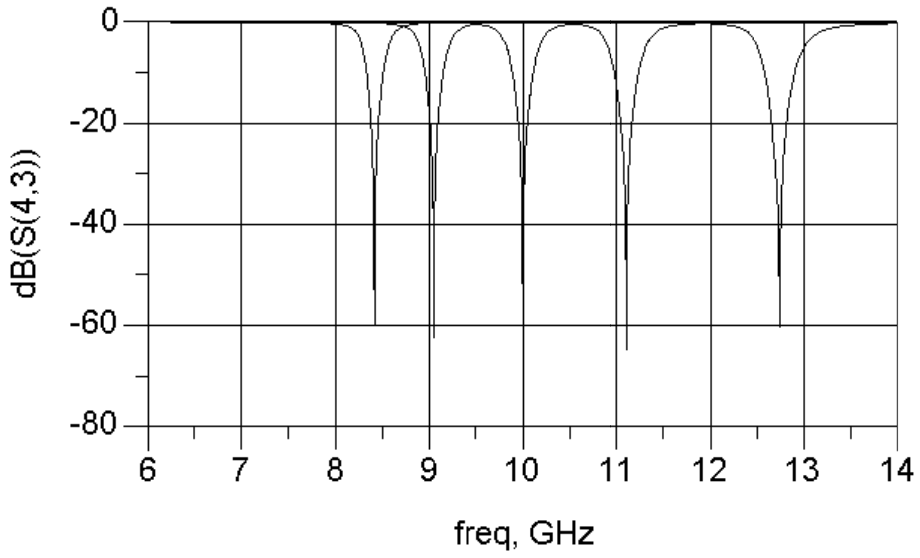

(b)

Figure 4.17 Tuning Results of Notch Filter.
(a) Table of Tuning Results. (b) Tuning Responses.

Deep notch depth is conserved during a wide tuning range over 4GHz as seen in Figure 4.17. Notch center frequency can be tuned even further with high notch depth when tuning capacitors are increased over 1.5pF. As center frequency increases,

notch bandwidths also increases and vice versa. This can be a limitation for determining the tuning range if notch bandwidths becomes too wide or too narrow after a frequency interval.

4.3.4 Bridged BSF type All-Pass Topology

All-pass filter response can also be obtained by a bridged BSF. A suitable topology for this purpose is directly connected delay line bridged BSF in section 3.2.2 in previous chapter. In this case, first a BSF is designed and then a cross-coupling quarter wavelength line is introduced to convert the BSF to all-pass filter by manual optimization of some parameters of BSF and impedance of delay line. Then all-pass filter response is transformed to bandstop response by detuning of resonators. The design steps for an example design which uses the same initial design specification in Figure 2.17 are as follows:

1) An initial circuit is synthesized using FILPRO Synthesis tool with the following specifications in Figure 4.18.

By Synthesis	Distr, LPF, Cheby
Ripple (dB)	0.01
Passband Corner (MHz)	9800
Transmission Zeros	2 Ninf, 3 NUE
Degree	5
f_q (MHz)	10000

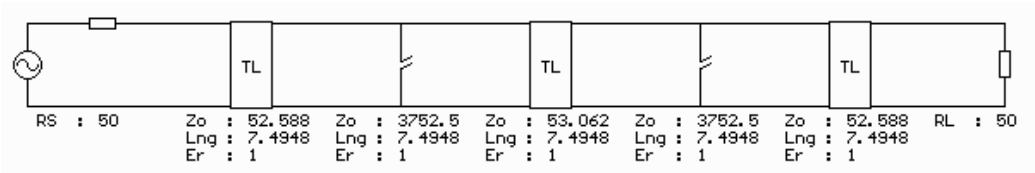

Figure 4.18 Initially Synthesized Circuit.

2) TL + shunt OC stub pairs in input and output are transformed to PCL equivalent configuration by using PCL L-resonator transformation in

Figure 2.18 of Chapter 2. Z_{ev} is chosen as 62Ω. Then tuning capacitors with initial value of 0.5pF are added to OC stub resonators of PCL configurations and lengths of OC stubs are shortened to turn the center frequency of resonators back to initial value. Then a bridging quarter wavelength delay line with an arbitrary initial high impedance value (which is taken as 100Ω for the example filter) is connected to input and output of the example filter as shown in Figure 4.19.

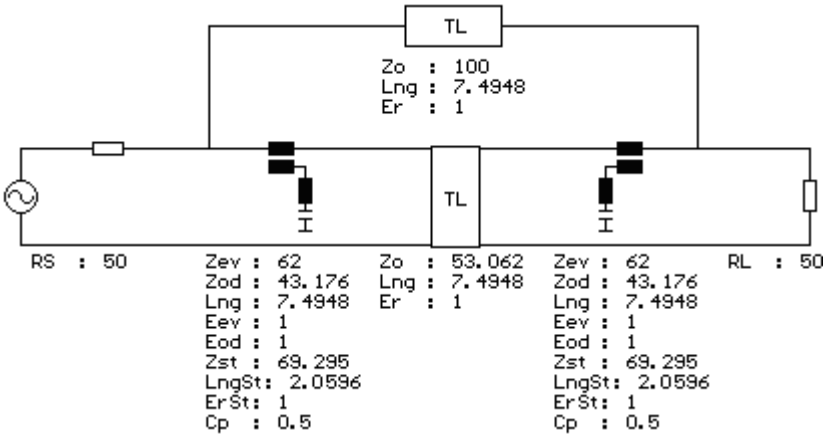

Figure 4.19 PCL L-resonator Transformations and Delay Line Bridge Addition.

3) Impedance of bridge line and the middle TL in Figure 4.19 are tuned until an all-pass filter response for an acceptable frequency range around center frequency is obtained. Note that in this topology, pure all-pass response can not be achieved. Even for lossless case, a small amount of notch depth is seen in the center frequency. Also, return loss and passband loss performances depend on the chosen impedance of tuning TLs. There is a trade-off between the chosen passband bandwidth and return loss performance. In the example circuit middle TL in the main filter is tuned to 80Ω and impedance of bridge line is tuned to 120Ω. The resultant all-pass circuit and its frequency responses of this filter are given in Figure 4.20.

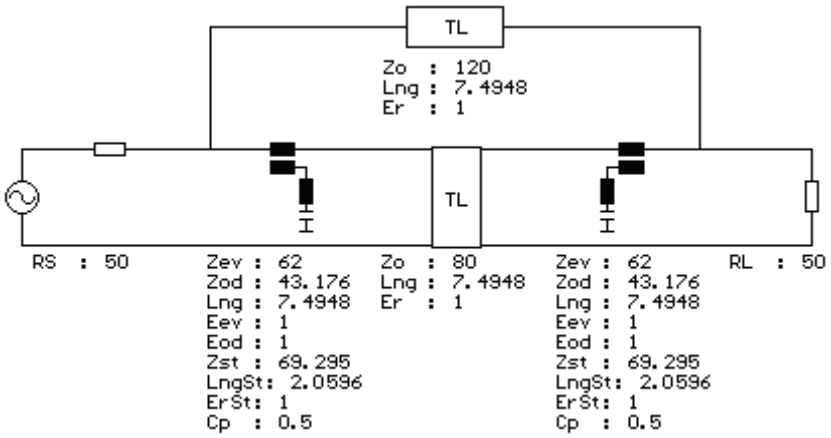

(a)

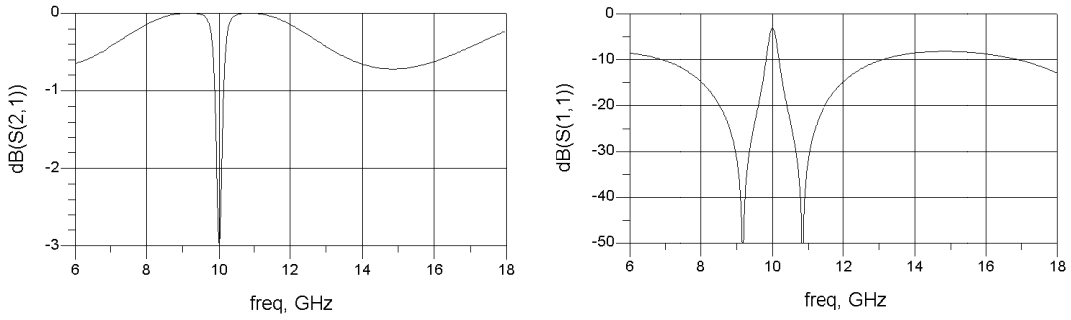

(b)

Figure 4.20 All-Pass Circuit.
(a) Circuit. (b) Frequency Responses.

Note that all-pass response obtained from BSF is obtained only for a limited frequency range around center frequency. At center frequency, an approximately 3dB notch is seen. Outside this notch around 0.6dB ripple exist in passband and return loss is below 15dB for a limited frequency range around center frequency.

4) After all-pass response is obtained, circuit losses are added to the design and center frequencies of the resonators are detuned. Performing manual optimization of capacitors, a deep notch is obtained at the center frequency. The resultant circuit and its frequency responses when this approach performed are shown in Figure 4.21. Lossy capacitors with Q=50 are used.

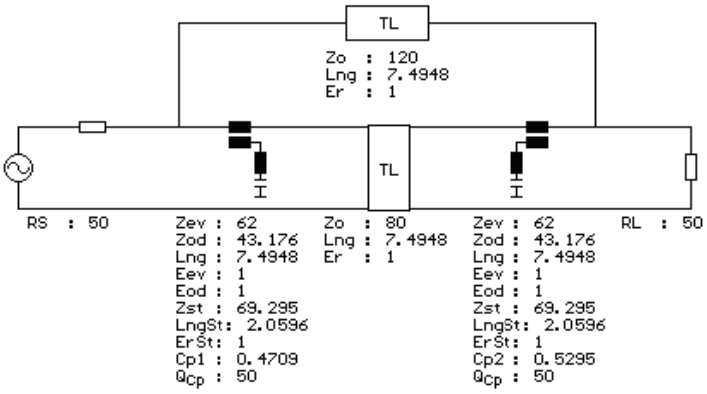

(a)

Notch Property	Value
Notch Depth	-63.254dB
Average PB Insertion Loss	0.1dB
3dBc Stopband BW	468 MHz
20dBc Stopband BW	96 MHz
30dBc Stopband BW	36 MHz

(b)

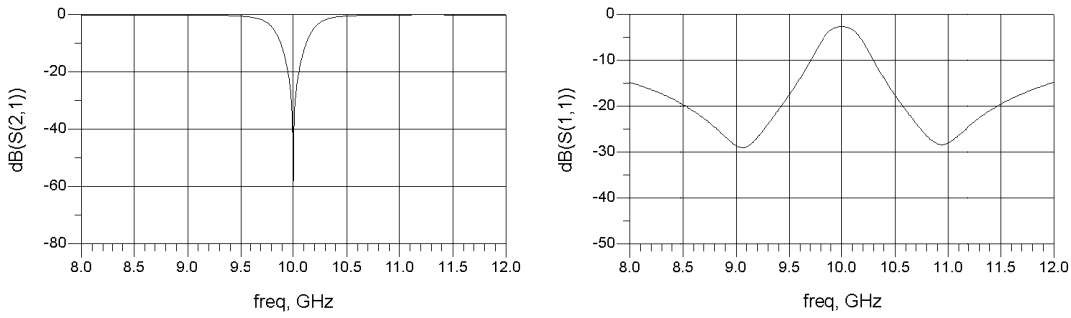

(c)

Figure 4.21 Notch Filter.
(a) Circuit. (b) Notch Characteristics. (c) Frequency Responses.

A deep notch is obtained as shown in Figure 4.21. As in the previous cases, the capacitors should be adjusted preciously for a very deep notch. Return loss goes below 15dB outside 8-12GHz.

5) Notch center frequency can be changed by tuning of capacitors. When the capacitors are tuned between minimum of 0.1pF and maximum of 1.5pF, the results are as shown in Figure 4.22.

Tuning Capacitor Values (pF)	Center Frequency (MHz)	3dBc Stopband BW (MHz)
Cp1=1.231 , Cp2=1.5	8481	390
Cp1=0.773 , Cp2=0.9	9103	439
Cp1=0.4709 , Cp2=0.5295	10000	468
Cp1=0.25 , Cp2=0.269	11468	388
Cp1=0.1 , Cp2=0.103	13675	226

(a)

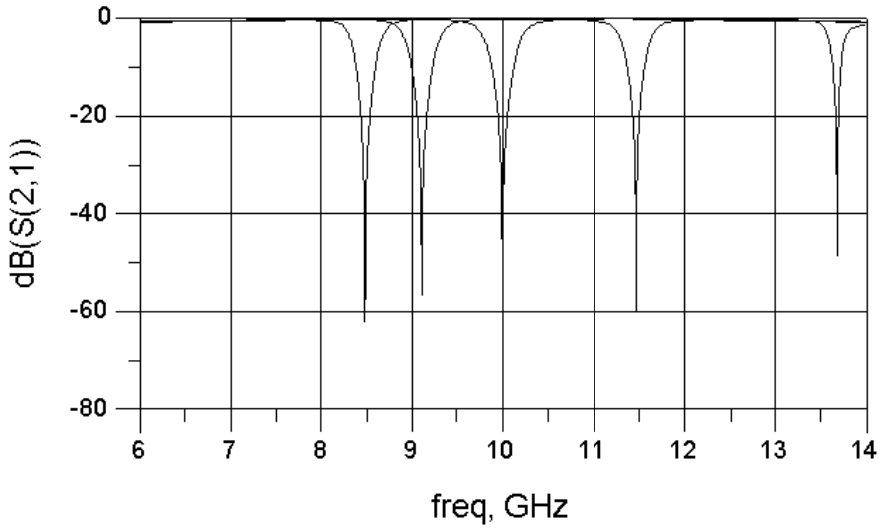

(b)

Figure 4.22 Tuning Results of Notch Filter.
(a) Table of Tuning Results. (b) Tuning Responses.

Deep notch depth is conserved during a wide tuning range over 5GHz as seen in Figure 4.22. Notch center frequency can be tuned even further with high notch depth when tuning capacitors are increased over 1.5pF as in the previous topology. As

center frequency is tuned away from the initial center frequency, notch bandwidths decreases different from the previous topology. So this can be a limitation for determining the tuning range if notch bandwidths becomes too narrow after a frequency interval. However main limitation for tuning range for this topology is the distortion in passband response (and return loss degradation) outside a frequency range.

4.4 Remarks

In this chapter, all-pass filter approach is introduced and bandstop filter topologies using this approach are given. Example filters with 2 resonators are designed and frequency responses are presented. It is shown that a high performance tunable notch filter can be obtained using all-pass filter approach. This approach is in fact an improvement over phase cancellation method, which is better useful for fixed notches.

CHAPTER 5

PROTOTYPE DESIGNS

5.1 Introduction

After the analysis of various filter topologies to design tunable notch filter in microwave frequencies, it is seen that best filter characteristics are obtained in all-pass filter approach according to the linear simulation results in which only tuning capacitor losses are considered. However, this approach should also be analyzed considering lossy circuit elements & transmission medium by using a realistic transmission medium and tuning capacitor (varactor) model to understand whether it will give good filter characteristics in practice. For this purpose, three prototype designs are done using all-pass filter approach. The topologies used are BLC type All-Pass filter of section 4.3.2, bridged BPF type All-Pass filter of section 4.3.3 and Bridged BSF type All-Pass filter of section 4.3.4. Initial designs of these prototype notch designs are performed in FILPRO. Circuit modifications and determination of physical parameters are done in ADS. EM simulation analysis are performed mainly in SONNET and also checked in CST. Finally these three designs are manufactured using the layouts of EM simulations and measurements are taken.

5.2 Fabrication & Measurement

All three prototype filters are designed in suspended stripline substrate (SSS) medium. The main reason of choosing SSS is some element values in prototype designs which are not possible to realize in microstrip form using standart PCB techniques. Low dissipation loss of SSS medium is also another reason that can improve filter performances. The dielectric material of SSS medium is Rogers RT/Duroid 5880 with dielectric constant of 2.2 and thickness of 10 mils and the air gap height of SSS medium is chosen as 39.37 mils (1mm) as shown in Figure 5.1. PCBs of these filters are manufactured in ILFA GmbH, a PCB manufacturer located

in Germany. Conductor lines are ¼ oz copper line with Galvanic Gold plating (4 um Ni and 1um Au).

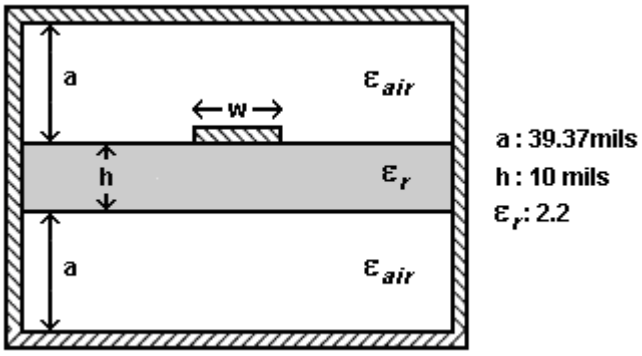

Figure 5.1 Cross Section of SSS Medium Used in Prototypes.

In these filters, MV20001 & MV20002 model GaAs varactor diodes of Microsemi are used. The datasheet of MV20000 series varactor diodes is given in appendix. To minimize package parasitics, unpackaged die form varactors are used. Information about varactor diode modeling, measurement and bias path used in example designs are given in section 5.3.

The mechanical cavities for SSS filters are manufactured in UYGUR Ltd. Şti. The mechanical tolerances of these cavities (especially air gap distance) are very important in SSS medium. These boxes are produced with air gap tolerances +-0.025mm. In order to reduce dissipation losses of SSS medium, cavities are plated with gold. A filter cavity is composed of two components: body with open top side and top cover which closes the open side of the body.

In order to connect these SSS cavities to network analyzer for measurement, SMA connectors and seal transitions are used in input and output of prototype filters. Also DC feedthrus are used to transmit DC bias to the filter bias path from outside. In prototype filters, M/A-COM Omni Spectra hermetic seals, Dynawave Inc. SMA Jack connectors and Special Hermetic Products, Inc DC hermetic feedthrus are used.

After varactors and bias elements are assembled to a PCB, this board is placed on the body. Seal transitions are mounted by conductive epoxy to the body and input & output lines of the board are soldered to open ends of seal transitions. Then connectors are mounted on the body and when top cover is placed on open side of body, the filter becomes ready for measurement.

The connections of varactors and bias elements to each other and layout are done by welding and bonding machines present in clean room facility of ASELSAN. The bondings for bias elements are performed using ball bonder machine Kulicke Soffa AG 4124 shown in Figure 5.2.a. Gold wire of diameter 1mil is used for bonds. Welding of varactors and DC feed thrus are performed using Unitek Peco Model UB25 welding machine shown in Figure 5.2.b. The pre-bonded ribbons of varactors have 3mils width and 10 mils width gold ribbons are used in DC feed thru connections.

(a)

Figure 5.2 Bonding and Welding Machines Used for Assembling.
(a) Bonding Machine.

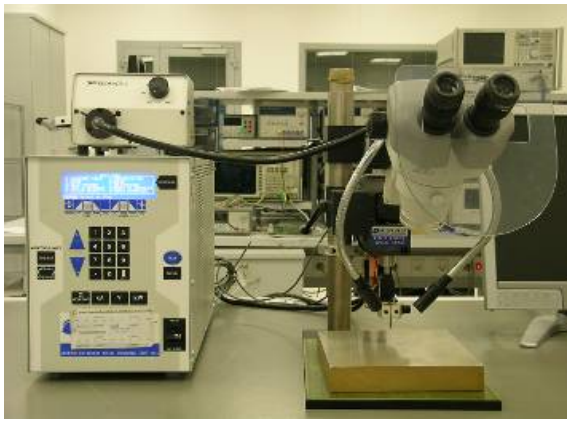

(b)

Figure 5.2 (continued) (b) Welding Machine.

The measurements are taken using Agilent E8362B PNA network analyzer. Since different DC biases should be given to varactors, two DC power supplies of Agilent E3631 are used. The measurement setup is shown in Figure 5.3.

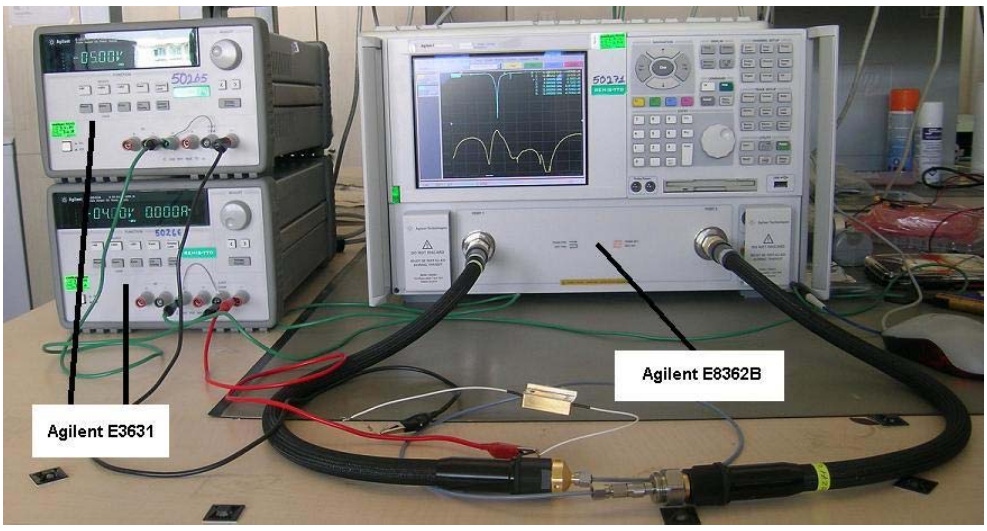

Figure 5.3 Measurement Setup.

5.3 Varactor Diodes

5.3.1 Basics

Varactor diodes, also called varicap diodes or just varactors, are the key elements which enables tuning of resonator center frequencies in prototype filters. They are semiconductor devices that are widely used in applications where a voltage controlled variable capacitance is required. A varactor consists of a PN junction which is optimized for its function as a variable capacitor. When the diode is in forward bias, PN junction allows current flowing (DC or AC) which is not desired for a capacitor. However in reverse bias, depletion region of the diode behaves like capacitor and capacitance of the diode depends on the width of depletion region which changes with applied reverse voltage. Hence varactors are always used in reverse bias.

The equivalent circuit model and the physical model corresponding to the equivalent circuit for most varactors are shown in Figure 5.4.

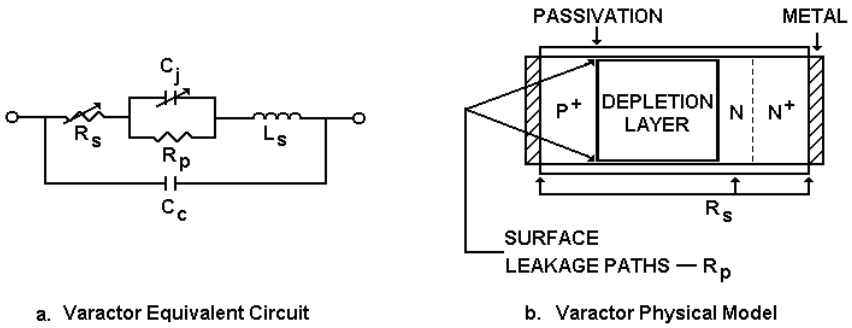

Figure 5.4 Varactor Equivalent Models.

In Figure 5.4, C_j is the variable depletion layer capacitance, R_s is the series resistance (contacts, leads and bulk resistance), and R_p is the parallel or leakage resistance across the junction. The case capacitance C_c and lead inductance L_s are important at microwave frequencies. The most important characteristics of a varactor diode are

capacitance value & capacitance-voltage change behavior, quality factor, and reverse breakdown voltage.

These characteristics depend on a number of factors including cross section area and length of depletion region, dielectric constant and dissipation loss parameter of semiconductor material and doping characteristics. There are two types of varactors classified according to the abruptness of PN junction named as abrupt and hyperabrupt. The type of the diode affects the tuning slope or gamma of the diode. Gamma parameter is used to characterize capacitor-voltage behavior of the diode. Abrupt varactors generally offer high level of Q factor and hyperabrupt varactors offer large changes in capacitance for a relatively small voltage change. As stated before, capacitance value of the diode depends on the width of depletion region and width of the depletion region inversely proportional to the reverse bias voltage. Maximum capacitance of a varactor is obtained at 0V reverse bias and minimum capacitance is obtained at reverse breakdown voltage.

5.3.2 Modeling & Measurement

The typical equivalent circuit model of a packaged varactor diode is shown in Figure 5.4.a. The equivalent circuit can be formed by using the information given in datasheet of the varactor. This equivalent circuit gives starting information about the performance of the diode. However for better modeling, after the formation of initial varactor model, parameters of the equivalent model should be updated by measuring an actual diode.

In prototype designs, MV20001 and MV20002 varactor diodes are used. These GaAs diodes have abrupt junctions and they are in unpackaged die form with a pre-bonded ribbon (named as 02 style outline). The physical structure of these diodes is given in Figure 5.5. Firstly, equivalent circuit model of these diodes are formed using datasheet given in the appendix. For equivalent circuit model, C_j, R_s, R_p, C_c and L_s are parameters should be found. C_j, R_s and R_p parameters depend on PN junction and C_c & L_s parameters depend on package.

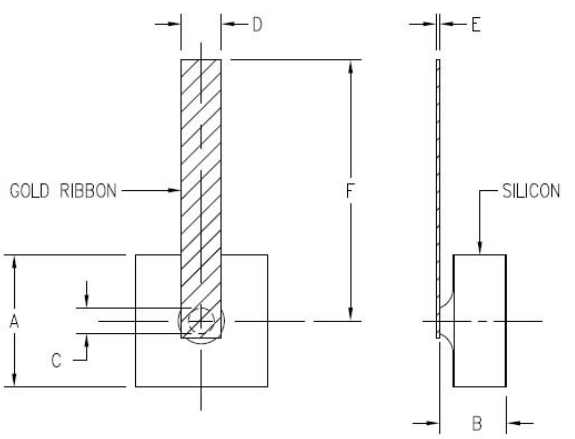

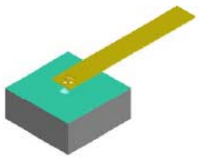

DIM	INCHES		MM	
	MIN	MAX	MIN	MAX
A	0.015	0.050	0.254	0.381
B	–	0.005 TYP	–	0.127 TYP
C	SEE NOTES		–	–
D	–	.003 TYP	–	.0762
E	–	.00025 TYP	–	.00635
F	.100	–	2.54	–

Figure 5.5 Physical Structure of 02 Outline MV20000 Series Varactors

Since the diodes are in die form, there is no package so package capacitance C_c can be taken as 0pF. The diode is connected to the filter via gold ribbon with 3 mils thickness which creates significant series inductance, so L_s parameter will take place in equivalent circuit.

The main diode parameter C_j can be found using the datasheet of varactor. Since these are abrupt junction diodes, gamma parameter is always 0.5. For an abrupt junction diode, capacitance and reverse bias voltage can be related using the following diode equation:

$$C_j = \frac{C_0}{\sqrt{(\frac{V}{\Phi}) + 1}} \qquad \textbf{(5-1)}$$

V: reverse bias voltage (has positive value), changes between 0V and V_B (breakdown voltage)

C_0: Zero-bias capacitance (when V=0V)

Φ: Built-in potential voltage, 1.3V for GaAs.

The dissipation losses of varactors are due to R_s and R_p resistances and these parameters determine Q factor of the varactor. In practice, R_p resistance value takes

very high values (e.g., on the order of tens of megaohms), so this parameter can also be neglected. Hence the loss parameter of a varactor can be modeled by a single series resistor. A resistance value for this parameter can be extracted from Q values given in datasheet of the varactor using the following formula.

$$R_s = \frac{1}{2\pi f_0 Q_{f_0} C_v} \qquad \textbf{(5-2)}$$

f_0: Frequency at which given Q value (Q_{f_0}) is measured (typically 50MHz)

C_v: Capacitance of diode for a given reverse bias (typically at 4V)

R_s value is found for a specific reverse bias voltage in (5-2). This value changes for different reverse bias voltages. However in equivalent circuit model, this value is taken as constant.

Note that in datasheets Q values of varactors are always given at low frequencies (ex. 50MHz) which have quite high values (ex. 8000 for MV20001) for GaAs abrupt diodes. However, this value is inversely proportional with frequency and gets very low values for high frequencies. For example at 10GHz Q of MV20002 can be approximated as 40.

From datasheet given in appendix and by using equations (5-1) and (5-2), the initial equivalent circuits of MV20001 and MV20002 varactors are given in Figure 5.6. Note that series inductance L_s is taken as 0.3nH. In practice, the value of L_s changes with the length of ribbon between varactor terminal and layout and since this length will always be different in each assembly. So an average estimated inductance value of 0.3nH is used in equivalent circuits.

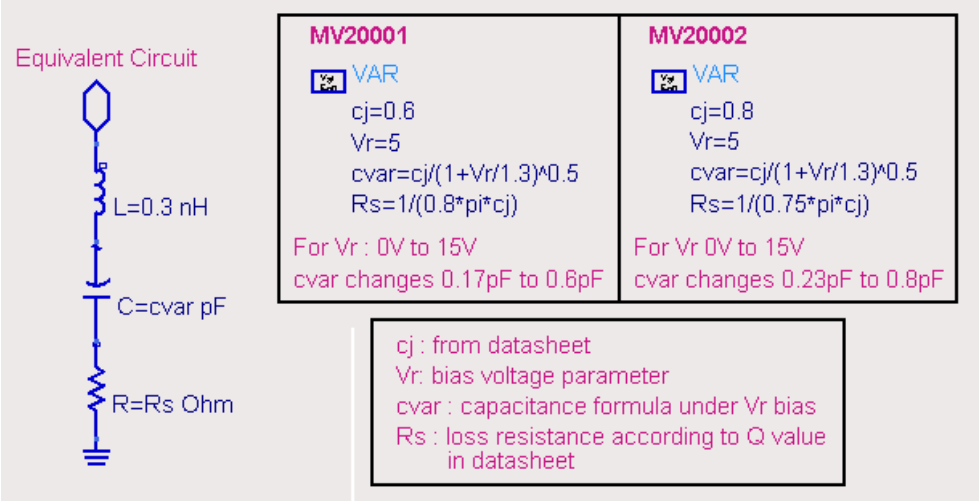

Figure 5.6 Initial Equivalent Circuits of MV20001 & MV20002 Varactors.

As stated before, it is better to update this initial varactor model in Figure 5.6 by measuring actual varactors. For this purpose, MV20001 and MV20002 varactors are measured by one port s-parameter measurement using the technique in [15]. In this technique, varactors are connected to end of a 50Ω TL piece, whose length is known, in shunt configuration and S11 of this configuration is measured by using network analyzer. For different bias voltages, measurements are taken. These measurements are then imported to a RF circuit simulator. The phase responses of S11 measurements are compared with initial equivalent circuit with different bias voltages and parameters of equivalent circuit are manually adjusted to give close results with measurement results. To apply this approach, the measurement test fixture in Figure 5.7.a is formed. In text fixture, a 50Ω microstrip line and an SMA connector is mounted on a metal piece as seen in Figure 5.7.a. Then a varactor is placed over a gold disc to elevate and the ribbon at top terminal of varactor is welded to end of microstrip line. Between network analyzer port and SMA connector of fixture, model 5585 Bias Tee of Picosecond Pulse Labs is connected for biasing the varactor. The equivalent circuit found by this way is shown in Figure 5.7.b. These final equivalent circuits are used in designing prototype tunable notch filters. Note that loss parameters of the varactor diode can not be extracted by this measurement technique. Also L_s value also varies according to the length of ribbon used. So in this

measurement only capacitance of varactor can be measured and as seen in Figure 5.7.b, it is close to the initial equivalent circuit value in Figure 5.6.

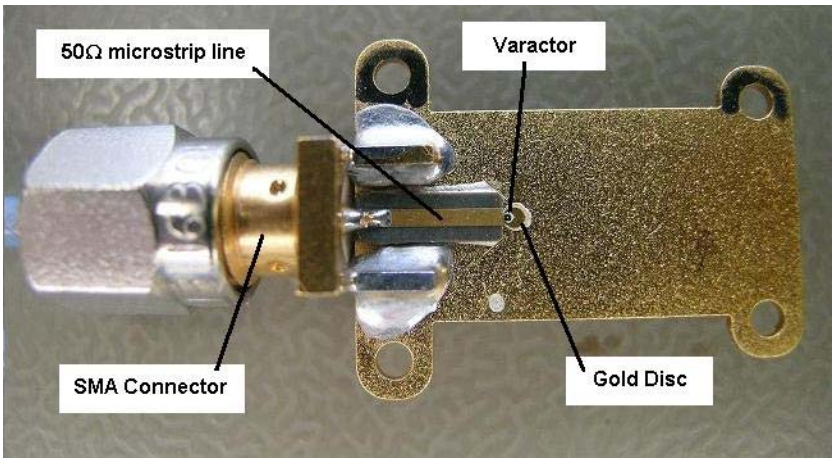

(a)

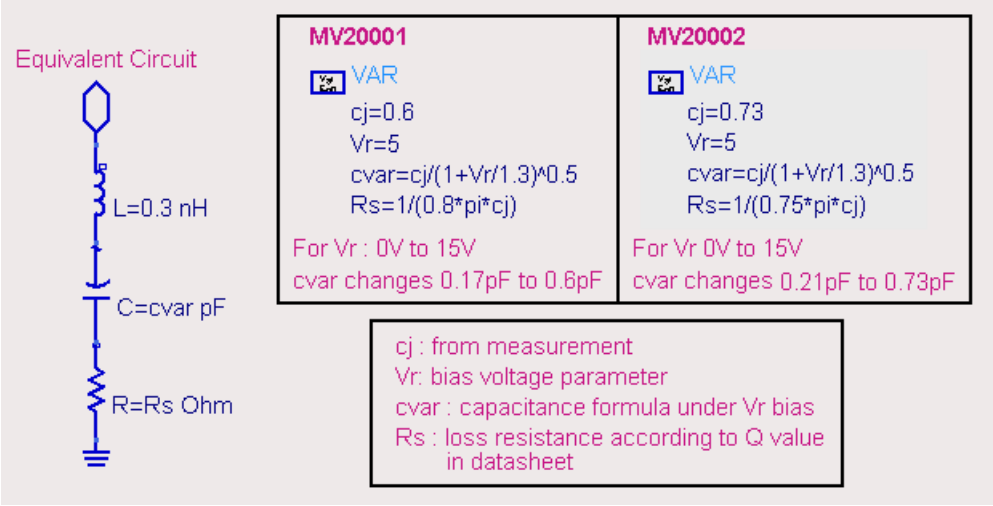

(b)

Figure 5.7 Measurement Test Fixture & Final Equivalent Circuits for Varactors. (a) Test Fixture. (b) Final Equivalent Circuits.

In prototype designs, bias circuit of varactors will be composed of only two resistors and a capacitor. Varactors are used in shunt configuration and in reverse bias, so DC current can not pass through varactor. This enables to use high value resistors in bias path instead of choke inductors. For biasing, two 4kΩ thin film resistors (8kΩ total)

of MSI Inc. and one 56pF single layer ceramic capacitor of Presidio Comp. Inc. are used. The schematic of the bias circuit is shown in Figure 5.8. In all prototype designs this bias circuit model will be used. Note that there is also a series inductor in the model. This inductor represents the effect of the bond used to attach the resistors to the layout and its estimated value is used.

Figure 5.8 Bias Circuit Model Used in Prototype Designs.

5.4 Bridged BPF Type Notch Filter

5.4.1 Linear Circuit Design & EM Simulations

The design of the prototype filter starts with synthesis of a narrowband BPF using synthesis tool of FILPRO as in first design step given in Chapter 4.3.3. An initial circuit is synthesized and first a narrowband BPF in FILPRO is obtained. Filter synthesis specifications, detailed list of transformations applied and the final BPF circuit are given in Figure 5.9.

Synthesis	Distr, BPF, Cheby
Ripple (dB)	0.01
Passband Corners (MHz)	9400-9600
Degree	4 (3Nzero, 1Ninf)
f_q (MHz)	19000

(a) Design Specifications

Figure 5.9 Formation of Realizable Narrowband BPF.

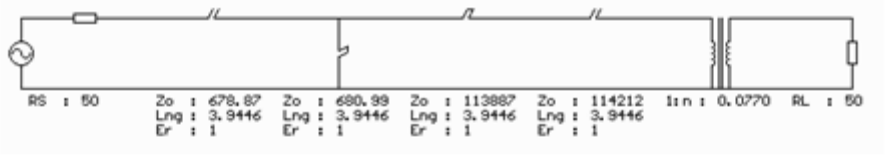

(b) Synthesized Circuit

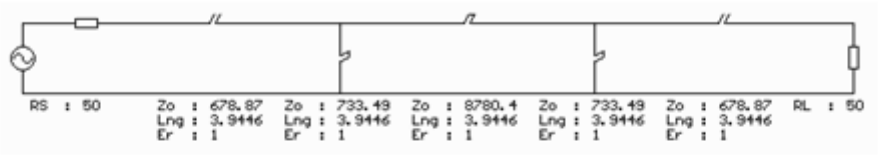

(c) L-Section SC Stubs to Pi-Section SC Stubs

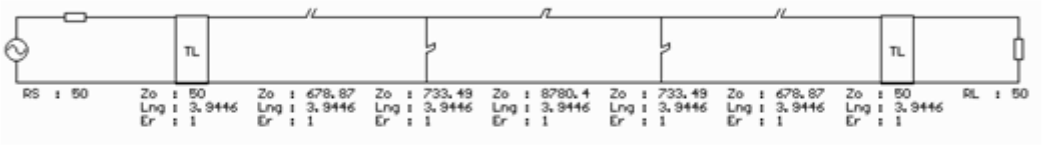

(d) 50Ω TLs Addition

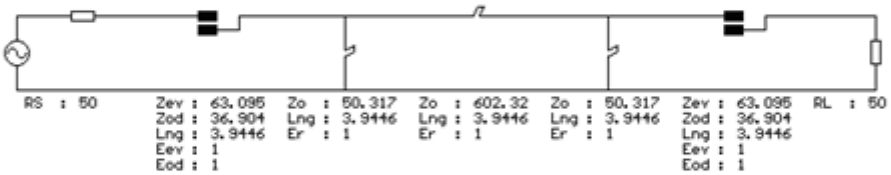

(e) Introduction of Edge-Coupled PCLs

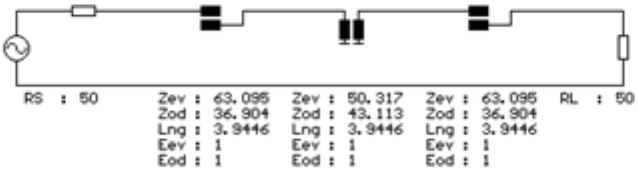

(f) Addition of Comb PCL

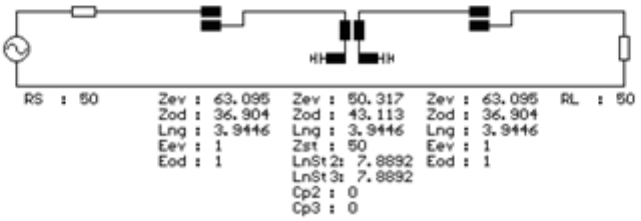

(g) Capacitor Addition to Comb PCL

Figure 5.9 (continued)

Note that center frequency of BPF is chosen as 9.5GHz. The tuning range of the tunable notch filter will be estimated after the addition of varactor diode models. The initial aim for the center frequency of the tuning range is 9.5GHz.

After the formation of the realizable narrowband BPF with tuning capacitor added, design stage in FILPRO is finished. The final circuit in Figure 5.9.g is transferred to ADS. Note that although tuning capacitors are added to the schematic, their values are 0pF for now. Their values will be added in ADS.

In ADS, first the bridge quarter wavelength 50Ohms TL is added to the circuit. Then capacitor values are entered. For now, lossless capacitors are used in the circuit. In this prototype filter, MV20002 model varactors will be used. According to the equivalent model of this varactor in Figure 5.7.b, capacitance change is expected between 0.21pF to 0.73pF. So for an initial value, capacitors are chosen as 0.4pF and OC stubs are shortened to preserve center frequency. Then even & odd mode impedances of interdigital PCLs are tuned to get an all-pass response. The resultant filter and its frequency responses are given in Figure 5.10. Note that the initial value for the capacitors and corresponding stub length are not critical. Capacitors could also be left as 0pF. In the following steps, they will be changed according to varactor model and layout.

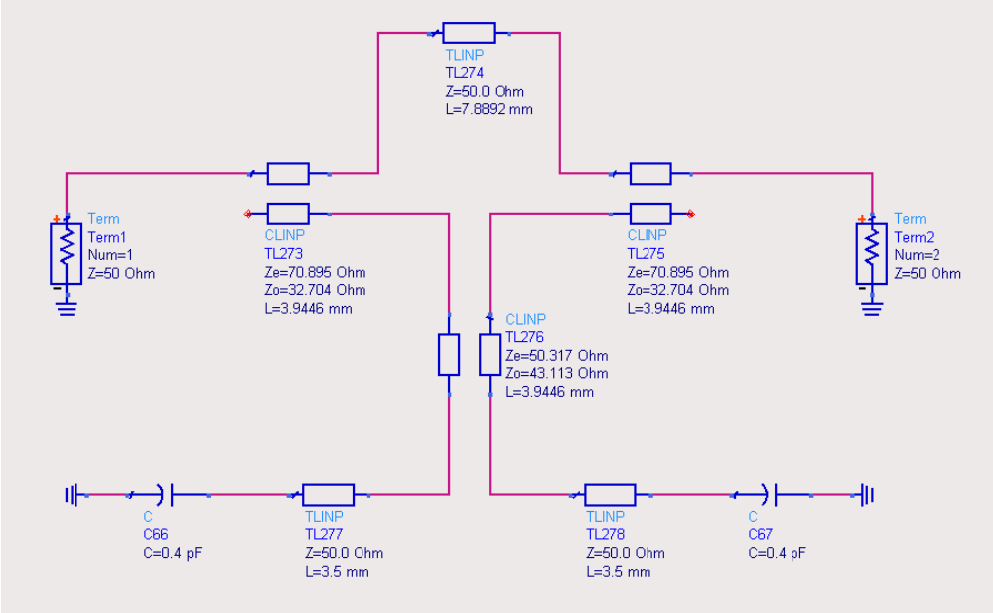

(a)

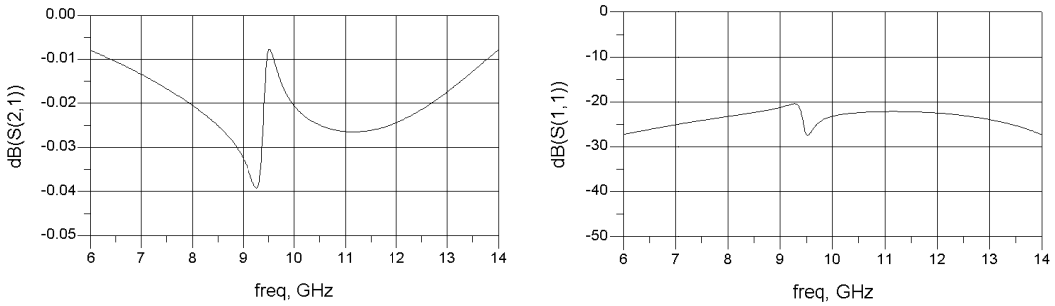

(b)

Figure 5.10 All-Pass Circuit.
(a) Circuit. (b) Frequency Responses.

The next step is to design a physically realizable layout for this filter schematic. Note that interdigital PCLs have -8.67dB coupling, which is a tight coupling, and comb type PCL has -22.26dB coupling, which is a loose coupling. In SSS, broadside offset coupled lines can be used to realize interdigital PCLs for this level tight coupling. So both side of the Duroid substrate will be used in this case. Coupling of comb type PCL can be achieved by side coupling. The problematic part of the schematic in Figure 5.10.a is the connection of interdigital PCLs to the comb PCL in the layout. Normally there should be a bend in the connection which means addition of a TL piece in between PCLs. This should be taken into account since it changes the filter

response. Fortunately, the effect of this bend will only be a shift in center frequency. So this can easily be compensated by shortening the length of OC stubs. However it can be such that this shift in center frequency cannot be compensated fully if the required shortening exceeds length of OC stubs. The effect of the bends can only be understood by EM simulation and the amount of the shortening in OC stubs can be decided according to EM simulation results.

The final SONNET layout of prototype filter and its circuit representation are given in Figure 5.11. The layout formation of the filter begins with design of PCLs. For this purpose, firstly physical parameters of interdigital and comb type PCLs are determined using ADS SSS model and are shown in Figure 5.11.a. As seen in the figure, comb type PCL have realizable values, but interdigital PCLs have very close spacing which can not be realized. Since there is no model for broadside offset coupled lines, these PCLs are designed individually by using EM simulation. However in circuit schematic, side coupled line model, which gives close frequency responses to offset coupled line, is left for representation of interdigital PCLs. Comb type PCLs are also designed individually using EM simulation. After the individual designs of PCLs, the bends that are necessary to connect PCLs to each other are designed using EM simulation. These bends are represented by 50Ω TL pieces in filter schematics of Figure 5.11.a and the length of these bends is derived from EM simulation results. After the design of PCLs and bends, 50Ω quarter-wave bridge line is introduced to the layout. Note that varactor model in Figure 5.7.b is used and to be able to add these models to EM simulation results, wall ports are introduced to ends of comb type PCL. SONNET layout formed after many trials is shown in Figure 5.11.b.

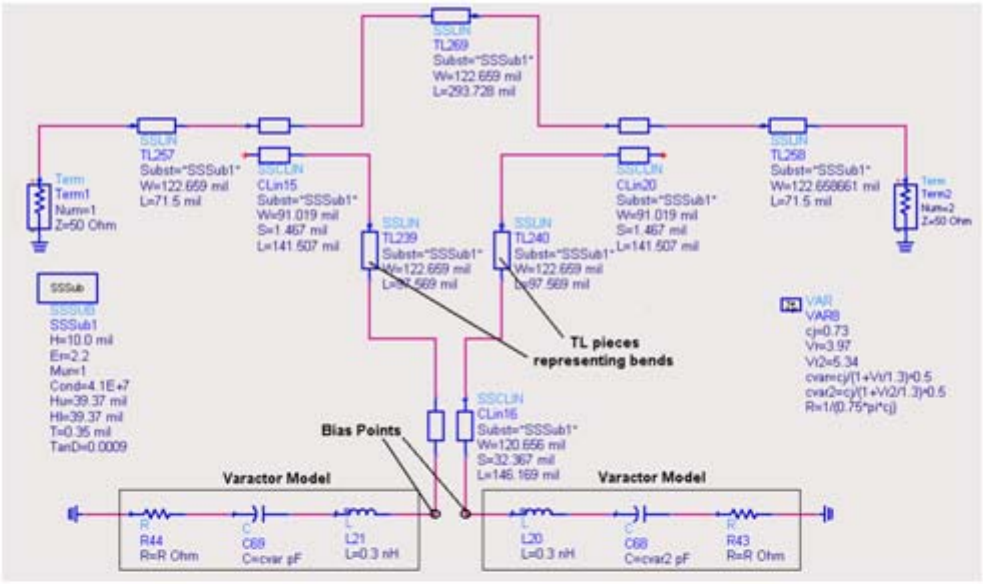

(a)

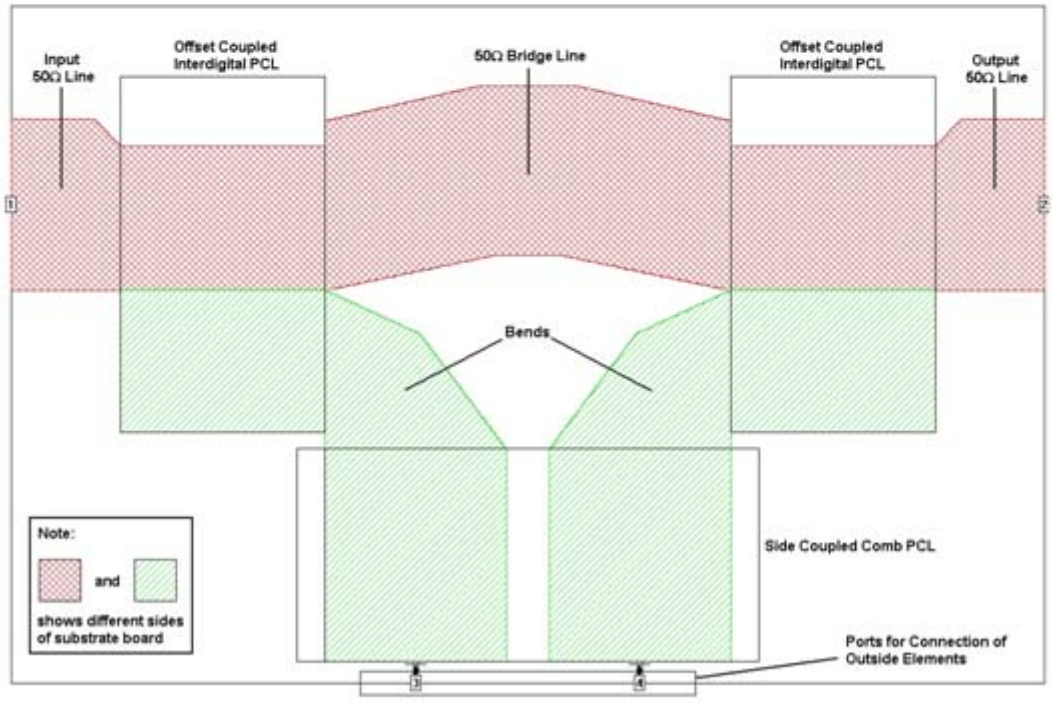

(b)

Figure 5.11 Final Filter Schematic and its SONNET Layout.
(a) ADS Schematics. (b) SONNET Layout

In the initial all-pass filter of Figure 5.10.a, tuning capacitors are connected to open ends of OC stubs. However in Figure 5.11.b, OC stubs are discarded to compensate

the frequency shift effects of bends. So varactors are directly connected to ends of comb type PCL.

In SONNET simulation, box metals and conductors are chosen as lossy metal (gold) and dielectric loss of substrate is included. After the execution of the simulation, simulation results are exported from SONNET in Touchstone format (s4p) and the results are analyzed in ADS. In analysis, varactor models are introduced to EM simulation results by using extra ports defined in SONNET layout.

The filter layout designed by SONNET is also simulated in CST for better evaluation. The 3D layout view in CST is given in Figure 5.12. Same with SONNET design, additional ports are introduced in CST to be able to connect varactor models to EM simulation result and simulation data is exported in Touchstone format to be evaluated in ADS.

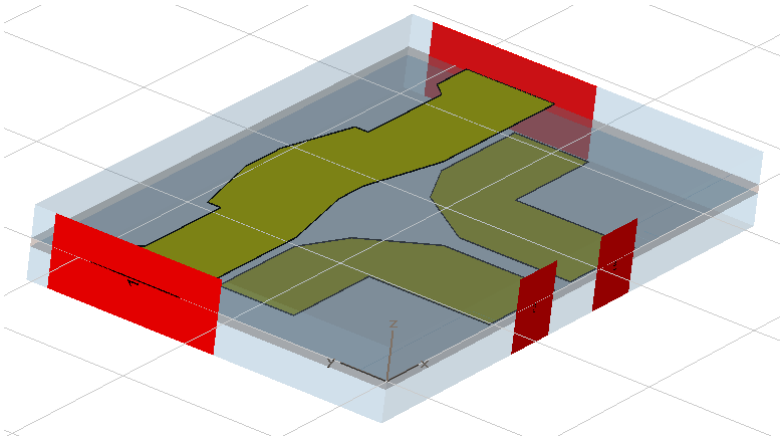

Figure 5.12 CST 3D Layout View.

After the simulations, all the results are combined in ADS and filter characteristics such as stopband bandwidths, notch depth, tuning range, return loss are investigated. For different capacitance values of varactors, the results for ADS SSS model simulation, SONNET simulation and CST simulation are given in Figure 5.13, Figure 5.14 and Figure 5.15 respectively. Note that bias points of this filter is at the

ends of comb PCL which is the same place with connection point of varactors. The bias circuit model in Figure 5.8 is connected to bias points in all three simulations and effects of the bias circuit are also included in the following figures.

Varactor Bias Voltage (pF)	Center Frequency (MHz)	Notch Depth (dB)	3dBc BW (MHz)	20dBc/30dBc BW (MHz)
Cp1=0 , Cp2=0.351	8140	-39.913	370	70/25
Cp1=3.72 , Cp2=5	9440	-71.486	440	100/40
Cp1=7.66 , Cp2=10	10090	-47.841	490	110/50
Cp1=11.57 , Cp2=15	10500	-57.225	530	130/50

(a)

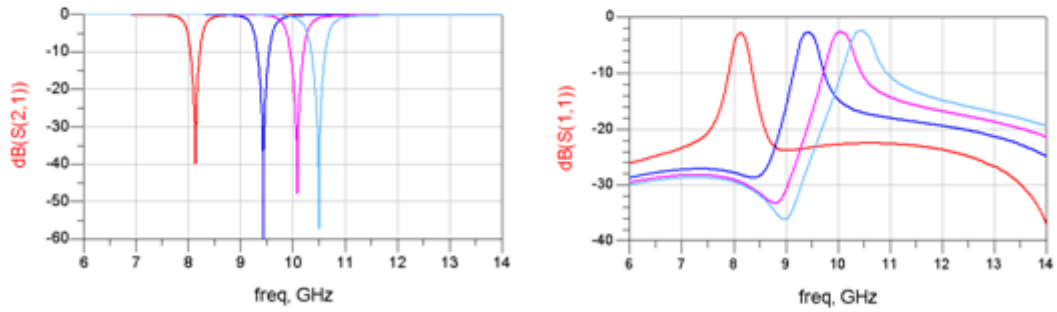

(b)

Figure 5.13 ADS SSS Model Results.
(a) Table of Tuning Results. (b) Tuning Responses.

Varactor Bias Voltage (pF)	Center Frequency (MHz)	Notch Depth (dB)	3dBc BW (MHz)	20dBc/30dBc BW (MHz)
Vp1=0 , Vp2=0.269	7940	-37.871	360	50/15
Vp1=3.88 , Vp2=5	9220	-40.663	420	70/25
Vp1=7.88 , Vp2=10	9820	-41.144	450	80/30
Vp1=11.85 , Vp2=15	10200	-51.182	480	90/30

(a)

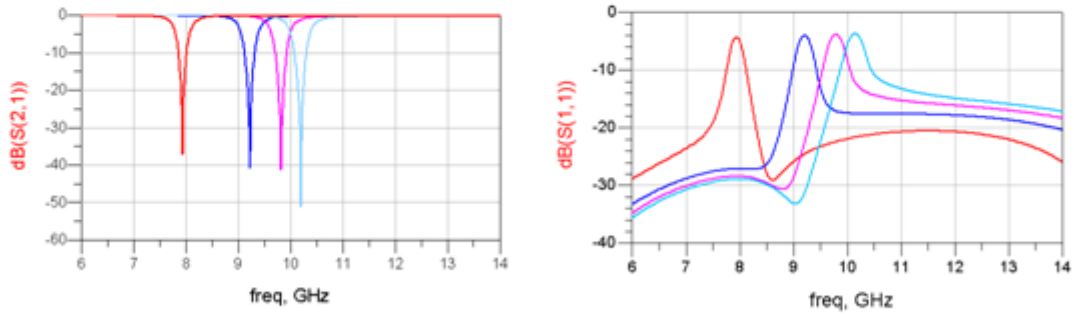

(b)

Figure 5.14 SONNET Simulation Results.
(a) Table of Tuning Results. (b) Tuning Responses.

Varactor Bias Voltage (pF)	Center Frequency (MHz)	Notch Depth (dB)	3dBc BW (MHz)	20dBc/30dBc BW (MHz)
Vp1=0 , Vp2=0.397	8080	-66.067	420	80/30
Vp1=3.54 , Vp2=5	9310	-65.834	490	110/40
Vp1=7.31 , Vp2=10	9900	-44.748	540	130/50
Vp1=11.05 , Vp2=15	10270	-47.541	570	140/60

(a)

Figure 5.15 CST Simulation Results.
(a) Table of Tuning Results.

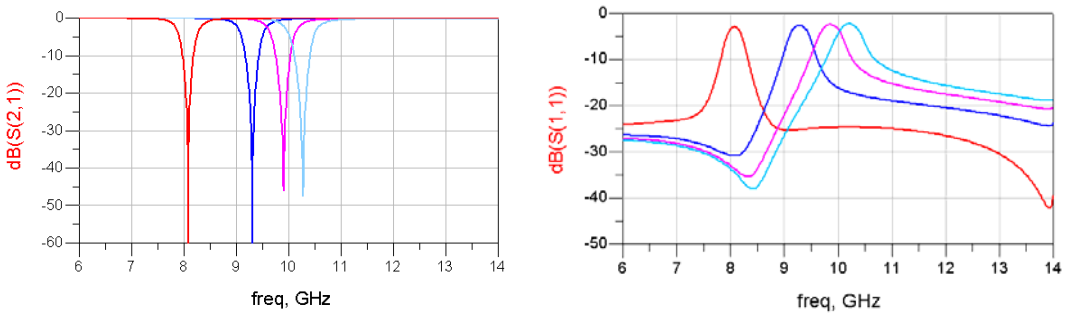

(b)

Figure 5.15 (continued) (b) Tuning Responses

5.4.2 Fabrication & Measurement Results

SONNET layout in Figure 5.11.b does not contain ground and resistor connection pads required for assembling of varactors & bias elements and grounding vias. These additional details does not have significant effect on filter responses except a small shift to lower frequency side in center frequency due to additional shunt capacitance of ground pads. After addition of ground and resistor pads, prototype layout is fabricated at ILFA. Parallel to fabrication of layout PCBs, mechanical cavities for SSS medium are also designed according to final layout and fabricated in UYGUR Ltd. Şti. with gold plating for low loss. After fabrication of these elements, all assembling processes are performed in clean room facilities of ASELSAN Inc. Varactor diodes, bias shunt capacitance and thin film resistors are mounted on corresponding pads using conductive epoxy. Varactor anode terminals are connected by welding its pre-bonded ribbons to ends of comb PCLs. Bias capacitor and resistor connections are done by bonding with a wire having 1mil diameter. SMA connectors and 50Ω transition seals are used to be able to connect the mechanical cavity to Agilent E8362B network analyzer for measurements. DC biases are transmitted to the filter board by using DC hermetic feedthrus of Special Hermetic Products, Inc. Connection of 50Ω transition seals to layout input & output and DC feedthrus to bias pads are done by soldering. The filter becomes ready for measurement when PCB is placed on the body and top cover is placed and fixed with bolds to the body. The picture of varactor mounted side of the fabricated filter board (a), connection of

elements (b), empty mechanical cavities (c) and two views of assembled filters with and without top cover (d) are given in Figure 5.16.

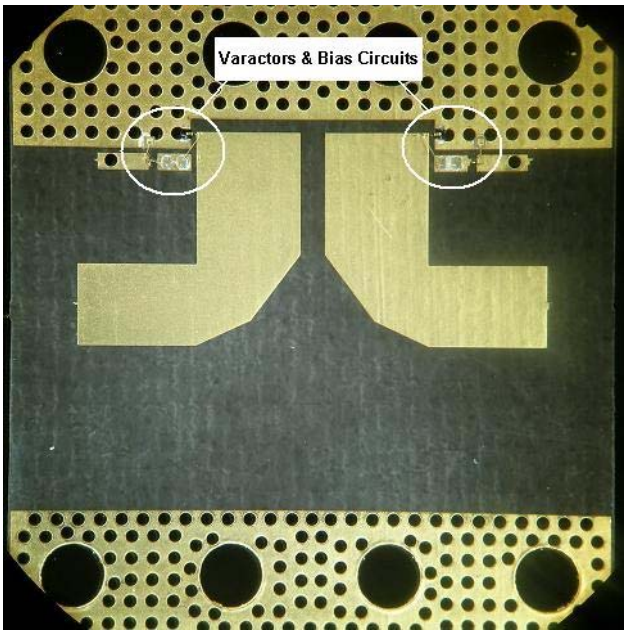

(a)

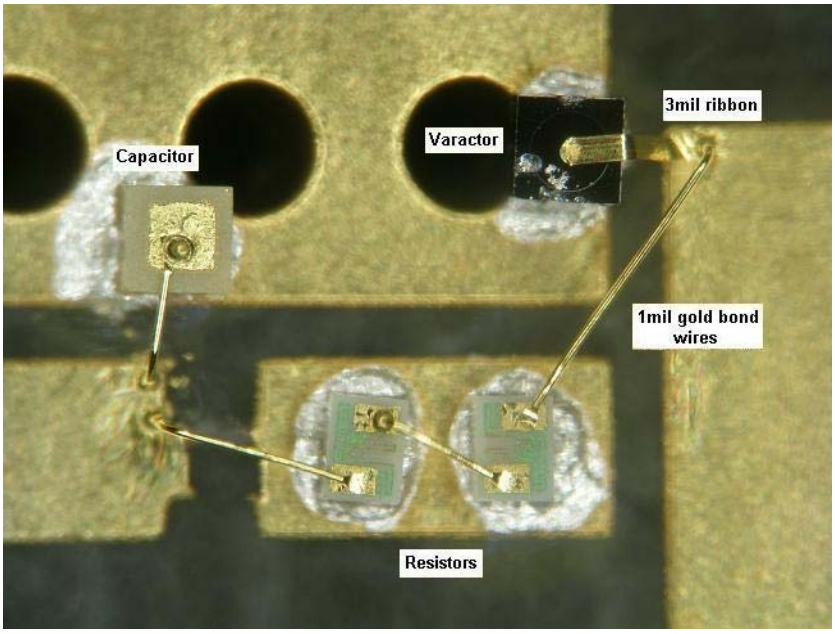

(b)

Figure 5.16 Fabricated and Assembled Components of the Prototype Filter. (a) Picture of Component Side of Layout. (b) Close View of Components & Connections.

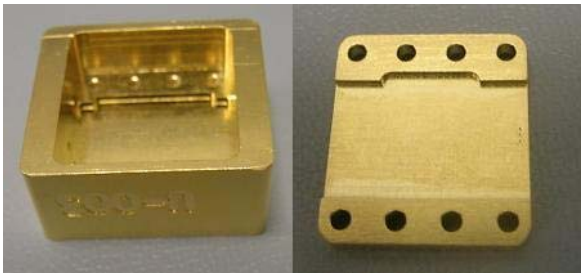

(c)

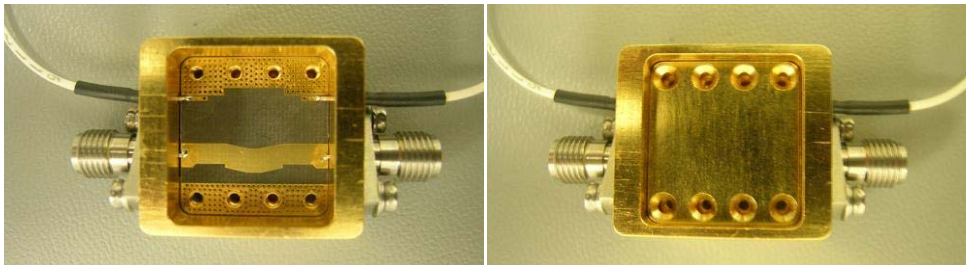

(d)

Figure 5.16 (continued) (c) Empty Cavities. (d) Ready to Measure Filter Pictures.

The measurement setup is given in Figure 5.3. For fixed bias voltages of 0V, 1V, 2V, 4V, 5V, 7.5V, 10V and 15V for one varactor, proper bias voltages are found by manual adjustment of second varactor to get a deepest possible notch depth and the results of measurement are given in Figure 5.17.

Varactor Bias Voltage (V)	Center Frequency (MHz)	Notch Depth (dB)	3dBc BW (MHz)	20dBc/30dBc BW (MHz)
Vp1=0 , Vp2=0.16	7320	-14.470	650	-/-
Vp1=1 , Vp2=1.13	7770	-16.879	610	-/-
Vp1=2 , Vp2=2.22	8100	-20.051	520	-/-
Vp1=4 , Vp2=4.49	8560	-30.190	510	50/-
Vp1=5 , Vp2=5.59	8730	-41.731	490	60/20
Vp1=7.5 , Vp2=9.6	9130	-46.355	520	60/20
Vp1=10 , Vp2=13.4	9400	-42.618	530	70/20
Vp1=11.05 , Vp2=15	9490	-59.846	530	70/20

(a)

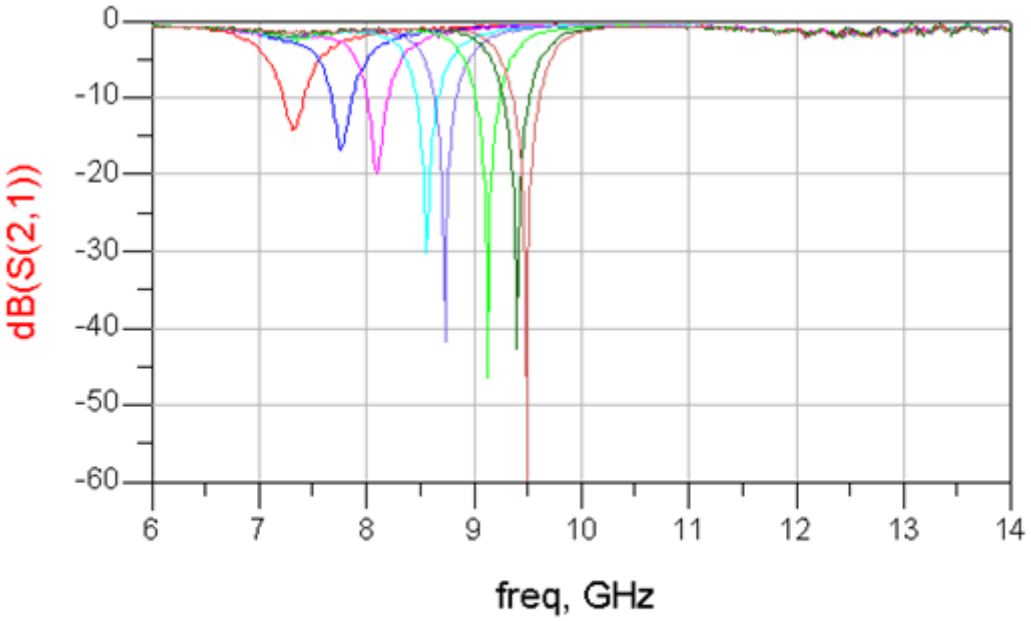

(b)

Figure 5.17 Measurement Results.
(a) Table of Tuning Results. (b) IL Tuning Responses.

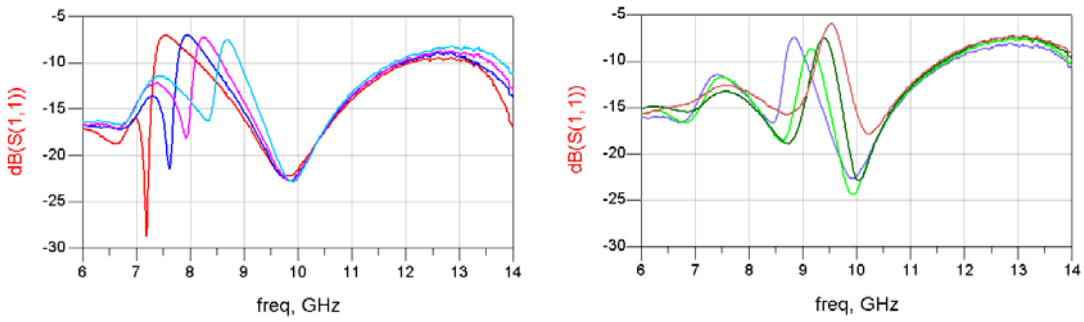

(c)

Figure 5.17 (continued) (c) RL Tuning Responses.

5.4.3 Comments

In Figure 5.17, it is seen that a tunable notch response is obtained in first prototype circuit with degradation in some properties compared to linear & EM simulation results.

First of all, deep notches are observed between 8560MHz and 9490MHz. 3dBc bandwidths of the notches are a little wider than linear & EM simulation results and conversely 20dBc/30dBc bandwidths are a little narrower than the simulation results. Changes in notch bandwidths are expected since losses of the PCB (dielectric & conductor losses) and metallization of the cavity in the practical filter are expected to be higher than simulation results. Also mechanical and PCB tolerances can also affect notch bandwidths.

For center frequencies between 7320MHz to 8560MHz, notch depths are below 30dB which is not desired. This can be due to two main reasons. One reason is a possible deviation in actual coupling values of offset-coupled lines in PCB from expected values due to PCB tolerances and inaccurate simulation results. These offset-coupled lines form the all-pass response and if their coupling values are not adjusted properly, notch depth starts to decrease when center frequency is tuned beyond a frequency range. Another reason is the bias circuitry which can distort the filter response.

Another major difference between simulation and measurement results are the shift in tuning range. In simulations, for bias voltages 0V to 15V, tuning range is approximately between 8000MHz and 10300MHz for all simulations and it is between 7320 MHz and 9490MHz. A small shift in tuning range is already expected due to PCB & cavity tolerances, extra fringing capacitance in cavities and varactor & its ribbon connections. However the main reason of this shift is the bias circuitry. The lumped element bias model used in simulations does not give accurate results.

As final observation, return loss responses (so also passband losses) are not as good as simulation results. Bias circuitry can cause return loss degradation however the main reason is the connection from seal transition and SSS medium. Pins of seals and SSS input & output lines have very different physical sizes (seal have 18mils diameter and input & output lines in SSS have 116mils width. These two are connected directly by soldering. This connection type is not an optimum solution.

Note that, although a tunable notch filter characteristics are obtained in prototype filter and this topology is verified, some improvements should be applied for the following prototype designs. Different bias circuits should be investigated to minimize its degrading effects on notch performances. An optimized transition from seal to SSS medium should be used.

5.5 Bridged BSF Type Notch Filter

5.5.1 Linear Circuit Design & EM Simulations

The design of the prototype filter starts with synthesis of a narrowband BSF using synthesis tool of FILPRO as in first design step given in Chapter 4.3.4. An initial circuit is synthesized and after the transformation of shunt OC stubs by PCL L-resonator transformation in Figure 2.18, a narrowband BSF is obtained. Filter synthesis specifications, initial synthesized filter and the final BSF circuit are given in Figure 5.18.

Synthesis	Distr, LPF, Cheby
Ripple (dB)	0.03
Passband Corners (MHz)	9400
Degree	5 (2Ninf, 3NUE)
f_q (MHz)	9500

(a)

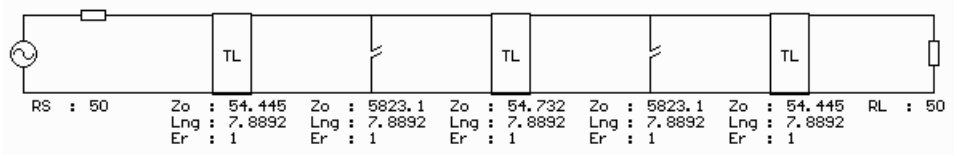

(b)

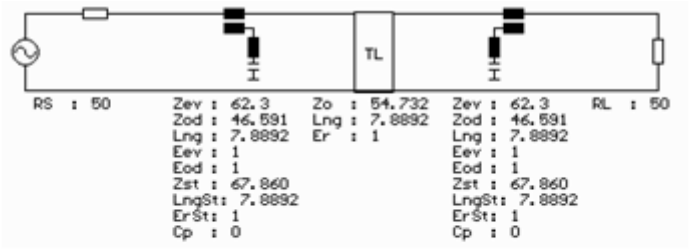

(c)

Figure 5.18 Formation of Realizable Narrowband BSF.
(a) Design Specifications. (b) Synthesized Circuit. (c) Final Circuit.

Center frequency of BSF is chosen as 9.5GHz. The tuning range of the tunable notch filter will be estimated after the addition of varactor diode models. The initial aim for the center frequency of the tuning range is 9.5GHz.

After the formation of realizable narrowband BSF with tuning capacitor added, design stage in FILPRO is finished. The final circuit in Figure 5.18.c is transferred to ADS. Note that although tuning capacitors are added to the schematic, their values are 0pF for now. Their values will be added in ADS.

In ADS, first the bridge quarter wavelength TL with 100Ω impedance is added to the circuit. In this topology, impedance of the bridge will be high and 100Ω impedance of bridge TL is chosen arbitrarily for a starting point in optimization. Then capacitor values are entered. For now, lossless capacitors are used in the circuit. In this example filter, MV20002 model varactors will be used. Similar to the previous case capacitors are chosen as 0.4pF as an initial value and OC stubs are shortened to preserve center frequency. Then impedances of bridge TL and middle TL are modified to get an all-pass response. However this time instead of a pure all-pass response, a frequency limited all-pass response with a small notch at center frequency can be obtained. During manual modification of TL impedances, this small notch is tried to be minimized. The frequency bandwidth in which all-pass response is observed will be the operating frequency range of the final tunable notch filter. The resultant filter and its frequency responses are given in Figure 5.19. Note that the initial value for the capacitors and corresponding stub length are not critical. Capacitors could also be left as 0pF. In the following steps, they will be changed according to varactor model and layout.

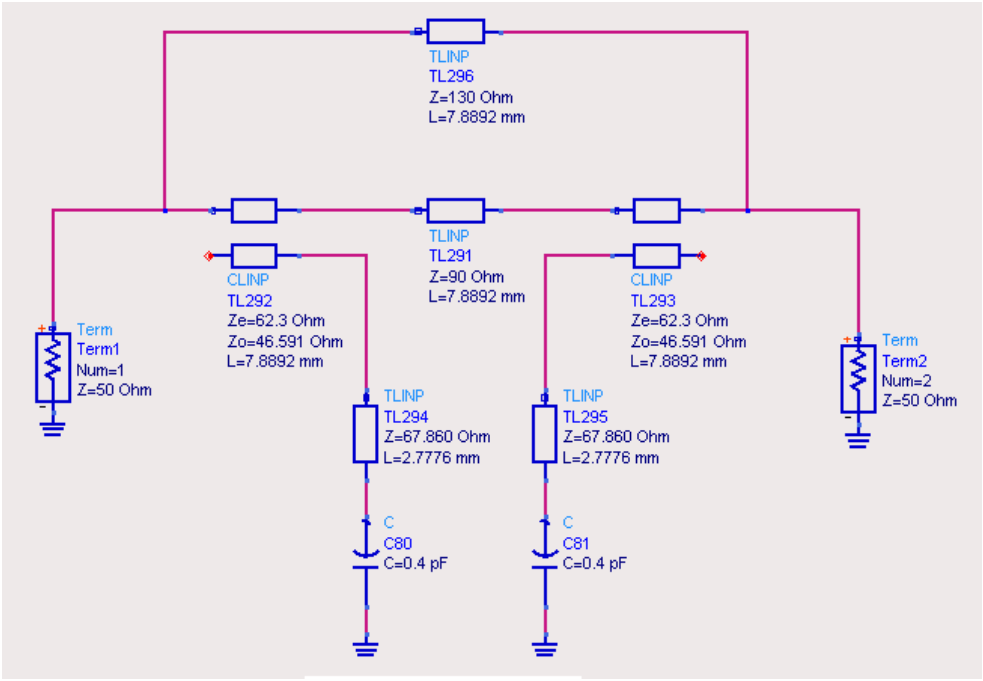

(a)

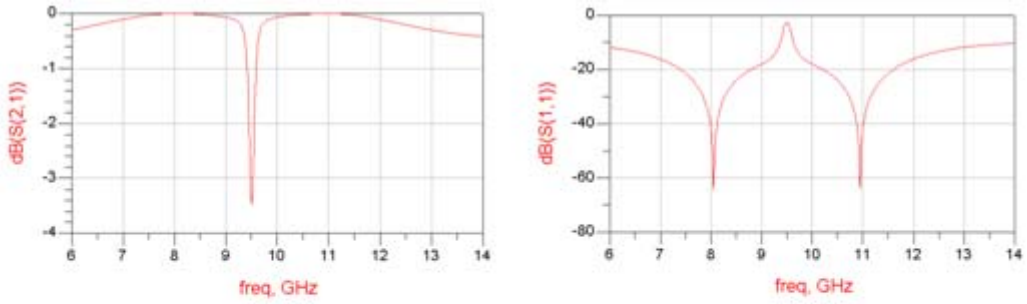

(b)

Figure 5.19 All-Pass like Circuit.
(a) Circuit. (b) Frequency Response.

The next step is to design a physically realizable layout for this filter schematic. Note that PCLs have -16.82dB coupling, which can easily be achieved by side coupling. The problematic part of the schematic in Figure 5.19.a is the connection of bridge TL to the main filter circuit. Since length of main filter is much longer than the bridge line, U-shaped layout should be used for main filter to be able to connect the bridge line to input and output ports. In this case, middle TL and bridge TL should be in U-shaped form. The physical layouts of these lines can best be formed by EM simulation.

The final SONNET layout of prototype filter and its circuit representation are given in Figure 5.20. The layout formation of the filter begins with design of PCL with L-resonator. For this purpose, firstly physical parameters of PCL are determined using ADS SSS model and are shown in Figure 5.20.a. Then PCL with L-resonator are designed individually using EM simulation. After the design of PCL, U-shaped bridge TL and middle TL are formed using EM simulation. In circuit schematics, they are still represented by simple TL pieces. After the design of PCLs and U-shaped lines, all components are combined to get a full layout. Note that in circuit schematics varactor model in Figure 5.7.b is used and to be able to add these models to EM simulation results, wall ports are introduced to ends of OC stubs of PCL L-resonators. SONNET layout formed after many trials is shown in Figure 5.20.b.

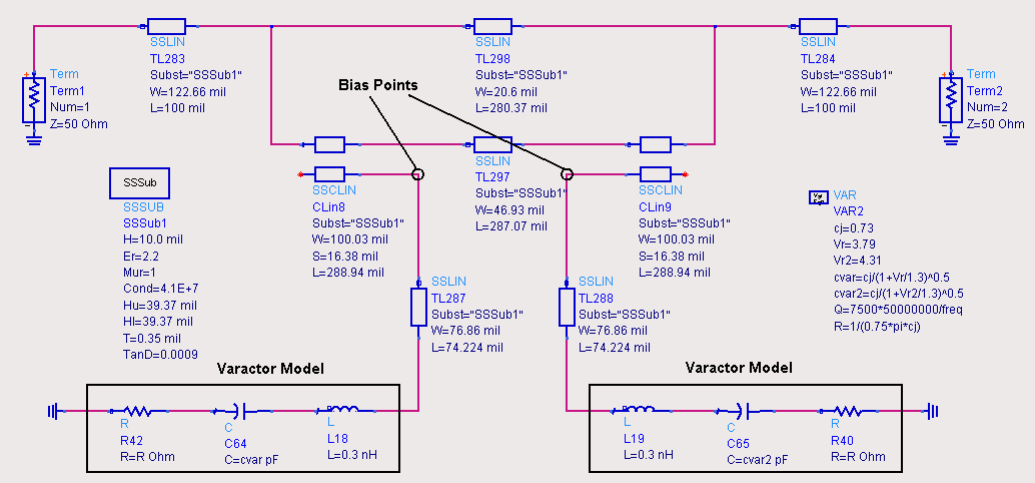

(a)

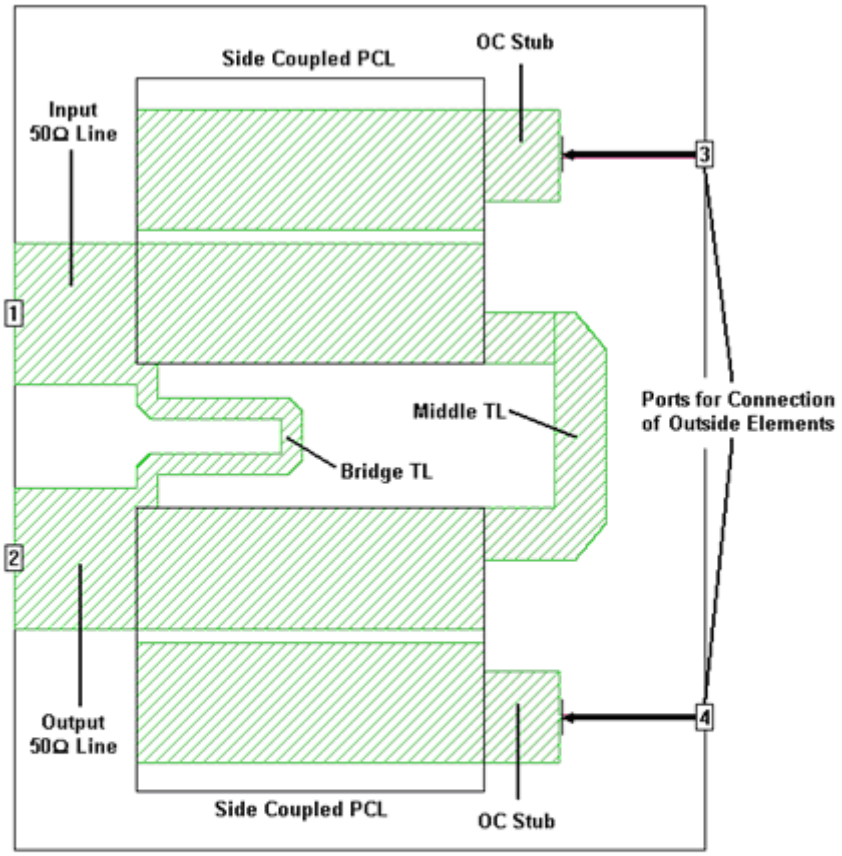

(b)

Figure 5.20 Final Filter Schematic and its SONNET Layout.
(a) ADS Schematics. (b) SONNET Layout.

In SONNET simulation, box metals and conductors are chosen as lossy metal (gold) and dielectric loss of substrate is included. After the execution of the simulation,

simulation results are exported from SONNET and analyzed in ADS. In analysis, varactors models are introduced to EM simulation results by using extra ports defined in SONNET layout.

The filter layout designed by SONNET is also simulated in CST for better evaluation. The 3D layout view in CST is given in Figure 5.21. Same with SONNET design, additional ports are introduced in CST.

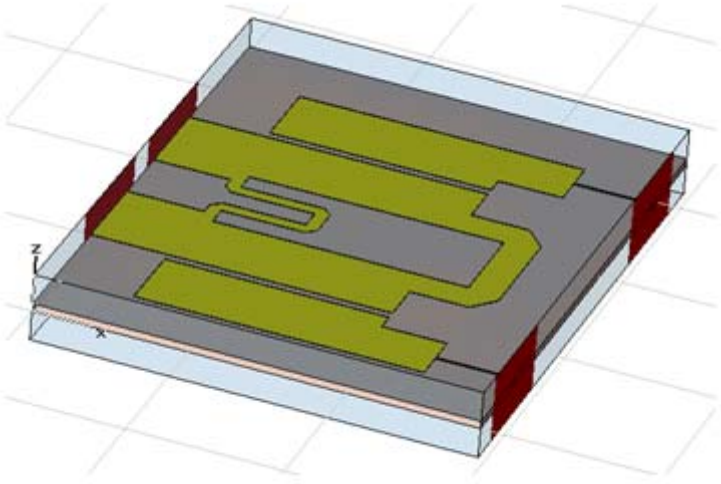

Figure 5.21 CST 3D Layout View.

After the simulations, all the results are combined in ADS and filter characteristics such as stopband bandwidths, notch depth, tuning range, return loss are investigated. For different capacitance values of varactors, the results for ADS SSS model simulation, SONNET simulation and CST simulation are given in Figure 5.22, Figure 5.23 and Figure 5.24 respectively. Note that bias points of this filter are at the beginning of OC stubs. The bias circuit model in Figure 5.8 is connected to bias points in all three simulations and effects of the bias circuit are also included in the following figures.

Varactor Capacitance (pF)	Center Frequency (MHz)	Notch Depth (dB)	3dBc BW (MHz)	20dBc/30dBc BW (MHz)
Cp1=0 , Cp2=0.176	8180	-44.707	270	40/15
Cp1=4.45 , Cp2=5	9640	-38.218	260	40/10
Cp1=9.2 , Cp2=10	10370	-37.688	230	35/10
Cp1=14.09 , Cp2=15	10860	-39.578	200	30/5

(a)

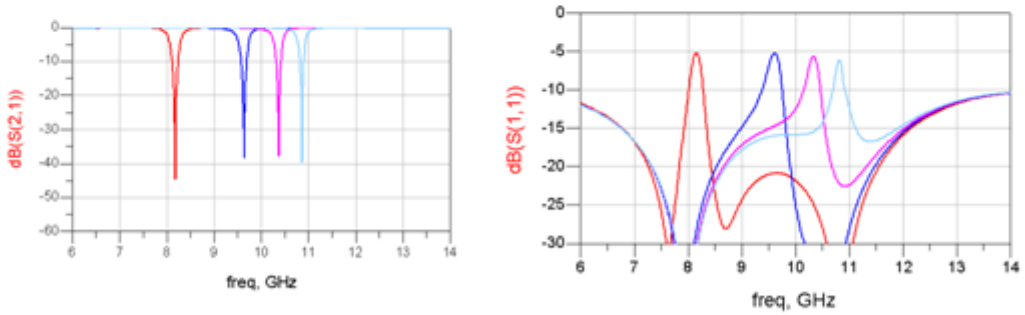

(b)

Figure 5.22 ADS SSS Model Results.
(a) Table of Tuning Results. (b) Tuning Responses.

Varactor Bias Voltage (pF)	Center Frequency (MHz)	Notch Depth (dB)	3dBc BW (MHz)	20dBc/30dBc BW (MHz)
Vp1=0 , Vp2=0.183	7820	-38.345	370	50/20
Vp1=4.47 , Vp2=5	9270	-54.362	410	35/25
Vp1=9.32 , Vp2=10	10000	-36.208	380	40/10
Vp1=14.44 , Vp2=15	10490	-30.845	350	30/-

(a)

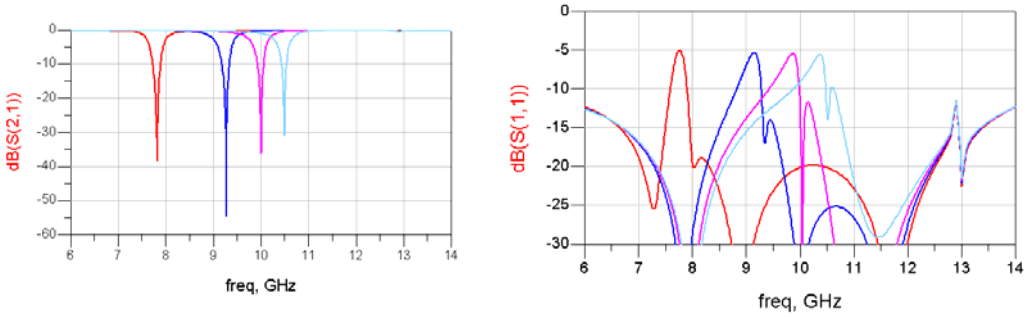

(b)

Figure 5.23 SONNET Simulation Results.
(a) Table of Tuning Results. (b) Tuning Responses.

Varactor Bias Voltage (pF)	Center Frequency (MHz)	Notch Depth (dB)	3dBc BW (MHz)	20dBc/30dBc BW (MHz)
Vp1=0 , Vp2=0.313	7990	-42.414	460	80/30
Vp1=4.06 , Vp2=5	9230	-44.843	490	80/25
Vp1=8.55 , Vp2=10	9870	-41.080	450	60/20
Vp1=13.3 , Vp2=15	10270	-53.082	420	50/15

(a)

Figure 5.24 CST Simulation Results.
(a) Table of Tuning Results.

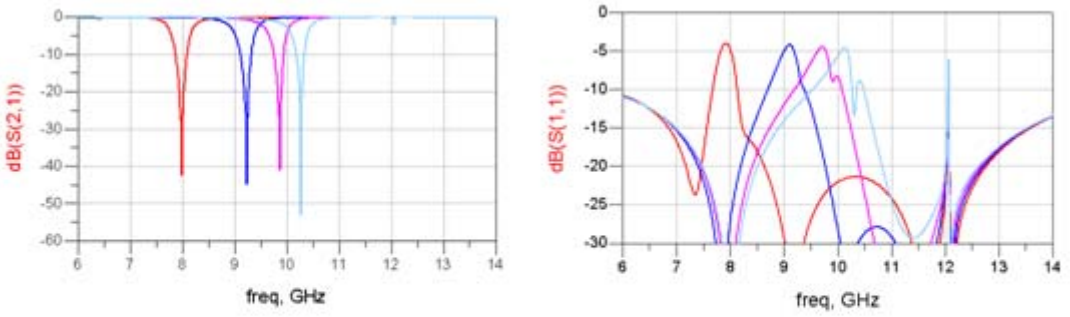

(b)

Figure 5.24 (continued) (b) Tuning Responses.

5.5.2 Fabrication & Measurement Results

SONNET layout in Figure 5.20.b does not contain ground and resistor connection pads required for assembling of varactors & bias elements and grounding vias as in the previous bridged BPF type prototype filter. The only effect of these details is a small shift to lower frequency side in center frequency due to additional shunt capacitance of ground pad. After addition of ground and resistor pads, prototype layout is fabricated and mechanical cavities for SSS medium are fabricated with gold plating. After fabrication of these elements, assembling processes are performed. Varactor diodes, bias shunt capacitance and thin film resistors are mounted on corresponding pads using conductive epoxy. Varactor anode terminals are connected by welding its pre-bonded ribbons to ends of OC stubs in PCL L-resonators. Bias capacitor and resistor connections are done by bonding with 1mil wire. SMA connectors, 50Ω transition seals and DC feedthrus are connected to the mechanical cavity. Connection of 50Ω transition seals to layout input & output are done by soldering and connection of DC feedthrus to bias pads are done by welding. The filter becomes ready for measurement when PCB is placed on the body and top cover is placed and fixed with bolds to the body. The picture of varactor mounted side of the fabricated filter board (a), connection of varactor & bias elements (b), empty mechanical cavities (c) and two views of assembled filters with and without top cover (d) are given in Figure 5.25.

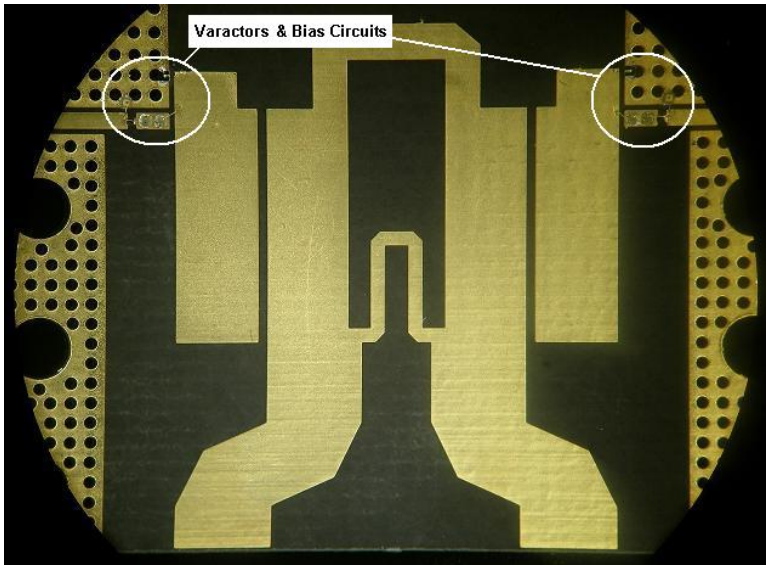

(a)

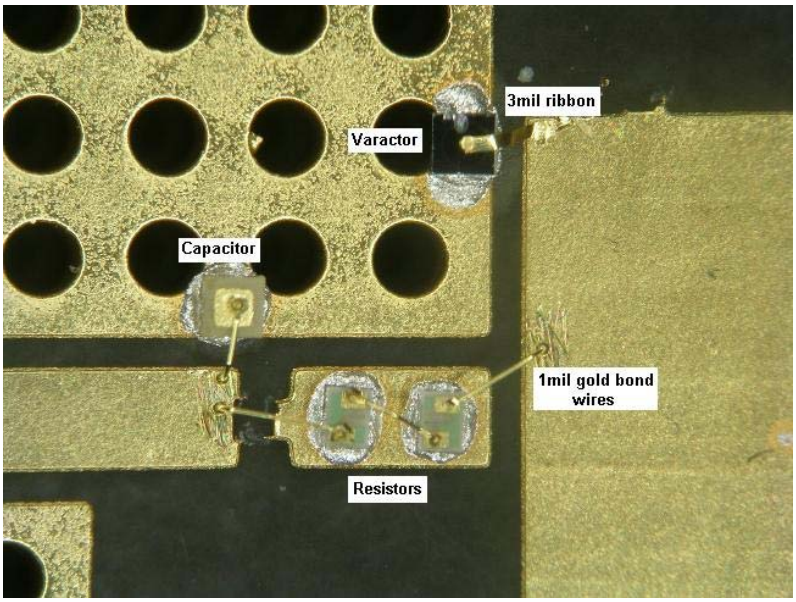

(b)

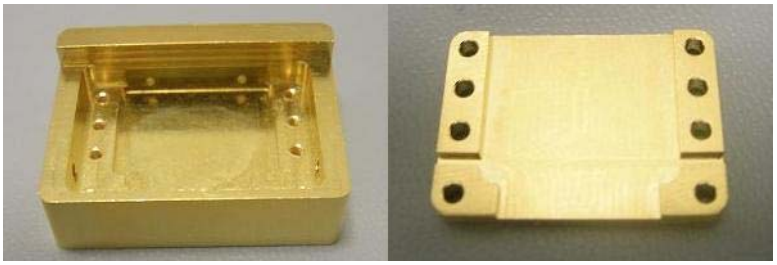

(c)

Figure 5.25 Fabricated and Assembled Components of the Prototype Filter.
(a) Picture of Component Side of Layout. (b) Close View of Components & Connections.
(c) Empty Cavities.

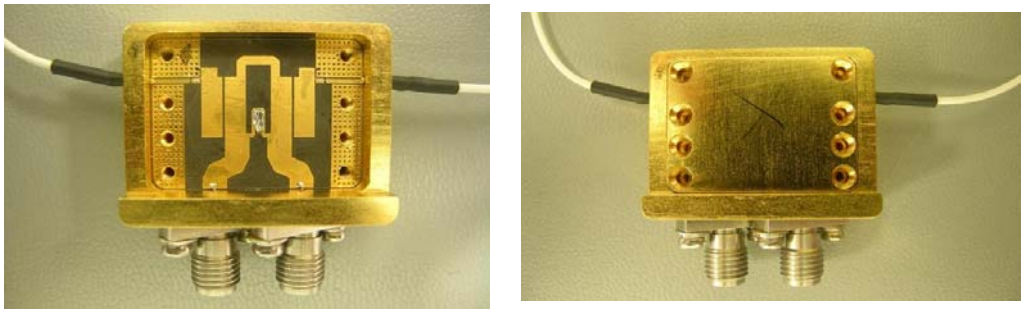

(d)

Figure 5.25 (continued) (d) Ready to Measure Filter Pictures.

The measurement setup is given in Figure 5.3. For fixed bias voltages of 0V, 1V, 2V, 4V, 5V, 7.5V, 10V and 15V for one varactor, proper bias voltages are found by manual adjustment of second varactor to get a deepest possible notch depth and the results of measurement are given in Figure 5.26. Note that in this prototype circuit, a small conductor piece is placed above cross-coupling bridge line for tuning. Without this piece, notch depths do not give satisfactory results.

Varactor Bias Voltage (V)	Center Frequency (MHz)	Notch Depth (dB)	3dBc BW (MHz)	20dBc/30dBc BW (MHz)
Vp1=0 , Vp2=0.1	7500	-26.403	550	50/-
Vp1=1 , Vp2=1.11	7960	-39.765	535	60/20
Vp1=2 , Vp2=2.04	8270	-56.004	530	65/25
Vp1=4 , Vp2=4.14	8740	-61.534	575	65/20
Vp1=5 , Vp2=5.39	8930	-43.674	600	70/20
Vp1=7.5 , Vp2=8.55	9310	-43.421	610	60/15
Vp1=10 , Vp2=12.45	9620	-40.338	610	50/15
Vp1=11.9 , Vp2=15	9800	-44.141	610	50/15

(a)

Figure 5.26 Measurement Results.
(a) Table of Tuning Results.

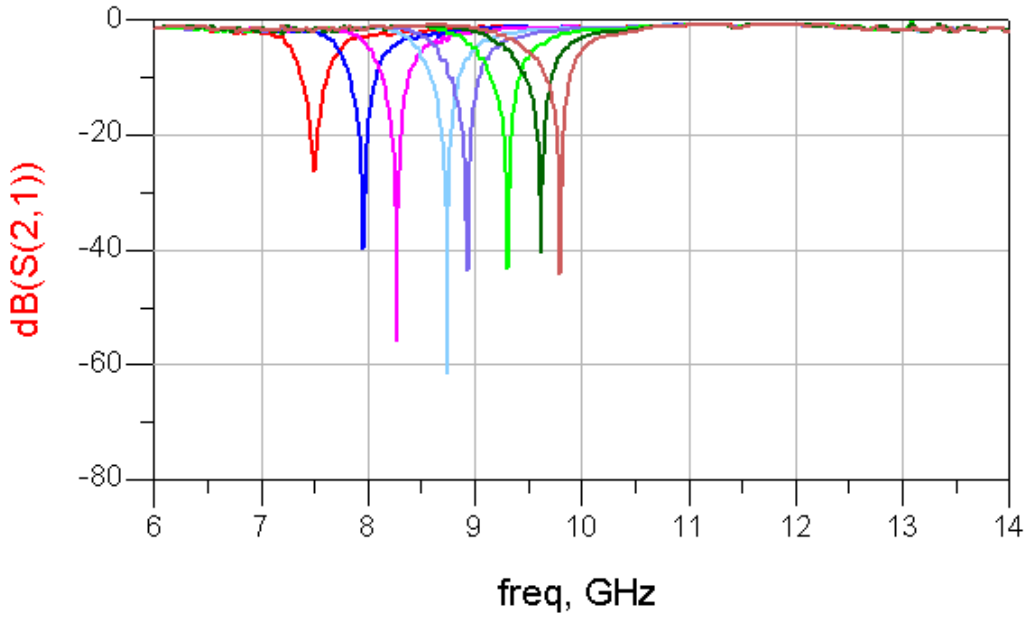

(b)

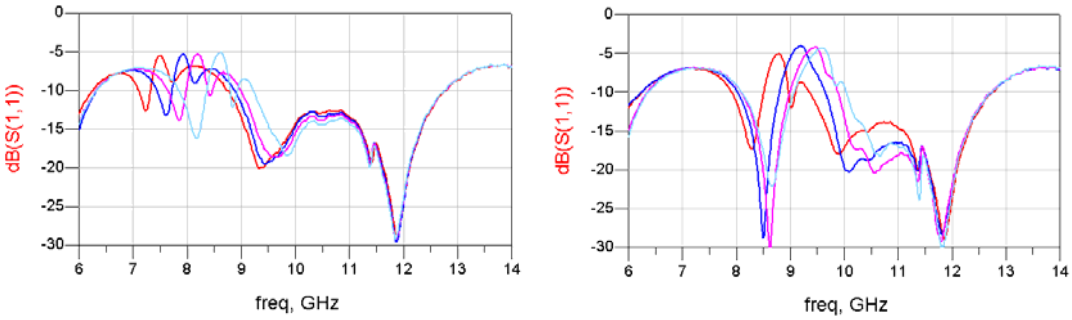

(c)

Figure 5.26 (continued)
(b) IL Tuning Responses. (c) RL Tuning Responses.

5.5.3 Comments

In Figure 5.26, it is seen that a tunable notch response is obtained in first prototype circuit with degradation in some properties compared to linear & EM simulation results.

First of all, deep notches are observed between 7800MHz and 9800MHz. 3dBc bandwidths of the notches are a little wider than linear & EM simulation results. Changes in notch bandwidth properties are expected due to losses of the PCB

(dielectric & conductor losses) and metallization of the cavity in the practical filter. Also mechanical and PCB tolerances can also affect notch bandwidths.

For center frequencies between 7500MHz to 7800MHz, notch depths go below 30dB. This can be due to 2 main reasons. One possible reason can be extra undesired couplings in between cross-coupling U-shaped bridge line and PCLs which are not seen in EM simulation results. Another reason is the bias circuitry which can distort the filter response.

Another major difference between simulation and measurement results are the shift in tuning range as in previous prototype circuit. In simulations, for bias voltages 0V to 15V, tuning range is approximately between 7900MHz and 10400MHz for all simulations and it is between 7500 MHz and 9800MHz. A small shift in tuning range is already expected due to PCB & cavity tolerances, extra fringing capacitance in cavities and varactor & its ribbon connections. However the main reason of this shift is the bias circuitry as in previous prototype circuit. The lumped element bias model used in simulations does not give accurate results.

As final observation, return loss responses (so also passband losses) are not as good as simulation results. The main reason is the connection from seal transition and SSS medium. However another reason is the tuning applied to this prototype circuit. The addition of conductor piece on cross-coupling bridge line, return loss in especially lower frequency side increases.

Note that a tunable notch filter characteristics are obtained in prototype filter and this topology is verified. However the improvements given for previous prototype filter should also be applied. In addition to them, layout of bridge line should also be reconsidered.

5.6 BLC Type Notch Filter

5.6.1 Linear Circuit Design & EM Simulations

The aim in first design stage of this filter is to find proper values for K23', Lng, C_p and Z_{sc} parameters of the topology given in Figure 4.6.b by trial and error until a desired frequency response is obtained. Firstly, K23' value is chosen. For narrowband notch response, this value should be high (above 1000). According to the chosen K23' value, an impedance transforming 3dB BLC is formed from Figure 3.11. For most cases Z_{sc} impedance can be chosen as 50Ω. Value of C_p depends mainly on the chosen center frequency for BLC (f_0) which specifies Lng parameter (quarter wavelength). So to make C_p value to take desired capacitance levels, center frequency of BLC (f_0) should be adjusted properly. To find proper values for K23', f_0 (so Lng), C_p and Z_{sc} some trials need to be performed. By starting from initial values like K23' as 1000, f_0 as expected center frequency of notch filter, Z_{sc} as 50Ω and tuning capacitance value C_p, a trial filter with topology given in Figure 4.6.b is formed. By detuning of capacitors, notch response is obtained and analyzed. If notch characteristics are not as expected (wide stopband etc), then parameters are modified and notch response is again analyzed for convenience. These trials are done until an appropriate response is obtained. When values for these parameters are decided, SC stubs and K23' inverter are entered to FILPRO to find impedance parameters of comb PCL configuration. Then the impedances found in FILPRO are transferred to ADS and the initial design is finished. Since capacitors have the same value, the present structure has all-pass response. The chosen values, comb transformation, final all-pass circuit and its frequency responses are given in Figure 5.27.

Parameter	Value
K23'	1174
F_0	11100 MHz
C_p	0.292pF
Z_{sc}	50Ω

(a)

Figure 5.27 All-Pass Circuit.
(a) Chosen Values.

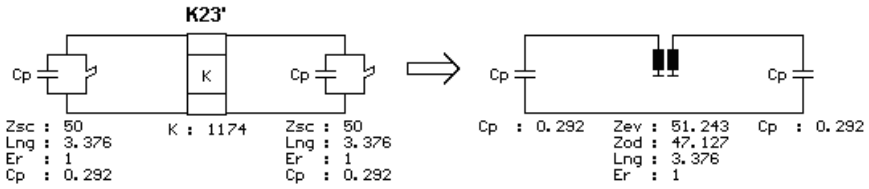

(b)

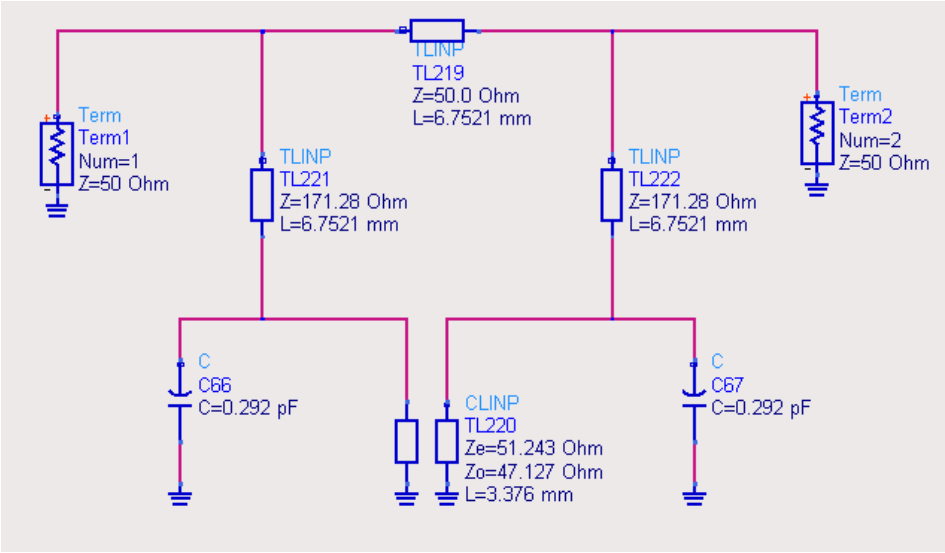

(c)

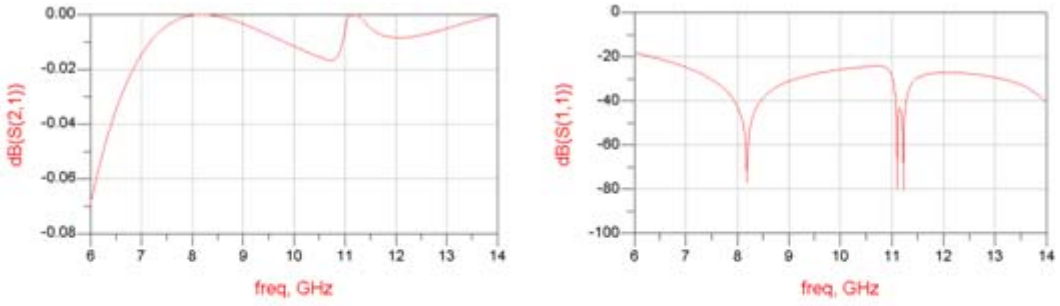

(d)

Figure 5.27 (continued) (b) Comb Transformation. (c) Circuit. (d) Frequency Responses.

Note that center frequency of BLC is chosen as 11.1GHz. The tuning range of the tunable notch filter will be estimated after the addition of varactor diode models. The initial aim for the center frequency of the tuning range is 9.5GHz.

The value of tuning capacitors in all-pass filter is chosen close to 0.3pF. In this prototype design, MV20001 model varactors will be used. Since all-pass response is formed, next step is to calculate physical parameters of the design in Figure 5.27.c in SSS and to insert varactor model to the design. The coupling of comb type PCL is -27.57dB which can be easily achieved by side coupling.

In this topology, bias and varactor connection points are the same which are both inputs of comb type PCL. Since there is a DC path between inputs of PCL, bias connections will be problematic. Since DC bias voltage of each varactor is different, bias circuits can not directly connected to PCL layout. In order to overcome this problem, varactors and bias points are connected to layout via a single layer capacitor. Since capacitance value is high (which is 56pF), effect of this capacitor on frequency responses of the filter is expected to be very little.

The final SONNET layout of prototype filter and its circuit representation are given in Figure 5.28. The layout formation of the filter begins with the design of PCL. For this purpose, firstly physical parameters of comb type PCL are determined using ADS SSS model and are shown in Figure 5.28.a. Then using these physical parameters, PCL is designed individually using EM simulation. TLs of BLC are also designed individually using EM simulation. Finally all TLs and the PCL are combined and a full layout shown in Figure 5.28.b is formed after many trials. Varactor model in Figure 5.7.b is used and to be able to add varactor model to EM simulation results, auto grounded ports with reference lines are introduced to inputs of comb type PCL.

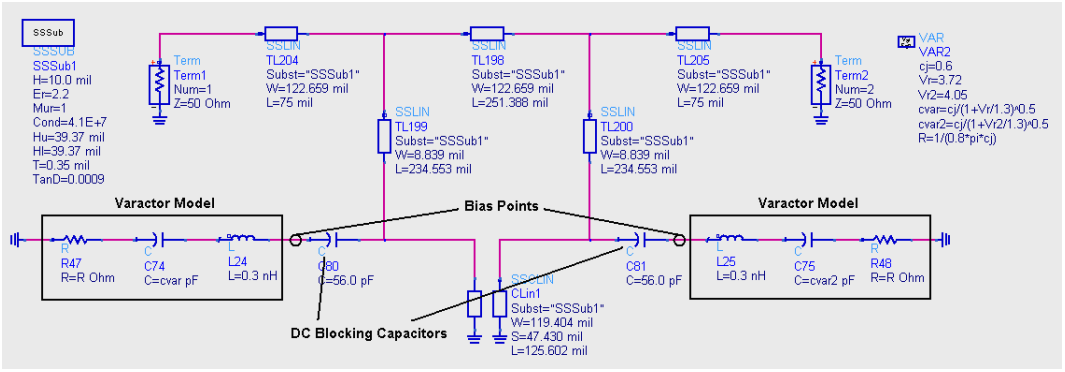

(a)

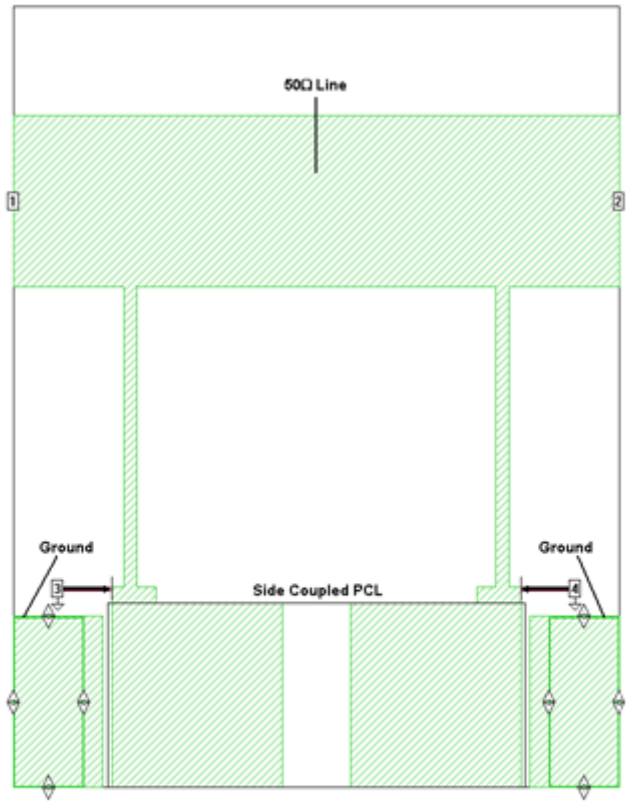

(b)

Figure 5.28 Final Filter Schematic and its SONNET Layout.
(a) ADS Schematics. (b) SONNET Layout.

In SONNET simulation, box metals and conductors are chosen as lossy metal (gold) and dielectric loss of substrate is included. After the execution of the simulation, simulation results are exported from SONNET and analyzed in ADS. In analysis, varactors models are introduced to EM simulation results by using extra ports defined in SONNET layout.

The filter layout designed by SONNET is also simulated in CST for better evaluation. The 3D layout view in CST is given in Figure 5.29. Same with SONNET design, additional ports are introduced in CST.

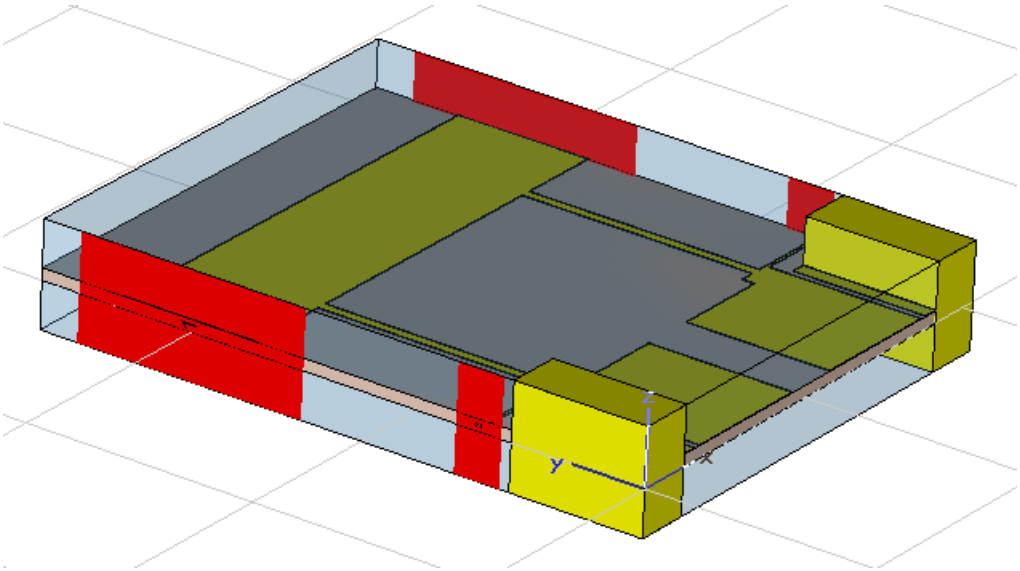

Figure 5.29 CST 3D Layout View.

After the simulations, all the results are combined in ADS and filter characteristics such as stopband bandwidths, notch depth, tuning range, return loss are investigated. For different capacitance values of varactors, the results for ADS SSS model simulation, SONNET simulation and CST simulation are given in Figure 5.30, Figure 5.31 and Figure 5.32 respectively. Bias point of this filter is the same place with the connection point of varactor. The bias circuit model in Figure 5.8 is

connected to bias points in all three simulations and effects of the bias circuit are also included in the following figures.

Varactor Capacitance (pF)	Center Frequency (MHz)	Notch Depth (dB)	3dBc BW (MHz)	20dBc/30dBc BW (MHz)
Cp1=0 , Cp2=0	7080	-21.104	290	-/-
Cp1=4.57 , Cp2=5	9880	-46.511	370	50/15
Cp1=8.98 , Cp2=10	11040	-38.076	440	70/15
Cp1=13.29 , Cp2=15	11760	-50.345	500	90/30

(a)

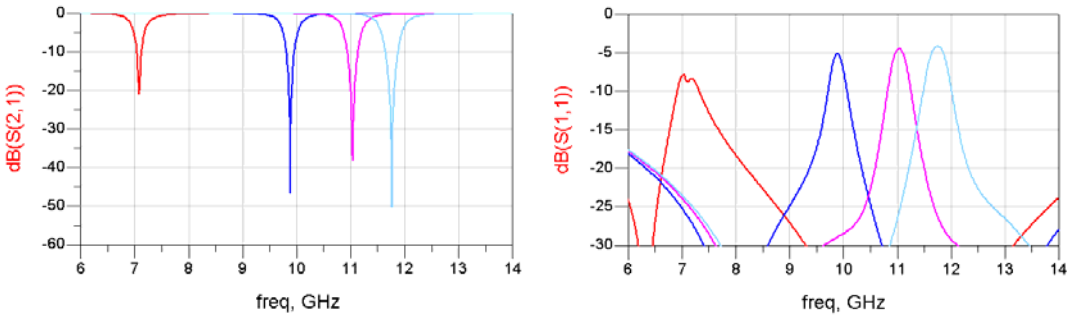

(b)

Figure 5.30 ADS SSS Model Results.
(a) Table of Tuning Results. (b) Tuning Responses.

Varactor Bias Voltage (pF)	Center Frequency (MHz)	Notch Depth (dB)	3dBc BW (MHz)	20dBc/30dBc BW (MHz)
Vp1=0 , Vp2=0	7450	-26.725	620	20/-
Vp1=4.53 , Vp2=5	10190	-47.826	700	120/40
Vp1=8.84 , Vp2=10	11250	-58.449	780	140/35
Vp1=13.01 , Vp2=15	11890	-47.207	820	170/60

(a)

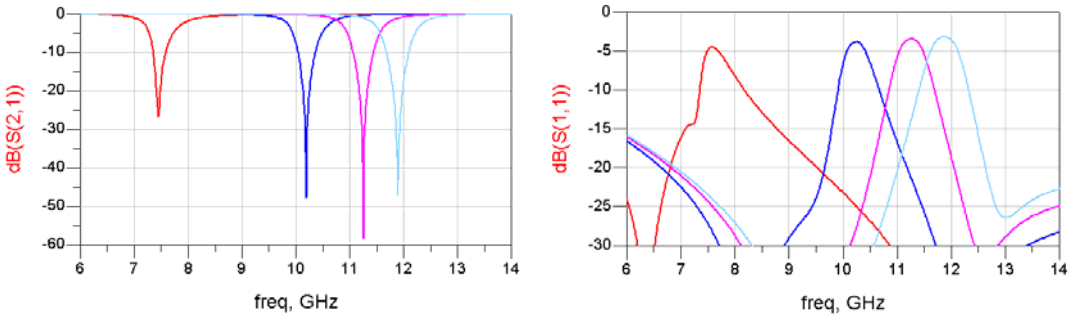

(b)

Figure 5.31 SONNET Simulation Results.
(a) Table of Tuning Results. (b) Tuning Responses.

Varactor Bias Voltage (pF)	Center Frequency (MHz)	Notch Depth (dB)	3dBc BW (MHz)	20dBc/30dBc BW (MHz)
Vp1=0 , Vp2=0	7650	-25.693	600	60/-
Vp1=4.62 , Vp2=5	10040	-55.358	600	100/30
Vp1=9.04 , Vp2=10	10940	-45.750	620	120/40
Vp1=13.38 , Vp2=15	11490	-47.850	640	120/45

(a)

Figure 5.32 CST Simulation Results.
(a) Table of Tuning Results.

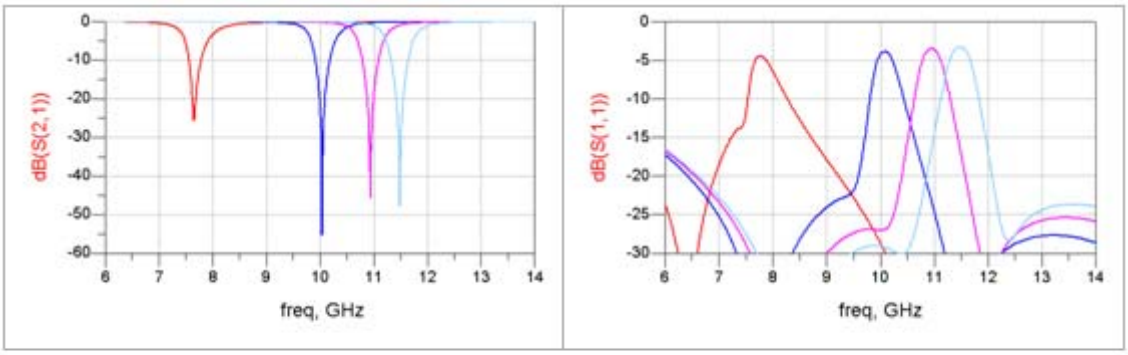

(b)

Figure 5.32 (continued) (b) Tuning Responses.

5.6.2 Fabrication & Measurement Results

SONNET layout in Figure 5.28.b does not contain ground and resistor connection pads required for assembling of varactors & bias elements and grounding vias. The only effect of these details is a small shift to lower frequency side in center frequency due to additional shunt capacitance of ground pad. After addition of ground and resistor pads, prototype layout is fabricated and mechanical cavities for SSS medium are fabricated with gold plating. After fabrication of these elements, assembling processes are performed. Varactor diodes, bias shunt capacitance and thin film resistors are mounted on corresponding pads using conductive epoxy. Varactor anode terminals are connected by welding its pre-bonded ribbons to ends of OC stubs in PCL L-resonators. Bias capacitor and resistor connections are done by bonding with 1mil wire. SMA connectors, 50Ω transition seals and DC feedthrus are connected to the mechanical cavity. Connection of 50Ω transition seals to layout input & output are done by soldering and connection of DC feedthrus to bias pads are done by welding. The filter becomes ready for measurement when PCB is placed on the body and top cover is placed and fixed with bolds to the body. The picture of varactor mounted side of the fabricated filter board (a), connection of varactor & bias

elements (b), empty mechanical cavities (c) and two views of assembled filters with and without top cover (d) are given in Figure 5.33.

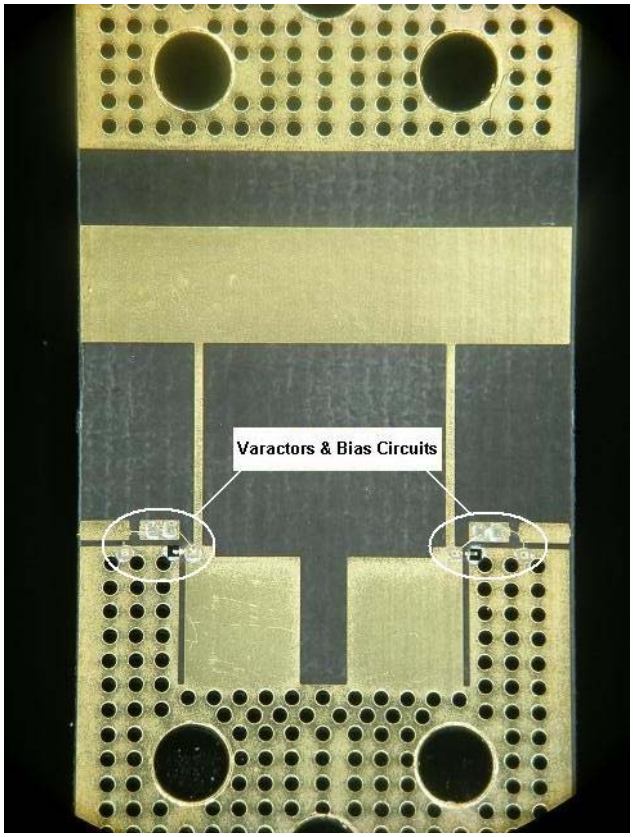

(a)

Figure 5.33 Fabricated and Assembled Components of the Prototype Filter.
(a) Picture of Component Side of Layout.

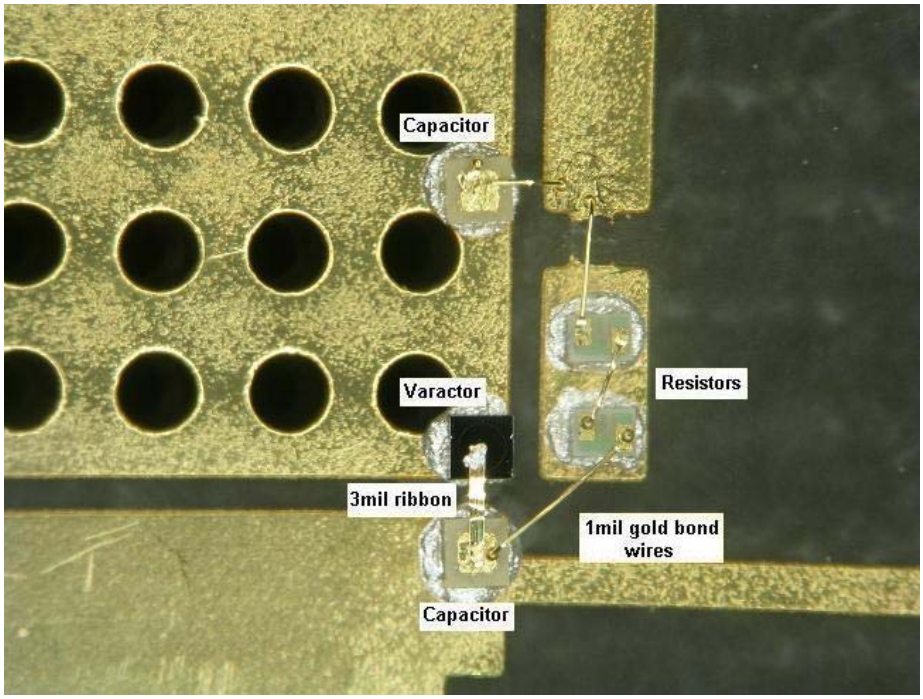

(b)

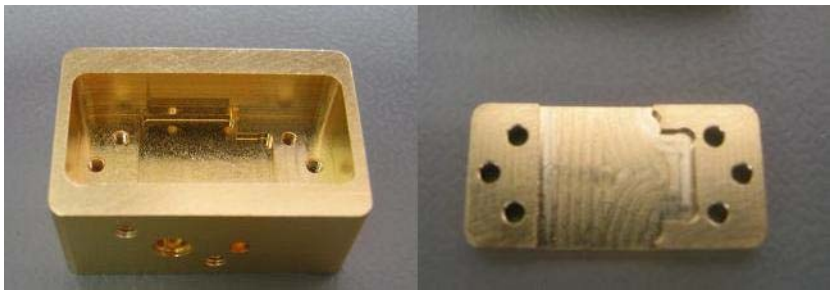

(c)

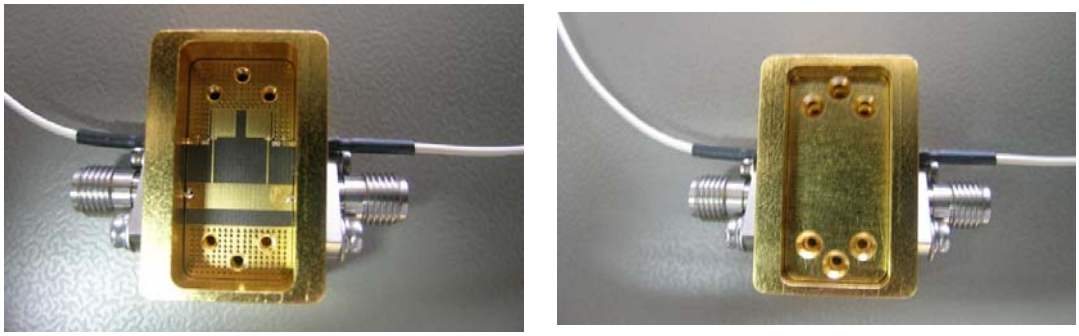

(d)

Figure 5.33 (continued) (b) Close View of Components & Connections. (c) Empty Cavities. (d) Ready to Measure Filter Pictures.

The measurement setup is given in Figure 5.3. For fixed bias voltages of 0V, 1V, 2V, 4V, 5V, 7.5V, 10V and 15V for one varactor, proper bias voltages are found by manual adjustment of second varactor to get a deepest possible notch depth and the results of measurement are given in Figure 5.34.

Varactor Bias Voltage (V)	Center Frequency (MHz)	Notch Depth (dB)
Vp1=0 , Vp2=0.2	6220	<10dB
Vp1=1 , Vp2=1.2	6950	<10dB
Vp1=2 , Vp2=2.4	7510	<10dB
Vp1=4 , Vp2=4.9	8210	<10dB
Vp1=5 , Vp2=5.9	8450	<10dB
Vp1=7.5 , Vp2=8.7	8930	<10dB
Vp1=10 , Vp2=12	9320	<10dB
Vp1=13.1 , Vp2=15	9640	<10dB

(a)

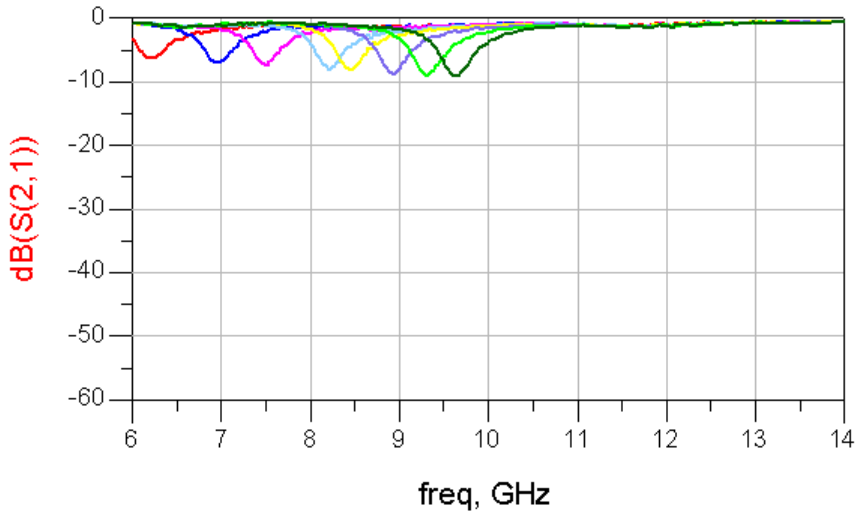

(b)

Figure 5.34 Measurement Results.
(a) Table of Tuning Results. (b) IL Tuning Responses.

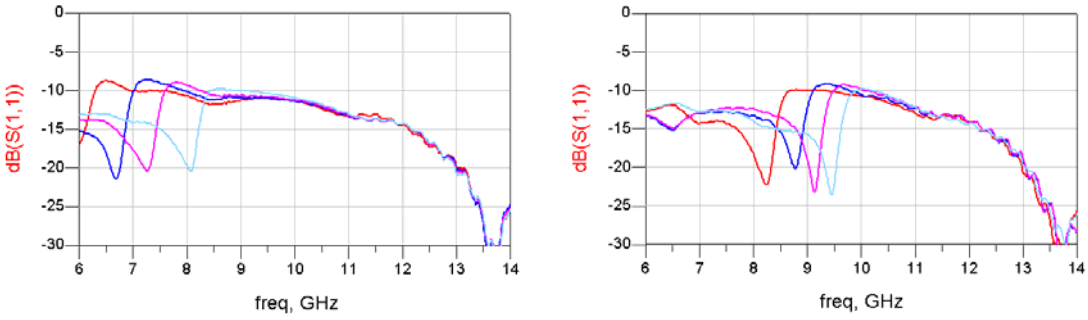

(c)

Figure 5.34 (continued) (c) RL Tuning Responses.

5.6.3 Comments

In Figure 5.34, it is seen that a tunable notch response is obtained with very low and unsatisfactory notch depths. So results of the prototype filter are problematic. Deep notches can not be obtained by changing bias voltages. Hence this prototype filter can not be used to verify the topology.

Possible reason of this response can be due to the connection of varactors and bias circuits to the layout by using a series connected single layer capacitor. Alternative ways should be searched for varactor and bias circuit connections.

CHAPTER 6

CONCLUSION

In this study, electronically tunable microwave bandstop filters are investigated. Especially narrowband tunable bandstop filters can be very useful and necessary for suppression of changing frequency interferences which can result from collocated transmitters and hostile emitters in order to prevent receiver desensitization. Typical position of these filters is receiver front-ends. So in order to minimize additional noise, signal distortion and receiver sensitivity degradation, losses and nonlinearities at passbands of the filter need be very small. Also suppression at tuned frequency should be high and suppressed frequency band should be narrow. These desired properties normally can be achieved by using high-Q resonators. However high-Q resonators can not be obtained by using planar transmission mediums and varactor diodes as tuning elements. In order to be able to design high performance tunable notch filters by using varactors and by using planar structures, filter topologies which take effects of circuit losses into account are necessary.

The main aim of this thesis is to investigate filter topologies that allow designing tunable narrowband bandstop filters with satisfactory performances using planar transmission mediums and varactor diodes. Note that during this work only filters with two resonators (and so two varactors) are introduced and analyzed.

For this purpose, firstly direct narrowband distributed bandstop designs are analyzed. These filters are first synthesized by using distributed filter theory and after application of some transformations, various realizable filter topologies are formed. However, all these filter topologies suffer from loss of circuit elements. Especially resonator losses due to planar mediums and varactor diodes severely decrease suppression levels and increase stopband bandwidth. So these topologies are not useful for tunable notch filter designing.

A method called as amplitude balanced phase cancellation can be useful for increasing performance of direct bandstop filters and for introducing new topologies with low-Q resonators. In this method, one or more extra paths are introduced between input and output ports in parallel with a narrowband bandstop or a narrowband bandpass filter and the signals are enforced to cancel each other at the output port by proper adjustment of amplitudes and phases. By this way, good notch characteristics can be obtained despite lossy resonators. The extra path can be a single transmission line or a transmission line and PCL combiner/splitters. Various filter topologies using this approach are introduced. The main drawback of this method is the bad tuning performances. At center frequency, a high quality notch response is obtained. However when center frequency is changed, notch depth decreases and outside a frequency range, notch depth becomes unsatisfactory and the tuning range when notch depth has acceptable levels is generally narrow.

After direct and phase cancellation methods, a novel systematic notch filter design method called as all-pass filter approach is introduced. All-pass filter approach is a special case of phase cancellation. In this approach first a bridged all-pass filter is designed by using either readily available all-pass topologies or by bridging a BPF or a BSF with two resonators. Then it is converted into a notch filter by detuning tuning capacitors until phase difference between the signal along the bridge path and main filter path becomes 180^0 and hence cancel each other at desired frequencies. This approach enables deep notch depths with narrow bandwidths and this notch characteristics is conserved during wide tuning ranges independent of resonator Q's. Three filter topologies are introduced and analyzed using this approach.

To better analyze and verify this approach, three prototype filters using all-pass approach are designed using both linear simulation and EM simulations. For linear simulation and designs, FILPRO and ADS are used. For EM simulations SONNET and CST are used. Using EM simulation layouts, prototype designs are implemented in suspended stripline substrate medium with GaAs varactor diodes. PCBs are manufactured at ILFA Inc. Mechanical cavities for SSS are manufactured in UYGUR Lti. Şti. All assembly processes are done in ASELSAN Inc. After measurement of these three prototype filters, good tunable notch filter characteristics

are obtained from two of the designs. One prototype filter did not give proper notch depths. There are two main reasons that deviate and distort all filter responses from expected simulation results. One is the bias circuit and the other one is the transition from coaxial line to SSS medium. As the result of measurements, two of the filter topologies are verified. To verify the third topology and to improve the responses of other two prototype filters, further trials and modifications on bias circuitry, transitions, etc. need to be done.

REFERENCES

[1] I. C. Hunter, J. D. Rhodes, “Electronically tunable microwave bandstop filters”, *IEEE Trans. MTT*, vol. 30, pp. 1361-1367, Sept. 1967.

[2] S. R. Chandler, I.C. Hunter and O.G. Gardiner, “Active Varactor Tunable Bandpass Filter”, IEEE Microwave and Guided Wave Letters, Vol. 3, No. 3, March 1993.

[3] D. R. Jachowski, “Passive enhancement of resonator Q in microwave notch filters”, 2004 IEEE MTTS Int. Mic. Symp Dig., pp. 1315-1325, June 2004.

[4] C. Rauscher, “A tunable X-Band active notch filter with low distortion passband response”, *IEEE Trans. MTT Digest*, 2000.

[5] C. Rauscher, “Varactor tuned active notch filter with low passband noise and signal distortion”, *IEEE Trans. MTT*, vol. 49, no. 8, Augst. 2001.

[6] J. D. Rhodes, “Hybrid notch filters”, Int. J. Circ. Theory appl. Vol. 23, pp. 49-58, 1995.

[7] J. D. Rhodes, I. C. Hunter, “Synthesis of reflection mode prototype networks with dissipative circuit elements”, IEE Proc. Mic. Antennas Propag, vol. 144, no. 6, pp. 437-442, 1997.

[8] D. R. Jachowski, “Compact frequency agile absorptive bandstop filters”, IEEE MTTS Int. Mic. Symp Dig., pp. 1315-1325, June 2005.

[9] A. C. Guyette, I. C. Hunter, R. D. Pollard and D. R. Jachowski, “Perfectly matched bandstop filters using lossy resonators”, IEEE MTTS Int. Mic. Symp Dig., pp. 517-520, June 2005.

[10] D. R. Jachowski and C. Rauscher, “Frequency agile bandstop filter with tunable attenuation”, IEEE MTTS Int. Mic. Symp Dig., pp. 649-653, June 2009.

[11] FILPRO Manual, METU, 2010.

[12] G. L. Matthaei, L.Young and E. M. T. Jones, “Microwave Filters, Impedance-Matching Networks, And Coupling Structures”, John Wiley & Sons, 2005.

[13] D.M. Pozar, “Microwave Engineering”, Artech House, 3rd Edition 1980.

[14] D.M. Pozar, “Microwave Engineering”, Artech House, 3rd Edition, pp 406, 1980.

[15] D. Q. Xu, G. R. Branner, “An Efficient Technique for Varactor Diode Characterization”, IEEE, 1997.

APPENDIX A

DATASHEET OF MV20000 SERIES GAAS VARACTORS

Microsemi

GaAs Varactor Diodes

Abrupt Junction

MV20001 – MV21010

Features

- High Q Values for Higher Frequency Performance
- Constant Gamma Design
- Low Reverse Current
- Available as Chip or Packaged Diodes
- Available in Chip-on-Board Packaging
- Custom Designs Available

Applications

- VCOs
- Phase-Locked Oscillators
- High Q Tunable Filters
- Phase Shifters
- Pre-Selectors

Description

Microsemi's GaAs abrupt junction varactors are fabricated from epitaxial layers grown at Microsemi using Chemical Vapor Deposition. The layers are processed using proprietary techniques resulting in a high Q factor and very repeatable tuning curves. The diodes are available in a variety of microwave ceramic packages or chips for operation from UHF to millimeter wave frequencies.

Maximum Ratings

Reverse Voltage	Breakdown Voltage
Forward Current	50 mA @ 25°C
Incident Power	+20 dBm @ 25°C
Operating Temperature	-55°C to +175°C
Storage Temperature	-55°C to +200°C

GaAs Varactor Diodes

Abrupt Junction

MV20001 – MV21010

Specifications @ 25°C

Gamma = 0.5

Part Number	C_T @ 4 V ± 10% (pF)[1,3,4]	Typ. $\frac{C_T @ 0\ V}{C_T @ V_{BR}}$[5]	Min. V_{BR} @ 10 µA (V)	Typ. Q @ -4 V[2]
MV20001	0.3	2.4	15	6000
MV20002	0.4	2.6	15	7500
MV20003	0.5	2.8	15	7000
MV20004	0.6	2.9	15	6500
MV20005	0.8	3.0	15	6000
MV20006	1.0	3.1	15	5700
MV20007	1.2	3.2	15	5000
MV20008	1.5	3.3	15	5000
MV20009	1.8	3.4	15	5000
MV20010	2.2	3.4	15	4000
MV21001	0.3	2.8	30	6000
MV21002	0.4	3.1	30	7500
MV21003	0.5	3.4	30	7000
MV21004	0.6	3.6	30	6500
MV21005	0.8	3.8	30	6000
MV21006	1.0	4.0	30	5700
MV21007	1.2	4.2	30	5000
MV21008	1.5	4.3	30	5000
MV21009	1.8	4.5	30	5000
MV21010	2.2	4.6	30	4000

[1]Capacitance is specified at 1 MHz.
[2]Measured by DeLoach Technique and referenced to 50 MHz.
[3]Tightened tolerances available upon request.
[4]Package capacitance of 0.15 pF is included in the above specification.
[5]The capacitance ratio is calculated using C_P = 0.15 pF. Ratios will vary depending upon package selection.

Typical Characteristics

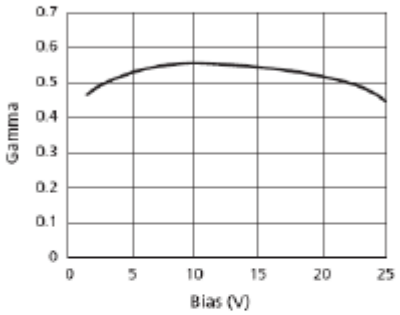

Typical Gamma vs. Bias
Gamma = 0.50

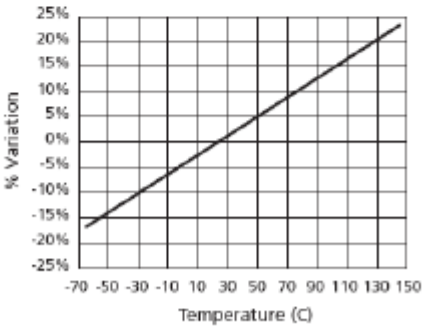

Variation of Breakdown
Voltage vs. Temperature
(Normalized to 25°C V_{BR} @ 10 µA)

Specifications @ 25°C

Gamma = 0.5

Part Number	C_T @ 4 V ± 10% (pF)[1,3,4]	Typ. $\frac{C_T @ 0\ V}{C_T @ V_{BR}}$[5]	Min. V_{BR} @ 10 µA (V)	Typ. Q @ -4 V[2]
MV20001	0.3	2.4	15	8000
MV20002	0.4	2.6	15	7500
MV20003	0.5	2.8	15	7000
MV20004	0.6	2.9	15	6500
MV20005	0.8	3.0	15	6000
MV20006	1.0	3.1	15	5700
MV20007	1.2	3.2	15	5000
MV20008	1.5	3.3	15	5000
MV20009	1.8	3.4	15	5000
MV20010	2.2	3.4	15	4000
MV21001	0.3	2.8	30	8000
MV21002	0.4	3.1	30	7500
MV21003	0.5	3.4	30	7000
MV21004	0.6	3.6	30	6500
MV21005	0.8	3.8	30	6000
MV21006	1.0	4.0	30	5700
MV21007	1.2	4.2	30	5000
MV21008	1.5	4.3	30	5000
MV21009	1.8	4.5	30	5000
MV21010	2.2	4.6	30	4000

[1] Capacitance is specified at 1 MHz.
[2] Measured by DeLoach Technique and referenced to 50 MHz.
[3] Tightened tolerances available upon request.
[4] Package capacitance of 0.15 pF is included in the above specification.
[5] The capacitance ratio is calculated using C_p = 0.15 pF. Ratios will vary depending upon package selection.

Typical Characteristics

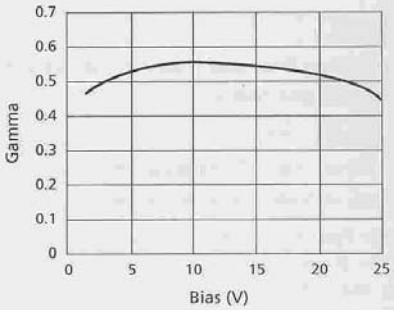

Typical Gamma vs. Bias
Gamma = 0.50

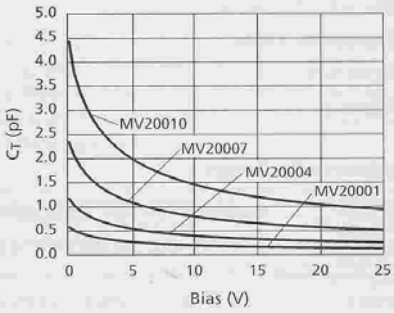

Total Capacitance vs. Bias

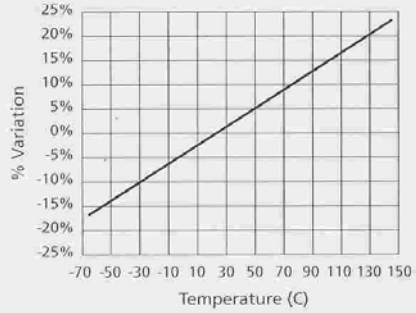

Variation of Breakdown
Voltage vs. Temperature
(Normalized to 25°C V_{BR} @ 10 µA)